GENETIC DETERMINANTS OF HUMAN SERUM STEROL LEVELS

APPROVED BY SUPERVISORY COMMITTEE

David W. Russell, Ph.D.

Ralph J. Deberardinis, M.D., Ph.D.

Jonathan C. Cohen, Ph.D.

Jay D. Horton, M.D.

I dedicate this thesis to my late undergraduate research advisor, David Sterling Marsh, Ph.D., who always showed enthusiasm and excitement for my research projects, taught me how to interpret unexpected results and revealed how new questions and hypotheses can arise from ‘uninterpretable’ data. My life would not have been the same without his endless sarcasm, wit and humor. I thank him for always making time for one of his ‘chilluns’; you will not be forgotten, Dave.

ACKNOWLEDGEMENTS

First and foremost, I thank my mentor and advisor, David Russell, for his endless support, patience, and guidance and for providing an excellent learning environment for my graduate studies. The knowledge and wisdom that I have acquired from working in his lab is priceless. Technical help of Daphne Rye, Bonne Thompson and Jeff McDonald over the years has been invaluable. I consider myself lucky to have been a student under such a great mentor, and it is an honor to be his last graduate student.

I am grateful to have been a student in the Department of Molecular Genetics; the cooperative and collaborative environment is unlike any other. I am also incredibly lucky to have distinguished scientists on my thesis committee. I appreciate the insight, suggestions and discussion on my project and future career.

Special thanks to my family. Thanks to my father, Ken Stiles, for instilling in me the value of a good education and hard work. Thanks to my mother, Sharon McNutt, for always supporting my decisions and for teaching me that time is scarce. To my younger siblings, I hope that my experience has instilled in you the importance of pursuing your dreams and achieving your goals, no matter how hard they may be. To the rest of my family, thank you for supporting me in every way and for doing more than your best to help me achieve my goals.

Finally, thanks to my best friend, my love, Marcus Long, for being one of my biggest supporters, I am thrilled to have you in my life and look forward to our future together. And to Cooper and Jane, our four-legged kids, thanks for always cheering me up; you bring a smile to my face.

GENETIC DETERMINANTS OF HUMAN SERUM STEROL LEVELS

by

ASHLEE RENEE STILES

DISSERTATION

Presented to the Faculty of the Graduate School of Biomedical Sciences

The University of Texas Southwestern Medical Center at Dallas

In Partial Fulfillment of the Requirements

For the Degree of

DOCTOR OF PHILOSOPHY

The University of Texas Southwestern Medical Center

Dallas, Texas

May, 2013

GENETIC DETERMINANTS OF HUMAN SERUM STEROL LEVELS

ASHLEE R. STILES, Ph.D.

The University of Texas Southwestern Medical Center at Dallas, 2013

DAVID W. RUSSELL, Ph.D.

Dozens of different cholesterol metabolites are synthesized by mammalian cells and are known to play important physiological roles in the liver, brain, and immune system. These metabolites are ultimately inactivated by conversion into bile acids in the liver and are thereafter excreted from the body. Mutations in several genes encoding enzymes that metabolize cholesterol have been identified and the clinical consequences of these mutations range from progressive central nervous system neuropathy to spastic paraplegia to liver failure in children. There are several genes in the cholesterol metabolic pathway in which human mutations and their clinical consequences have not yet been identified. For example, the metabolite 24-hydroxycholesterol is produced in the brain by cholesterol 24-hydroxylase (encoded by the CYP46A1 gene). Disruption of this gene in the mouse causes severe learning defects, but it is not known whether mutations in the human gene cause the same phenotype. To overcome the uncertainty inherent in guessing what the phenotype arising from mutations in the human *CYP46A1* gene might be and to detect mutations in other genes specifying cholesterol metabolic enzymes, we developed mass-spectrometry based methods to measure >60 different sterol metabolites in small volumes (200 µl) of human serum. We applied these methods to

quantify sterols in 3,230 serum samples derived from clinically well-characterized subjects participating in the Dallas Heart Study. Large intra-individual variation was detected in the serum levels of approximately 22 of the >60 sterols assessed. To identify the genes underlying the observed variation, we took both targeted and untargeted approaches. In the targeted approach, advantage was taken of the fact that the substrates and products of many sterol metabolizing enzymes are known and we thus sequenced the corresponding genes in subjects with very high or low levels of the sterol in question. In the untargeted approach, the 3,230 individuals whose sterol levels were measured were genotyped for 9,229 non-synonymous (amino acid-changing) variations (SNPs) in multiple human genes. For 24-hydroxycholesterol, the metabolite mentioned above, both approaches yielded concordant results. Direct sequencing of the oxysterol 7α-hydroxylase gene (*CYP39A1*), which uses 24-hydroxycholesterol as a substrate, identified several mutations that decrease enzyme activity and thus lead to increased serum levels of this sterol substrate. In the genetic linkage analysis, a SNP in *CYP39A1* was strongly ($P=2.1 \times 10^{-27}$) correlated with serum 24-hydroxycholesterol levels. Expression analysis indicated that this SNP also decreased CYP39A1 enzyme activity. Together, these results illustrate that our approach has the ability to identify genetic determinants of serum sterol levels. Additional correlations were identified between a SNP in *EPHX2* and levels of 24,25-epoxycholesterol ($P=9.6 \times 10^{-25}$) and a SNP in *SDR42E1* and levels of 8-dehydrocholesterol levels ($P=1.5 \times 10^{-15}$). Biochemical assays were performed to characterize these previously unidentified genetic associations and to reveal their effect on oxysterol and sterol metabolism. Simultaneously, SNP genotypes and sterol levels were correlated with specific clinical phenotypes in an effort to shed light on the role of non-cholesterol sterols in disease. The next step is to apply these methods to the other 19 sterols that are routinely detected in serum and to correlate the analytical and genetic findings with the >100 clinical phenotypes of the 3,230 subjects whose sterol levels we have measured.

TABLE OF CONTENTS

PRIOR PUBLICATIONS

Stiles AR, McDonald JG, Bauman DR, Russell DW. CYP7B1: one cytochrome P450, two human genetic diseases, and multiple physiological functions. J Biol Chem. 2009 284:28485-9.

Stiles AR and Russell DW. SRD5A3: a surprising role in glycosylation. Cell 2010 23:196-8.

McDonald JG, Smith DD, **Stiles AR,** Russell DW. A comprehensive method for extraction and quantitative analysis of sterols and secosteroids from human plasma. J Lipid Res. 2012 53:1399-409.

LIST OF FIGURES AND TABLES

CHAPTER 1

CHAPTER 2

CHAPTER 3

CHAPTER 4

LIST OF APPENDICES

LIST OF ABBREVIATIONS

ABC, ATP-binding cassette transporter

ACAT, acyl-CoA acyltransferase

ACN, acetonitrile

APCI, atmospheric pressure chemical ionization

BHT, butylated hydroxytoluene

BMI, body mass index

cDNA, complimentary deoxyribonucleic acid

CH25H, cholesterol 25-hydroxylase

$CHCl_3$, chloroform

$CHCl_3$:MeOH, chloroform:methanol

CID, collision-induced dissociation

CTX, cerebrotendinous xanthomatosis

CYP, cytochrome P450 enzyme

CYP3A5, cytochrome P450 3A5

CYP7A1, cholesterol 7α-hydroxylase

CYP27A1, sterol 27-hydroxylase

CYP39A1, oxysterol 7α-hydroxylase

CYP46A1, cholesterol 24-hydroxylase

DCM, dichloromethane

DHCR7, 7-dehydrocholesterol recductase

DHS, Dallas Heart Study

DMEM, Dulbecco's modified eagle medium

DNA, deoxyribonucleic acid

DPBS, Dulbecco's phosphate-buffered saline

EPHX2, epoxide hydrolase 2

ER, endoplasmic reticulum

ESI, electrospray ionization

EtOH, ethanol

FWHM, full width-half maximum

GC, gas chromatography

GC-MS, gas chromatography-mass spectrometry

HDL, high density lipoprotein

HEK-293, human embryonic kidney-293 cells

HMG-CoA, 3-hydroxy-3-methylglutaryl CoA reductase

HPLC, high-performance liquid chromatography

HPLC-MS, high-performance liquid chromatography-mass spectrometry

HSD3B7, 3β-hydroxy-Δ^5-C_{27} steroid oxidoreductase

IDL, instrument detection limit

IgA, immunoglobulin A

KOH, potassium hydroxide

LB, luria broth

LC, liquid chromatography

LDL, low density lipoprotein

LTP, long-term potentiation

LXR, liver X receptor

MDL, method detection limit

MeOH:DCM, methanol:dichloromethane

MICAL1, microtubule associated monoxygenase, calponin and LIM domain containing 1

MRI, magnetic resonance imaging

mRNA, messenger ribonucleic acid

MS, mass spectrometry

MTBSTFA, *N*-methyl-*N*-*tert*-butyldimethylsilyl trifluoroacetamide

N_2, nitrogen

NADPH, nicotinamide adenine dinucleotide phosphate

NH_4I, ammonium iodide

NH_4OAc, ammonium acetate

NMR, nuclear magnetic resonance

PCR, polymerase chain reaction

PMPCA, peptidase (mitochondrial processing) alpha

PTFE, polytetrafluoroethylene

RCT, reverse cholesterol transport

RIC, reconstructed ion chromatogram

RPM, revolutions per minute

RRF, relative response factor

RSE, relative standard error

SDR42E1, short-chain dehydrogenase/reductase family 42E member 1

SDS-PAGE, sodium dodecyl sulfate polyacrylamide gel electrophoresis

SERM, selective estrogen receptor modulator

SMRM, scheduled multiple reference monitoring

SNP, single nucleotide polymorphism

SPE, solid phase extraction

SREBP, sterol response element binding proteins

SRM, standard reference material

TBDMCS, *tert*-butyldimethylchlorsilane

TLC, thin-layer chromatography

TLR, Toll-like receptor

UPLC, ultra pure liquid chromatography

UV, ultraviolet

CHAPTER ONE:

Introduction

History of Sterol Detection and Analysis

Over 230 years ago, the first known sterol, cholesterol, was discovered by French chemists as a crystalline component of human gallstones. The first connection between cholesterol and human health appeared in 1843 when it was shown that cholesterol was present in arterial plaques. Since its initial discovery, we have learned the structure of cholesterol, determined the biochemical pathway of its synthesis, understood its metabolic regulation and the feedback mechanisms that regulate its synthesis, learned that cholesterol is the precursor of steroid hormones, oxysterols, and bile acids, and is a structural component of cellular membranes [1]. The identification of a number of inherited disorders due to defects in the cholesterol biosynthetic pathway and the bile acid synthetic pathway has made it clear that cholesterol and its derivatives play crucial roles in human embryogenesis and development [2]. The ability to improve methods of sterol detection and measurement has shed light on cholesterol homeostasis and the pathways involved in its synthesis and degradation.

Cholesterol and related sterols that possess the 1,2-cyclopentanoperhydrophenanthrene ring system, are derived from isoprenoid biosynthesis and are characterized by the presence of a fused four-membered ring structure with a side chain. Cholesterol biosynthesis from the first intermediate containing the four-membered ring structure (lanosterol) occurs via two different routes with the choice of pathways determined by the stage at which the double bond at carbon-24 (C_{24}) of the side chain is reduced. If C_{24} double bond reduction is retained until the last reaction, cholesterol synthesis proceeds via desmosterol through the Bloch pathway. If there is

early reduction of the C_{24} double bond of lanosterol, then the pathway proceeds via 7-dehydrocholesterol through the Kandutsch-Russell pathway (Figure 1). The skin and intestine have higher levels of sterol Δ24-reductase and thus utilize the Kandutsch-Russell pathway. In contrast, cholesterol biosynthesis in the liver and brain occur through the Bloch pathway as there are higher levels of lanosterol 14α-demethylase activity in these tissues [3].

Early attempts at natural product surveys of sterols were based on measurements of melting point, color reaction, optical rotation and crystalline form. In the mid- to late 20th century, research changed to focus on biomimetic chemistry, tracer work, enzymology, and structure determination using high-field nuclear magnetic resonance (NMR) and x-ray diffraction methods. During this time, there was a renewed focus on the regulation of cholesterol synthesis and human physiology. These studies ultimately led to the development of statins, which inhibit the activity of a biosynthetic enzyme, 3-hydroxy-3-methylglutaryl CoA reductase (HMG-CoA) [4], and lead to a reduction in blood cholesterol levels. Central to the advances of the last decades has been the development of molecular genetic approaches including gene cloning, primary amino acid sequence determination, and functional characterizations. These methods have revealed a large number of enzymes that act on sterols and several inborn errors of cholesterol metabolism [3].

Historically, sterols have been analyzed via thin-layer chromatography (TLC) and gas chromatography (GC). The advent of mass spectrometry (MS) provided instruments with picogram sensitivity that could be coupled to both GC and liquid chromatography (LC) to provide molecular weight, elemental composition and structural information. In using a mass spectrometer for quantitative measurements, isotope-dilution methods are employed, which are one- to two-orders of magnitude more sensitive than conventional TLC or GC methods [5]. Deuterium-labeled sterols are used as internal standards in this approach and are added to samples prior to the extraction of lipids via organic solvents. Assumptions made in using

isotope dilution methods for quantitation include that the internal deuterated standard will be degraded or lost to the same degree as the sterol to be measured (the analyte) due to its near identical physiochemical properties [6]. In order for sterols to be analyzed by GC-MS, hydroxyl groups and carboxylic acids must first be derivatized to tri-methylsilyl ethers or *tert*-butyldimethylsilyl ethers, and any conjugating groups such as sulfate, glucose, fatty acids, or glucuronic acid must be removed to enhance volatility.

Sterols are typically analyzed by GC-MS methods using electron ionization (EI) at 70eV or chemical ionization (CI). EI is most commonly used because this method allows determination of fragment-ion formation, which is valuable for structural characterization. There are additional benefits to EI in that extensive libraries of mass spectra are available which provide detailed information and retention index values for sterols that provide additional guides to analyte identification. Selected ion monitoring (SIM) can be employed in combination with isotope dilution methods to provide maximum sensitivity. In this approach, only the region around selected ion(s) where ion current is monitored with chromatographic time are analyzed. An advantage associated with GC-MS is chromatographic resolution; many sterols are effectively resolved by GC and for this reason, GC-MS methods are still used today. GC-MS is an excellent approach for sterol profiling; however, the introduction of soft-ionization and atmospheric pressure ionization (API) methods of electrospray ionization (ESI) and atmospheric pressure chemical ionization (APCI) have made the LC-MS-based screening of biological samples simpler, quicker, and more sensitive leading to more informative, higher throughput and faster processing [7].

There are several disadvantages to GC-MS however, including the need to derivatize molecules prior to analysis, which requires additional steps in sample preparation, increases instrument maintenance requirements and can increase the complexity of the resulting chromatogram. Additionally, the molecular ions of polyhydroxylated molecules (such as those

arising from trihydroxylated sterols) may be weak or not observable [8]. Oxysterols, which are sterols with more than one hydroxyl group located on the ring structure or side chain, are traditionally difficult to analyze. These compounds are thermally labile, present in trace quantities relative to cholesterol in biological samples, and can form spontaneously when cholesterol or other sterols are exposed to oxygen. Many of these challenges are overcome by using LC-MS [9],[10]. LC-MS is capable of fully resolving and separating oxysterols from cholesterol, can distinguish isomeric pairs of oxysterols, and can be paired with different ionization and chromatographic methods to enhance resolution and detection [11].

A further advantage that LC-MS has over GC-MS is that the former method is more compatible with polar molecules. Sterols are also more amenable to separation in their native state by LC-MS. While the quantitation and identification of oxysterols by GC-MS is an order of magnitude higher in sensitivity than high-pressure liquid chromatography (HPLC) alone, GC-MS analysis of oxysterols requires derivatization and exposure to high temperatures, which can lead to oxysterol decomposition [11]. Tandem MS/MS (MS/MS), the arrangement of two mass-spectrometers in series in space or in time, and precursor/product ion scans are superior to GC-MS systems that rely on a single quadrupole, electron impact MS [8]. Multiple reaction monitoring (MRM) scans in which the formation of multiple ions from a single precursor is monitored in MS/MS provides maximum sensitivity and minimizes background interference. In this approach, MS_1 is fixed on a precursor ion and MS_2 is fixed on a fragment ion that allows the incorporation of multiple product-fragment pairs [7]. The type of ionization used for mass spectrometric analysis of lipids varies depending upon the characteristics of the desired analyte. APCI produces gentle fragmentation with large structurally informative fragments along with some protonated molecules and is used for neutral molecules such as phytosterols. ESI yields almost exclusively protonated molecules or molecular adduct ions with little to no fragmentation and is optimal for the detection of more polar molecules such as oxysterols [12].

The extraction and analysis of sterols from biological samples such as plasma is challenging. First, sterols and oxysterols exhibit a wide array of chemical properties based upon structural differences in their functional groups. Second, circulating sterols are sequestered in lipoprotein particles and ~80% of sterols exist as steryl esters making them highly insoluble [13]. Third, there are magnitudes of difference in the levels of individual sterols in plasma and other samples with concentrations of cholesterol at 1 to 3 mg/ml and 25-hydroxycholesterol, present at 1 to 3 ng/ml. Finally, plasma contains proteins and other lipids such as triglycerides, phospholipids and sphingolipids at levels similar to that of total cholesterol and these components further confound sterol analysis. These factors can be overcome through multiple extraction steps, a saponification step to hydrolyze steryl esters and solid phase extraction using an amino-propyl column to separate sterols and oxysterols from non-polar lipids, polar lipids and fatty acids. The saponification step is not always effective in hydrolyzing all oxysterols and steryl esters. The efficiency of hydrolysis increases with increasing temperature, time, or concentration of potassium hydroxide; however, some sterols, such as 7-oxocholesterol decompose at extremes of hydrolysis. For example, temperatures greater than 22 ^{o}C, concentrations of potassium hydroxide from 0.35 to 0.70 M and incubation time from 1 hr to 14 hrs degrade almost 50% of 7-oxocholesterol [10]. In order to prevent artifacts arising from cholesterol autoxidation during sample preparation, antioxidants and metal chelators can be added to the sample to minimize non-enzymatic oxidative reactions [6].

Cholesterol Homeostasis

Rudolf Schoenheimer demonstrated in 1933 that mice fed a high cholesterol diet exhibit a net destruction of cholesterol whereas those fed a diet low in cholesterol synthesize cholesterol [13]. During the 1950's and 60's, scientists elucidated the pathway by which a 2-carbon acetate precursor is converted to a 27-carbon cholesterol with 4 conjoined rings and an 8-carbon side

chain. It is now known that cholesterol can be obtained by the body from multiple sources: the sterol can be obtained from the circulation via metabolism of low density lipoproteins, synthesized *de novo* from acetyl-coenzyme A, or obtained from dietary sources. When cells require lipids such as sterols and fatty acids, sterol regulatory element binding proteins (SREBPs) transcriptionally activate a cascade of enzymes required for endogenous lipid synthesis. Cholesterol synthesis occurs in almost all cells with the liver accounting for as much *de novo* cholesterol synthesis as all extrahepatic tissues combined. Cholesterol is synthesized in the endoplasmic reticulum (ER) and cytoplasm from acetyl-CoA through the mevalonate pathway [1], which as noted above splits after lanosterol into the Bloch and Kandutsch-Russell pathways. In order to prevent the accumulation of excess cholesterol in the plasma and intracellular membranes, cholesterol is converted to cholesteryl esters, highly insoluble hydrophobic molecules stored in lipid droplets [14].

In addition to serving as a major structural lipid of the plasma membrane, cholesterol is a precursor for the synthesis of metabolites such as bile acids, steroids, and fat-soluble vitamins. The breakdown pathways of cholesterol are of equal physiological importance to the supply pathways. Cholesterol is converted into bile acids in the liver, which are ampipathic polar compounds that function as signaling molecules and as detergents. The synthesis of bile acids is the major pathway of cholesterol breakdown and accounts for ~90% of cholesterol removal. This pathway involves at least 16 different enzymes and can be divided into two major pathways, the classic/neutral pathway and the alternative/acidic pathway [15]. Conversion into bile acids involves multiple hydroxylations of the ring structures of the starting cholesterol molecule and the oxidation and shortening of the side chain to produce a C_{24} bile acid. More minor routes of cholesterol disposal include the conversion of cholesterol into steroid hormones by endocrine tissues, the synthesis of oxysterols by the lung and brain, which are ultimately

converted into bile acids via the alternate pathway, and the chemical and enzymatic conversion of 7-dehydrocholesterol into activated vitamin D_3 by the skin, liver, and kidneys.

Oxysterol Enzymes in the Alternate Pathway of Bile Acid Synthesis

Bile acid biosynthesis is initiated and controlled by a liver-specific enzyme, cholesterol 7α-hydroxylase (CYP7A1), which converts cholesterol to 7α-hydroxycholesterol (Figure 2). This reaction represents the first and rate-limiting step in the classic pathway of bile acid synthesis, which is the predominant pathway under normal physiological conditions. Approximately 400 to 600 mg of cholesterol are converted into bile acids through this pathway on a daily basis by the human liver. Humans lacking cholesterol 7α-hydroxylase as a result of an inherited mutation in the *CYP7A1* gene have significant elevations of total and LDL cholesterol levels in the plasma, accumulation of cholesterol in the liver, and a decreased rate of bile acid excretion [16].

When the classic pathway of bile acid synthesis is suppressed, the alternate pathway of bile acid synthesis becomes the major route for the synthesis of bile acids. Under normal conditions, this pathway is initiated for the most part in extrahepatic tissues and accounts for a daily elimination of 18 to 20 mg of cholesterol. The alternate pathway complements reverse cholesterol transport from the peripheral tissues to the liver via high density lipoprotein (HDL) and is initiated by one of three enzymes. A ubiquitously expressed sterol 27-hydroxylase (CYP27A1) that converts cholesterol to 27-hydroxycholesterol via direct hydroxylation on the side chain at the C_{27} position. CYP27A1 is a polyfunctional enzyme and in addition to hydroxylation of cholesterol in extrahepatic tissues, also hydroxylates bile acid intermediates and vitamin D_2 and D_3 in the liver. This enzyme is an unusual cytochrome P450 in that it catalyzes multiple oxidation reactions at carbon-27 of sterol substrates. The first reaction is a hydroxylation event, followed by oxidation of the hydroxyl to an aldehyde and thereafter to a

carboxylic acid. The importance of this enzyme is reflected in the finding that inherited mutations in the coding gene (*CYP27A1*) cause a disease known as cerebrotendinous xanthomatosis (CTX), which is characterized by abnormal synthesis of bile acids and the accumulation of cholesterol and other sterols (chiefly cholestanol) in multiple tissues [17].

A second source of oxysterol substrates for the alternate pathway of bile acid synthesis is found in the brain and involves the metabolism of cholesterol to 24*S*-hydroxycholesterol by cholesterol 24-hydroxylase, another member of the cytochrome P450 family of enzymes (CYP46A1). Cholesterol 24-hydroxylase converts cholesterol, a non-polar membrane lipid, to 24*S*-hydroxycholesterol, an itinerant polar oxysterol that diffuses from the brain and is metabolized by the liver. This conversion represents a major pathway of cholesterol turnover in the vertebrate brain as cholesterol itself is unable to traverse the blood brain barrier. Cholesterol 24-hydroxylase is a highly conserved cytochrome P450 that is expressed in large, metabolically active neurons of the brain such as pyramidal cells of the hippocampus and cortex and Purkinje cells of the cerebellum [18]. The enzyme is found in the endoplasmic reticulum, which extends throughout neuronal cell bodies and dendrites. Disruption of the mouse cholesterol 24-hydroxylase gene causes an ~50% decrease in cholesterol turnover, which is compensated for by an equivalent decrease (~50%) in the rate of *de novo* cholesterol synthesis, but no changes in the steady-state cholesterol pool in this or any other organ. The decrease in cholesterol synthesis reduces the flow of metabolites through the biosynthetic pathway, producing a codominant phenotype as observed in the mouse model. Cholesterol 24-hydroxylase knockout mice are deficient in spatial, associative, and motor learning, and have abnormal hippocampal long-term potentiation (LTP). The defect in LTP can be reversed by geranylgeraniol, a polyisoprenoid end-product of the cholesterol biosynthetic pathway. Geranylgeraniol acts quickly and specifically to restore LTP in hippocampal slices [19]. The striking phenotype observed in *Cyp46a1* knockout mice raises several questions, including 1)

are there naturally-occurring mutations in the human cholesterol 24-hydroxylase gene, and if so, what are their clinical consequences? 2) Do these mutations generate a codominant phenotype as observed in the mouse model? 3) Are there compensatory mechanisms that protect against mutations in *CYP46A1*?

After crossing the blood brain barrier, 24*S*-hydroxycholesterol is taken up by lipoprotein particles in the serum and transported to the liver for further processing. In the liver, an oxysterol 7α-hydroxylase (CYP39A1) hydroxylates the metabolite at the 7α position, a hallmark feature of most mammalian bile acids. No mutations that disrupt the *CYP39A1* gene in either humans or mice are known to exist. After 7α-hydroxylation, bile acid intermediates in both the classic and alternate pathways are metabolized by 3β-hydroxy-Δ^5-C_{27} steroid oxidoreductase (HSD3B7). Mutations in *HSD3B7* eliminate bile acid synthesis and cause liver failure in humans and mouse models [20, 21].

Cholesterol 25-hydroxylase (CH25H) represents a third source of oxysterols for the alternate pathway of bile acid synthesis. 25-hydroxycholesterol was first shown to suppress cholesterol synthesis in cultured cells and later it was found that 25-hydroxycholesterol interferes with the activation of transcription factors (SREBPs) that regulate the expression of genes involved in fatty acid and cholesterol synthesis [22]. It is now known that 25-hydroxycholesterol is a cholesterol metabolite that is produced and secreted by macrophages and dendritic cells in response to Toll-like receptor (TLR) activation. This oxysterol has potent and wide-ranging effects in the immune system that include suppressing the production of immunoglobulin A (IgA) by B cells, directing the migration of activated B cells in the germinal follicle, and controlling the differentiation of monocytes into macrophages [23]. The synthesis of 25-hydroxycholesterol is catalyzed by the enzyme cholesterol 25-hydroxylase, which uses cholesterol and molecular oxygen as substrates and NADPH as a cofactor. *CH25H*, the gene encoding cholesterol 25-hydroxylase, is present in a majority of vertebrate species but absent

from lower organisms such as yeast and flies. *Ch25h* is expressed at low levels in the mouse lung, heart and kidney, but not in tissues involved in fatty acid and cholesterol synthesis, such as the liver underscoring a role for the enzyme outside of lipid metabolism (i.e., in the immune system). In support of this function, 25-hydroxylase knockout mice regulate fatty acid and cholesterol metabolism normally [24].

Human Sterolomics

The goal of my graduate work has focused on understanding the roles of sterols, oxysterols, and secosteroids in a human cohort. To achieve this goal, a mass-spectrometry based analytical method first had to be developed that allows for the quantitation and detection of sterols in human serum. After the development of a semi-high-throughput, repeatable, reliable method, 22 sterols, oxysterols, and secosteroids routinely found in human plasma were measured in a well characterized population cohort of 3,230 individuals, the Dallas Heart Study 2 [25]. Once all of the analytes were measured in our cohort, sterol-sterol correlation analyses and linkage analyses were performed to identify genetic determinants of human serum sterol levels using targeted and untargeted approaches. Finally, upon identification of variant alleles in genes that correlated to sterol levels, variants were recreated in an expression vector encoding normal enzyme and *in vitro* biochemical analyses were performed to understand the metabolic consequences of the variant allele.

To develop a mass-spectrometry based analytical method, several factors had to be overcome in order to measure and detect a spectrum of sterols ranging from non-polar sterols to polar tri-hydroxy oxysterols. The analytical challenges we were faced with due to the insolubility of sterols in human plasma, the sequestration of sterols within lipoproteins, the existence of sterols in free and esterified forms, and the dramatic differences in levels of

individual sterols were addressed and overcame in this modified-Bligh-Dyer extraction method. Using a streamlined extraction procedure and a combination of LC-MS-ESI, LC-MS-APCI, and GC-MS, this method can detect 60 sterols from a single extraction of 200 μL of plasma. This method was applied to quantify sterols in 3,230 samples derived from clinically well-characterized subjects participating in the Dallas Heart Study, a multi-ethnic, genetically diverse population apart of a longitudinal study whose genomic DNAs and clinical histories are maintained in a relational database on campus. Large intra-individual variation was detected in the serum levels of approximately 22 of the 60 sterols assessed.

Sterol-sterol correlation analyses revealed numerous statistically significant associations between sterols. Levels of dietary plant sterols such as sitosterol, campesterol, and stigmastanol correlated with each other as expected given that these sterols are substrates for the ABCG5/ABCG8 transporter, which is responsible both for their absorption from the diet in the gut and for their excretion from the liver. Unexpected correlations were also identified: serum levels of the cholesterol biosynthetic intermediate 14-desmethylanosterol was shown to correlate with plant sterols suggesting an exogenous dietary origin for serum 14-desmethylanosterol and that this sterol is an ABCG5/ABCG8 substrate. These suggestions are supported by the absence of correlations between 14-desmethylanosterol and those of other intermediates in the cholesterol biosynthetic pathway such as lanosterol and lathosterol. Additional sterol-sterol correlations detected among cholesterol biosynthesis intermediates may reflect the common regulation of this pathway by sterol regulatory element binding protein (SREBP) transcription factors.

Targeted and untargeted approaches were taken to identify genes underlying the observed variation in 22 of the 60 sterols measured. In the targeted approach, advantage was taken of the fact that the substrates and products of many sterol metabolizing enzymes are known and thus direct sequencing of the corresponding genes in subjects with very high (above the 95th

percentile) or low (below the 5th percentile) levels of the sterol in question was performed. In the untargeted approach, the 3,230 individuals whose DNAs were genotyped for 9,229 non-synonymous sequence variations in multiple human genes revealed statistically significant associations ($P < 10^{-5}$) of SNPs that resulted in an increase or decrease in sterol levels. Three SNPs were found to be in high linkage to levels of sterols: SNP rs2277119, in *CYP39A1* was associated with increased levels of 24*S*-hydroxycholesterol ($P = 2.18 \times 10^{-27}$), SNP rs751141, in *EPHX2* was found to be associated with increased levels of 24,25-epoxycholesterol ($P = 9.46 \times 10^{-25}$) and SNP rs6564956, in *SDR42E1* was associated with decreased levels of 8-dehydrocholesterol ($P = 1.51 \times 10^{-15}$).

We are particularly interested in 24*S*-hydroxycholesterol, 8-dehydrocholesterol, and 24,25-epoxycholesterol for the following reasons: 24*S*-hydroxycholesterol as mentioned, is a unique oxysterol synthesized in the brain and transported to the liver as a means of reverse cholesterol transport and to maintain cholesterol homeostasis in the brain. Mutation of the cholesterol 24-hydroxylase gene in the mouse disrupts cholesterol synthesis and turnover in the brain and results in a learning phenotype. No human mutations exist in the gene encoding the enzyme that synthesizes 24*S*-hydroxycholesterol in the brain, cholesterol 24-hydroxylase (CYP46A1), or the gene encoding the enzyme that converts 24*S*-hydroxycholesterol to 7α,24-dihydroxycholesterol in the liver, oxysterol 7α-hydroxylase (CYP39A1). I have identified mutations in *CYP39A1* and have performed additional genetic and functional studies to determine the effect of the encoded variants on CYP39A1 enzymatic activity and subsequently, levels of 24*S*-hydroxycholesterol.

24,25-epoxycholesterol has a unique origin; this oxysterol is synthesized in a shunt pathway tangential to the cholesterol biosynthetic pathway. It is hypothesized that 24,25-epoxycholesterol is produced to help maintain cholesterol homeostasis in the serum. The presence of the oxysterol in the plasma acts as an indicator for total cholesterol levels and when

in excess, binds to transcription factors SREBPs causing cholesterol synthesis to cease. 24,25-epoxycholesterol is also able to bind and activate liver X receptors, which are important regulators of cholesterol, fatty acid, and glucose homeostasis [26]. While the biosynthesis of 24,25-epoxycholesterol is well characterized, little is known about the catabolism of this metabolite. In the current studies, a missense mutation in the epoxide hydrolase 2 (*EPHX2*) gene resulting in an arginine to glutamine at codon 287 was found to be associated to increased levels of 24,25-epoxycholesterol. The biological function of this enzyme is well characterized; EPHX2 is known to convert epoxide-containing compounds into diols, which are less toxic and easier to excrete.

Correlation analyses between sterols revealed a strong, positive linear relationship between levels of 7-dehydrocholesterol and 8-dehydrocholesterol ($r = 0.65$). Much is known about the metabolism of 7-dehydrocholesterol; however, the biological function and role of 8-dehydrocholesterol is unknown. 7-dehydrocholesterol is a key intermediate of the Kandutsch-Russell pathway of cholesterol biosynthesis and necessary for cholesterol synthesis in the skin, kidney, and liver. Mutations in Δ7-Sterol reductase, *DHCR7*, encoding the enzyme that converts 7-dehydrocholesterol to cholesterol, result in Smith-Lemli-Opitz syndrome, a disorder of cholesterol biosynthesis resulting in mental retardation and with an incidence rate of 1 in 60,000 births. In the skin, 7-dehydrocholesterol is also converted into vitamin D_3 by UV radiation present in sunlight. Both 7- and 8-dehydrocholesterol accumulate in Smith-Lemli-Opitz patients [26, 27], which raises the following question: Is the formation of 8-dehydrocholesterol catalyzed by an enzyme that isomerizes the double bond in the B-ring of 7-dehydrocholesterol? In attempting to answer this question, I identified a polymorphism in the *SDR42E1* locus, which encodes short-chain dehydrogenase/reductase family 42E member 1, and found that this alteration was correlated to decreased levels of 8-dehydrocholesterol in a population cohort.

Figure 1. Schematic of cholesterol synthesis. Arrows indicate the flow of intermediates.

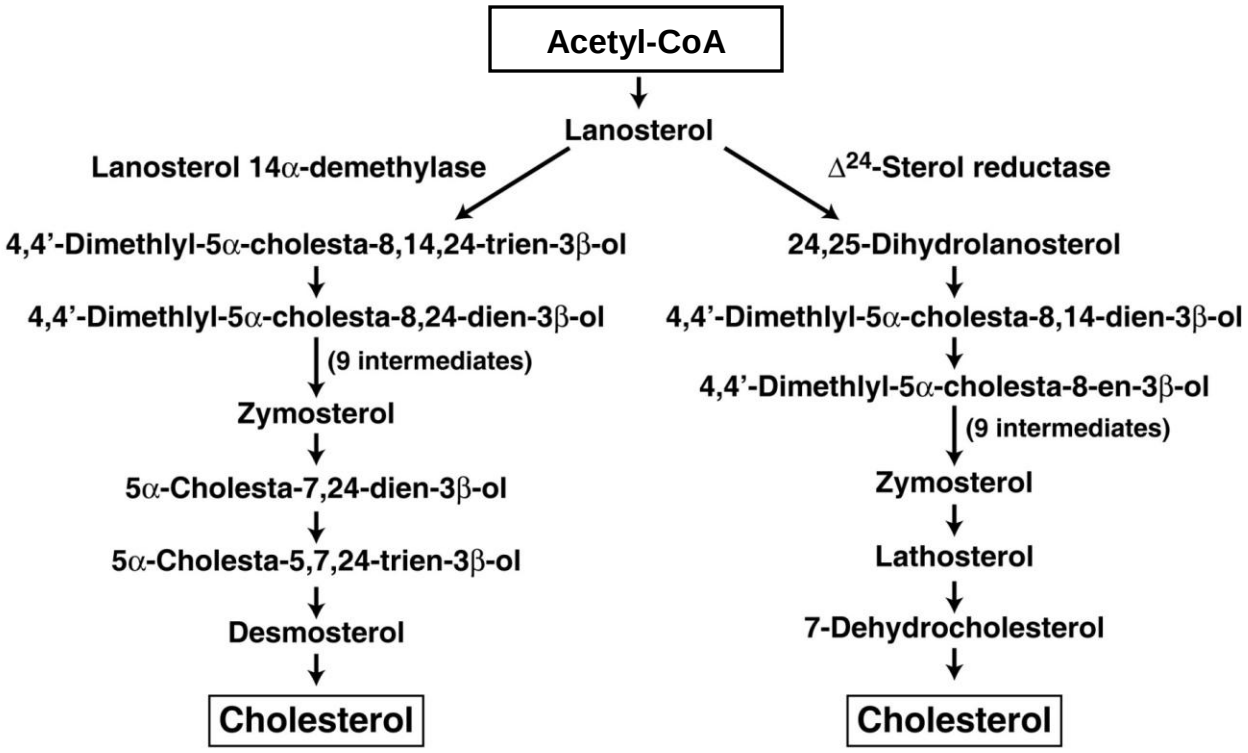

Bloch Pathway

Kandutsch-Russell Pathway

Figure 2. Enzymes in the bile acid synthetic pathway. Arrows indicate the flow of intermediates. Phenotypic consequences of mutations in genes in the bile acid synthetic pathway described in mouse and human. *Blue,* no described phenotype from mutations in humans.

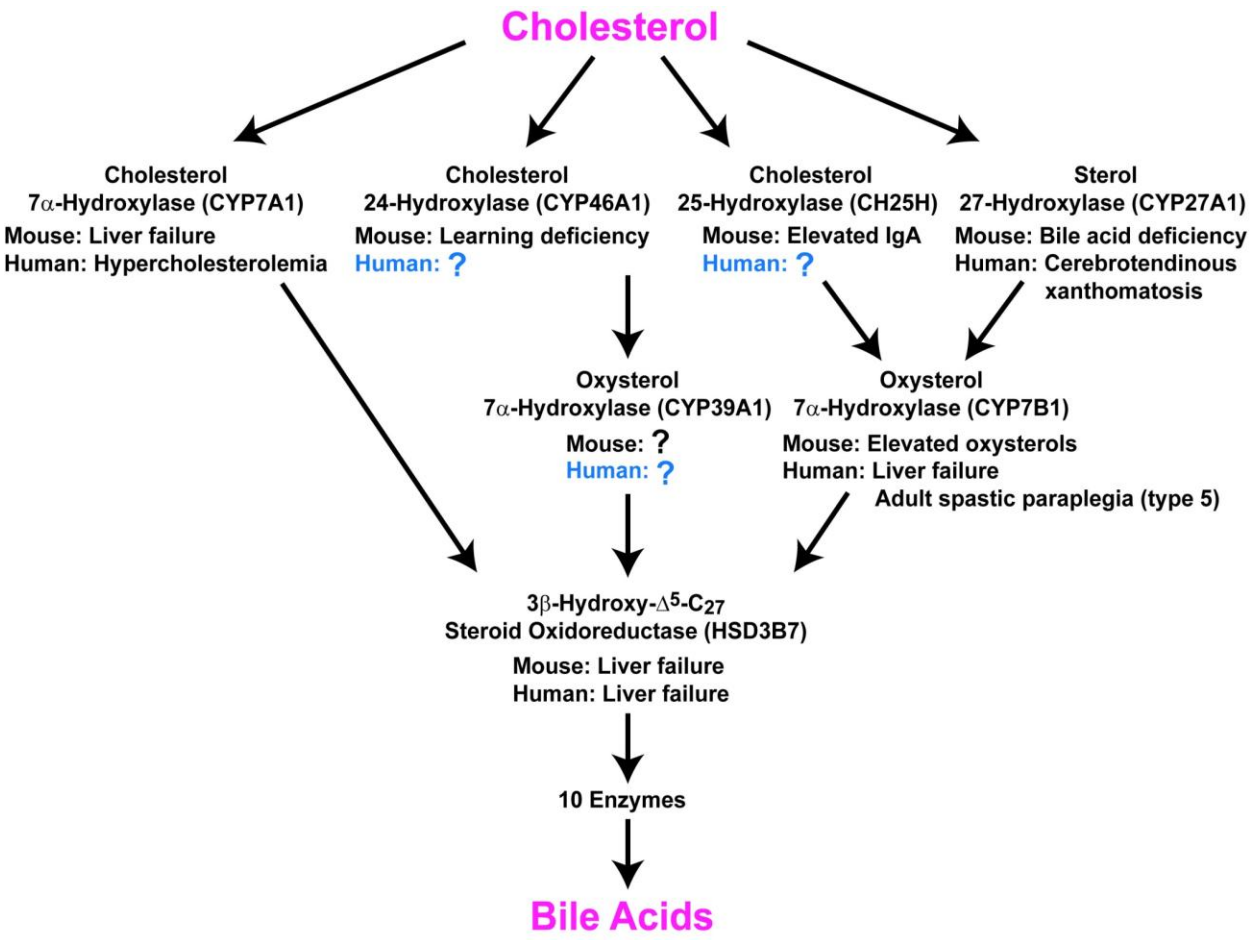
Cholesterol
Cholesterol
7α-Hydroxylase (CYP7A1)
Mouse: Liver failure
Human: Hypercholesterolemia
Cholesterol
24-Hydroxylase (CYP46A1)
Mouse: Learning deficiency
Human: ?
Cholesterol
25-Hydroxylase (CH25H)
Mouse: Elevated IgA
Human: ?
Sterol
27-Hydroxylase (CYP27A1)
Mouse: Bile acid deficiency
Human: Cerebrotendinous xanthomatosis
Oxysterol
7α-Hydroxylase (CYP39A1)
Mouse: ?
Human: ?
Oxysterol
7α-Hydroxylase (CYP7B1)
Mouse: Elevated oxysterols
Human: Liver failure
Adult spastic paraplegia (type 5)
3β-Hydroxy-Δ5-C27
Steroid Oxidoreductase (HSD3B7)
Mouse: Liver failure
Human: Liver failure
10 Enzymes
Bile Acids

CHAPTER TWO:

A Comprehensive Method for Extraction and Quantitative Analysis of Sterols and Secosteroids from Human Plasma

We describe the development of a method for the extraction and analysis of 62 sterols, oxysterols, and secosteroids from human plasma using a combination of high-performance liquid chromatography-mass spectrometry (HPLC-MS) and gas chromatography-mass spectrometry (GC-MS). Deuterated standards are added to 200 μL of human plasma. Bulk lipids are extracted with methanol:dichloromethane (MeOH:DCM), the sample is hydrolyzed using a novel procedure, and sterols and secosteroids are isolated using solid-phase extraction. Compounds are resolved on C_{18} core-shell HPLC columns and by gas chromatography (GC). Sterols and oxysterols are measured using triple quadrupole mass spectrometers and lathosterol is measured using GC-MS. Detection for each compound measured by HPLC-MS was ≤ 1ng/mL of plasma. Extraction efficiency was between 85 and 110%; day-to-day variability showed a relative standard error of <10%. Numerous oxysterols were detected including the side chain oxysterols 22-, 24-, 25-, and 27-hydroxycholesterol, as well as ring-structure oxysterols 7α- and 4β-hydroxycholesterol. Intermediates from the cholesterol biosynthetic pathway were also detected and included zymosterol, desmosterol, and lanosterol. This method also allowed the quantification of six secosteroids, including the 25-hydroxylated species of vitamins D_2 and D_3. Application of this method to plasma samples revealed that at least 50 samples could be extracted in a routine day.

INTRODUCTION

Sterols play essential roles in the physiological processes of virtually all living organisms. Members of this lipid class are integral building blocks in the cellular membranes of animals and have important functions in signaling, regulation, and metabolism [28]. To date, the majority of studies have focused on cholesterol, the most abundant sterol in mammals that serves as both a precursor and product to a host of important molecules including steroid hormones, bile acids, oxysterols, and intermediates in the cholesterol biosynthetic pathway [3, 29, 30]. While cholesterol has gained significant notoriety due to the compound's negative impact on health, other sterols, such as plant-derived phytosterols, are thought to offer potential human health benefits by lowering circulating cholesterol levels [31, 32].

Novel functions for sterols and secosteroids continue to be identified. For example, the cholesterol metabolites 25-hydroxycholesterol and 7α,25-dihydroxycholesterol have recently been shown to play important signaling roles in the immune system [4, 33, 34]. 24*S*-hydroxycholesterol has been shown to be involved in cholesterol turnover in the brain which plays a role in memory [35] and glucose metabolism [36]. Alterations in vitamin D_3 levels arising from the lack of sun exposure and/or use of sunscreen are postulated to have a negative impact on health [37, 38]. These findings together with the large number of sterols suggest that there may be undiscovered roles for sterols in biology and they highlight the need for continued research into the biochemical pathways associated with these compounds.

The extraction and analysis of sterols in human plasma presents a unique challenge due to their virtual insolubility, sequestration within lipoproteins, and dramatic differences in the levels of individual sterols. Cholesterol is the most abundant sterol, with circulating levels on the order of 1 to 3 mg/mL, whereas 25-hydroxycholesterol is a million-fold less abundant at 1-3 ng/mL [39, 40]. The circulating form of sterols in humans is primarily as steryl esters in which a fatty acid is esterified to carbon 3 of the sterol; however, a small variable percentage of free sterols also exist. Enzymatically formed oxysterols are typically between 59 to 91% esterified [40].

This duality poses additional analytical challenges as free versus esterified sterols must either be isolated or measured separately or steryl esters must first be converted to free sterols. Other lipids, such as triglycerides, phospholipids, and sphingolipids that are present in the plasma at concentrations similar to cholesterol further confound the analysis of sterols.

Traditionally, the extraction of sterols has relied on two classic methods, the Bligh/Dyer or Folch extraction methods [41, 42]. Both make use of a mixture of chloroform and methanol to simultaneously disrupt lipoproteins and solubilize lipids. An alkaline hydrolysis step is employed to cleave sterol-fatty acid conjugates; a strong base in alcohol is added to the extract, which is then often incubated at room temperature, or elevated temperature (60 – 100 °C) for 1-2 hours [43-45]. Hydrolysis also serves to degrade other abundant lipid classes such as triglycerides and phospholipids, which reduces sample complexity. Alternatively, if the goal is to measure only free, unesterified sterols, the alkaline hydrolysis step is eliminated. Lastly, solid phase extraction (SPE) is utilized to isolate sterols from other components. Ideally, cholesterol could be isolated from the sample as it would simplify subsequent instrumental analysis of other less abundant sterol species; however, SPE does not yet have the inherent resolution or reproducibility to quantitatively isolate cholesterol from all other sterols [43, 46]. Although many variations of these extraction procedures have been reported in the literature, the fundamental steps of the various methods are the same.

Instrumental analysis of sterols and related compounds in plasma has typically focused on either a single analyte or a limited group of analytes. Historically, these methods have employed GC and GC-MS for the analysis of select sterols [43, 47, 48]. GC and GC-MS have limitations with regard to sample composition, injection volume, sensitivity, and mass spectral scanning functions. Despite these limitations, GC and GC-MS are still widely used for sterol analysis due to their chromatographic resolving capacity, ease of use, and relative low cost of the acquisition and operation of the instruments.

Recently, methods have been developed for sterol analysis using LC-MS [49-51]. Like GC and GC-MS, these methods are typically optimized for the detection of one or two analytes. In 2007, our laboratory described a method for analyzing a diverse group of sterols and oxysterols using LC-MS [46]. The method was optimized for detection of 12 common sterols and oxysterols in a single extraction. Since then, high performance liquid chromatography (HPLC) has become more widely used in the analysis of sterols and is often coupled to triple quadrupole mass spectrometers for quantitative analysis to enhance sensitivity and selectivity. Similarly, improvements in ionization and ion transfer into the mass spectrometer have enhanced the ability to measure low-level metabolites in biological systems.

Here we report a method for the quantitative analysis of sterols, oxysterols, and secosteroids in plasma. Using a streamlined extraction procedure and a combination of LC-MS (electrospray ionization and atmospheric pressure chemical ionization), this method allows for the analysis of approximately 60 sterols from a single extraction of 200 µL of plasma. The extraction procedure is flexible and can be tailored to sample type and information sought. Since many sterols are positional isomers, chromatographic resolution remains crucial for the analysis of sterols and related compounds as the mass spectrometer (MS) cannot differentiate between isobaric compounds. The instrumental analysis used in this method employs recent advances in HPLC column technology that provide increased resolution and sensitivity, and the throughput is such that 50 samples can be readily assayed per day. The method lends itself to translational research involving large cohorts of clinically well-characterized patients and can be adapted to serum, tissues, or other biological matrices.

EXPERIMENTAL SECTION

Materials. Human plasma samples were obtained from 200 subjects of The Cooper Institute (Dallas, TX) following protocols approved by the Institutional Review Board of the University of Texas Southwestern Medical Center. Written consent was obtained from each patient prior to

sample collection. Pooled normal human plasma was purchased from Innovative Research, (Novi, Michigan) for use as a control sample. Primary and deuterated sterol and secosteroid standards were obtained from Avanti Polar Lipids (Alabaster, AL) unless otherwise noted. A complete list of analytes is given in Table 1. Dichloromethane (DCM) and hexane were from Burdick & Jackson (Honeywell; Morristown, NJ), methanol (MeOH), chloroform ($CHCl_3$), acetonitrile (ACN), and water were from Fisher Scientific (Fair Lawn, NJ). Dulbecco's phosphate-buffered saline (DPBS) was from Mediatech (Manassas, VA). Ammonium acetate (NH_4OAc) and butylated hydroxytoluene (BHT) were from Sigma-Aldrich (St. Louis, MO), 10N potassium hydroxide (KOH) was from Fisher Scientific, ammonium iodide (NH_4I) was from Acros Organics (Geel, Belgium) and *N*-methyl-*N*-*tert*-butyldimethylsilyl trifluoroacetamide with 1% *tert*-butyldimethylchlorosilane (MTBSTFA with 1% TBDMCS) was from Restek (Bellefonte, PA). All solvents were HPLC-grade or better; all chemicals were ACS-grade or better.

Extraction, Hydrolysis, and Isolation of Sterols and Secosteroids from Human Plasma.

Frozen plasma samples (stored at -80 °C) were equilibrated to room temperature for approximately 30 min. To ensure homogeneity, each sample was pipetted 3 times with a 1-mL air-displacement pipette (fitted with a disposable 1-mL barrier tip). 200 µL of plasma were then added drop-wise to 3 mL of 1:1 DCM:MeOH in a 16 × 100 glass tube placed in a 30 °C ultrasonic bath. The tube also contained 20 µL of a deuterated sterol and secosteroid standard cocktail and BHT at 50 µg/mL (see Supplemental Material for standard amounts). The tube was flushed with N_2 for several seconds to displace oxygen, sealed with a PTFE-lined screw cap, and incubated at 30 °C in the ultrasonic bath for 10 min. Following incubation, the sample was centrifuged at 3500 rpm for 5 min at 25 °C to pellet protein and other insoluble material. The supernatant from each sample was decanted into a 16 × 100 mm glass screw-cap tube and set aside. A 1:1 DCM:MeOH solution (3 mL) was added to the pelleted material, the tube capped, and vigorously agitated until the pellet was dislodged and disrupted. The sample was then

centrifuged at 3500 rpm for 5 min at 25 °C and the resulting supernatant decanted back into the tube containing the supernatant from the initial extraction.

Hydrolysis was performed by adding 300 µL of 10N KOH to each tube, flushing with N_2 for several seconds, followed by placement in a water bath at 35 °C for 1.5 hrs. Following hydrolysis, 3 mL of DPBS were added to each sample, the tubes capped, and the samples agitated for several seconds. Samples were centrifuged at 3500 rpm for 5 min at 25 °C. The organic (lower) layer was removed with a 9" Pasteur pipette and transferred to a 16 × 100 glass tube and set aside. DCM (3 mL) was added to the remaining sample, the tube capped, vortexed for several seconds, and centrifuged at 3500 rpm for 5 min at 25 °C. Using a 9" Pasteur pipette, the organic layer (lower layer) was removed and transferred to the 16 × 100 glass culture tube containing the initial sample. To maximize extraction efficiency, the same pipette was used for each liquid-liquid step and the pipette was placed into a separate glass culture tube between steps. Hydrolyzed samples were then dried under N_2 using a 27-port drying manifold (Pierce; Fisher Scientific, Fair Lawn, NJ).

Sterols and secosteroids were isolated using 200 mg, 3-mL aminopropyl solid-phase extraction columns (Biotage; Charlotte, NC). The column was rinsed and conditioned with 2 × 3 mL of hexane. The extracted and dried plasma sample was dissolved in approximately 1 mL of hexane and gently swirled for several seconds. The sample (and any insoluble material) was then transferred to the SPE column using a 6" Pasteur pipette and eluted to waste. The extract tube was rinsed with 1 mL of hexane, gently swirled, and this rinse transferred to the column and eluted to waste. Again, to minimize sample loss, the same Pasteur pipette was used at each step. Following the addition of sample, the column was rinsed with 1 mL of hexane to elute non-polar compounds. Sterols were then eluted from the column with 4.5 mL (1.5 column volumes) of 23:1 $CHCl_3$:MeOH into a new 16 × 100 glass culture tube. The eluted sample was dried under N_2.

To prepare the sample for instrumental analysis, 400 µL of warm (37 °C) 90% MeOH was added and the tube placed in an ultrasonic bath for 5 min at 30 °C. The sample was then transferred to an autosampler vial containing a 500-µL deactivated insert (Restek, Bellefonte, PA) and 20 µL of d6-6α-hydroxycholestanol as an internal standard. If particulate matter was observed in the sample during dissolution, then the vial insert was carefully transferred to a standard microcentrifuge tube using fine-point tweezers and centrifuged at room temperature for 5 min at 6000 rpm in a micro centrifuge. The vial insert was then carefully transferred back to the autosampler vial and stored at room temperature until analysis.

A 50 µL aliquot of the sample was removed and transferred to a new autosampler vial for analysis by GC-MS. The sample was dried under N_2. Derivatization of sterols was performed by adding 100 µL of 1:1 pyridine:MTBSTFA (1%TBDMCS) with 2 mg/mL NH_4I (dissolved first in pyridine), flushing the sample with N_2, capping the vial, and incubation at 70 °C for 30 min. The derivatized sample was dried under N_2, dissolved in 150 µL of hexane, vortexed for 5 min, and stored at room temperature until analysis.

Instrumental Analysis. Quantitative analysis of sterols, oxysterols, and secosteroids was performed using a combination of techniques that included HPLC-MS-APCI, HPLC-MS-ESI, and GC-MS. Oxysterols were analyzed using a tertiary Shimadzu LC-20XR HPLC system (Shimadzu Scientific Instruments, Columbia, MD) equipped with an ultrasonic degasser, column oven and autosampler. The HPLC was coupled to an AB Sciex API-5000 MS equipped with Turbo V ESI source (Foster City, CA). Oxysterols were resolved with a binary solvent gradient using a Kinetex C_{18} HPLC column (150 × 2.1 mm, 2.6 µm particle size; Phenomenex, Torrance, CA). The mobile phases were (A) 70% ACN with 5 mM NH_4OAc (dissolved in water first) and (B) 1:1 IPA:ACN with 5 mM NH_4OAc (dissolved first in IPA for 10-12 hours). Following preparation, mobile phases were allowed to come to thermal equilibrium overnight at 25 °C. After injection of 30 uL of extract, the gradient was started at 0% B and ramped to 100% B over

7 min, held at 100% B for 3 min, and returned to 0% B for a 2 min equilibration. The flow rate was 0.5 mL/min and the column was maintained at 18 °C.

Sterols were analyzed using a binary Shimadzu LC-10ADvp system with a column oven and CTC LC PAL autosampler (Leap Technologies, Carrboro, NC) coupled to an AB Sciex 4000 QTrap mass spectrometer equipped with a Turbo V APCI source. Sterols were resolved with a two-step isocratic elution using a Poroshell 120 SB-C18 HPLC column (150 x 2.1 mm, 2.7 µM particle size; Agilent Technologies, Wilmington, DE). The mobile phases were (A) 96% MeOH with 0.1% acetic acid (AA) and (B) MeOH with 0.1% AA. The autosampler was equipped with a 5-µL injection loop that was loaded with 15 µL of extract. The elution began at 100% A for 7.5 min, increased to 100% B at 8 min, was held at 100% B for 6 min, and returned to 100% A for a 6 min equilibration. The flow rate was 0.4 mL/min and the column was maintained at 30 °C.

Both MS instruments were operated in scheduled multiple-reaction monitoring (SMRM) mode. Transitions for each compound were optimized by flow injection via syringe pump using a representative solvent flow rate of 1:1 A:B for each instrument. MRM transitions for oxysterols in ESI mode were primarily optimized for the ammonium adduct $[M+NH_4]^+$ or the protonated molecular ion $[M+H]^+$ generated through the loss of NH_3. The transitions included the loss of one or more -OH groups as H_2O, depending on the specific compound. Sterols in APCI mode were optimized for either the protonated adduct $[M+H]^+$ or the loss of -OH as H_2O $[M+H-H_2O]^+$. The transition includes a nondescript, low-mass fragment often at *m/z* 81, 95, or 109, although there were several exceptions in which fragments of various masses were generated. A complete list of transitions for sterols and oxysterols and a detailed description of instrument settings and parameters for both HPLC-MS analyses are provided in Supplementary Materials.

Lathosterol was analyzed using an Agilent 7890 GC coupled to an Agilent 5975C mass-selective detector (MSD; Wilmington, DE). The instrument was equipped with a 40-m Agilent J&W DB-5MS column (180 µm i.d., 0.18 µm film thickness; Folsom, CA). The injection port was

maintained at 300 °C and 1 µL injections were performed using splitless conditions with a purge to split vent at 0.5 min. Hydrogen was used as the carrier gas and was generated with a Parker Balston H2PD-150 hydrogen generator (Haverhill, MA) at an average linear velocity of 55 cm/s in constant flow mode. The temperature program began at 150 °C for 1 min, then was ramped at 10 °C/min to 325 °C and held for 6.5 minutes. The transfer line was heated to 300 °C, the ion source to 230 °C and the quadrupole to 150 °C. Electron ionization was used at 70 eV and selected ion monitoring (SIM) was used for data acquisition. A complete description of instrument configuration and settings is provided in Appendices B-D.

Aliquots of plasma were sent to a commercial clinical chemistry laboratory for measurement of total cholesterol.

An extensive and detailed discussion of each step of the extraction and instrumental analysis is provided in Supplementary Material. Here the reader can gain useful tips and tricks as well as read discussion explaining how and why each step of the procedure was implemented.

Quantitation. Integration of areas under elution curves for LC-MS and GC-MS was done using Analyst™ 1.5.1 and Chemstation™ software, respectively. Quantitative values were calculated using isotope dilution and single point calibration through a relative response factor (RRF) calculation. The RRF standard was run at the beginning, middle, and end of each sample set; typically 54 samples per set. Deuterated analogs were not available for every analyte, thus a deuterated compound of similar chemical composition was substituted when necessary. A table of primary compounds and the respective deuterated analog used for quantitation is given in Appendix E.

RESULTS

Chromatography. Reconstructed ion chromatograms (RIC) for standard mixes and extracts of a pooled plasma sample for sterols, oxysterols, and lathosterol are shown in Figure 2*A*-*F*. To improve the clarity of data presented in the figure, deuterated analogs are not included in the RIC's. The chromatographic peaks are labeled alphabetically and correspond to compounds listed in Table 1.

The 22 sterol and sterol-derived compounds routinely detected in plasma by this method are either resolved, or have unique masses that allow them to be uniquely identified by mass spectrometry. Sterols are labeled with capital letters and correspond to labels given in Table 1. Sterols elute between 6.5 and 11.5 min from the HPLC columns. Less polar compounds such as zymosterol and desmosterol elute early (D, E), and methylated sterols such as sitosterol and 24,25-dihydrolanosterol elute later in the chromatogram (T,U). Use of the core-shell HPLC column resulted in chromatographic peak widths on the order of 6-8 sec at full width-half maximum (FWHM). Figure 2*E* depicts the resolution of lathosterol and cholesterol (L and M), respectively by GC-MS; however, in a plasma extract the physiological levels of cholesterol overwhelm the lathosterol signal causing inadequate resolution (Figure 2*F*). In order to maintain a common scale, the cholesterol signal in Figure 2*B* is plotted at 0.1× scale. The split peak shown in Figure 2*B* is not an unresolved lathosterol and cholesterol signal but rather the result of the extreme abundance of cholesterol causing splitting and overload of the HPLC column.

Oxysterols elute between 1.5 to 7.5 min in three general groups as shown in Figure 2*C* and 2*D*. The use of core-shell HPLC columns yielded chromatographic peak widths on the order of 3-6 sec FWHM. Polar hydroxylated sterols such as 7α,27-dihydroxycholesterol (c) elute in the first group between 1.5 and 3 min. The 25-hydroxylated vitamin D_2 and D_3 (i, j) compounds elute with the side-chain oxysterols 24-, 25-, and 27-hydroxycholesterol (l, m, o) between 4 and 5.5 min. The least polar compounds, ring structure oxysterols such as 7α- and 4β-hydroxycholesterol (x, *k*), elute in the third group between 5.5 and 7.5 min.

The known enzymatically formed oxysterols are resolved from other isobaric species with several exceptions, the first being the separation of 7α- and 7β-hydroxycholesterol. Previous work has shown that 7β-hydroxycholesterol is present in human plasma at approximately 10% of the level of 7α-hydroxycholesterol [39]. While the two compounds can be resolved by GC-MS, we were not able to resolve them with the HPLC parameters described here; therefore, the values for 7α-hydroxycholesterol include any 7β-hydroxycholesterol present in the sample. The second set of co-eluting compounds of biological importance are 8,(14)-dehydrocholesterol and 7,(8)-dehydrocholesterol. The origins of 8,(14)-dehydrocholesterol are not well understood, and it is unclear if the compound is present in our samples. Thus, 7,(8)-dehydrocholesterol may include unknown quantities of 8,(14)-dehydrocholesterol. The third set of co-eluting compounds is 24,25-dihydrolanosterol and an unknown compound. 24,25-dihydrolanosterol is poorly resolved and is further complicated by the very low signal level observed in most of the human plasma samples analyzed here. The unknown compound has an isobaric signal, elutes after 24,25-dihydrolanosterol, and with manual integration a reasonable estimate of the peak area can be achieved. The fourth set of co-eluting compounds is composed of 20-hydroxycholesterol and 15α-hydroxycholestenone. The origin of these compounds is poorly understood. Their co-elution does not appear to be of major significance as in the 200 plasma samples analyzed here, only trace-level signals were detected for their MRM pairs corresponding to the correct retention time.

Due to the similar structures of lathosterol (J) and cholesterol ($\Delta^{7,8}$ versus $\Delta^{5,6}$) and considerably disparate concentration levels (cholesterol is 1000× more abundant), the HPLC method used to resolve sterols does not sufficiently separate lathosterol from cholesterol; however, the GC-MS method described herein is able to resolve lathosterol from cholesterol (Figure 2*E* and 2*F*). Separation is accomplished through the use of hydrogen as a carrier gas in

conjunction with a very high resolving column. A chromatographic signal for lathosterol is produced with a peak width of 2 sec at FWHM.

Mass Spectrometry. Representative mass spectra for selected sterols, oxysterols, and secosteroids are shown in Figure 3. Examples, including 7α,27-dihydroxycholesterol, 25-hydroxyvitamin D_3, and 7α-hydroxycholesterol ionized under electrospray conditions are shown in Figures 3*A-C*. The oxysterols are neutral and ionize poorly with electrospray alone; ammonium acetate is added to the mobile phase, which results in the formation of readily detectable ammonium adducts. All oxysterols show common features of ionization and fragmentation with collision-induced dissociation (CID) using mild collision energies (10-20 V). These features arise from both in-source decay and during CID. Mass spectral features common to most oxysterols include an ammonium adduct at $[M+18]^+$, a protonated ion at $[M+18-NH_3]^+$, and ions derived from sequential losses of 17 and 18 mass units for each alcohol group depending on the specific compound. Due to the 4-ring structure and isooctyl side chain found in all oxysterols (Figure 1), no unique mass spectral information was obtained for isomeric compounds using CID. High-energy CID (50-60 V) yielded a heavily fragmented collision spectrum consisting of methylene groups spaced 14 mass units apart with no unique mass spectral information. For quantitative purposes it was determined that mild CID conditions yielded better oxysterol signal intensity in conjunction with MRM.

Respective mass spectra for two sterols, desmosterol and lanosterol, are shown in Figures 3*D-E*. Like oxysterols, sterols are neutral but they are less polar and therefore more efficiently ionized by APCI. The pseudo-molecular ion formed for most sterols is the loss of the alcohol group as water at $[M+H-H_2O]^+$. Because the pseudo-molecular ion is a result of water loss, there are no additional alcohols to dissociate under mild CID conditions as with the oxysterols. Therefore, a high energy CID is used (e.g., 50-60 V) to generate a heavily fragmented collision spectrum. For quantitation, the MRM transition was typically the pseudo-molecular ion and the

most intense fragment ion, usually *m/z* 81, 95, or 109. Additional sterol mass spectra can be found at http://www.lipidmaps.org.

The electron ionization mass spectrum for MTBSTFA-derivatized lathosterol is shown in Figure 3*F*. The base peak is observed at *m/z* 443 resulting from the loss of the isopropyl group at $[M-57]^+$. A smaller signal is also present at *m/z* 367, which arises from the loss of the entire MTBS group with the oxygen at the C_3 position along with an additional unsaturation forming at an unknown location in the sterol molecule. The signal at *m/z* 443 was monitored with SIM for quantitation.

QA/QC. The recovery of sterols, oxysterols, and secosteroids from the solvent spike QC sample showed that for the 10 oxysterols reported in Table 2, recovery was between 99.6% and 109%, indicating virtual complete recovery. The nine sterols detected had a slightly wider recovery range between 94.6% and 111% with the exception of 7-dehydrocholesterol at 85%. The solvent spike gives an accurate measure of the extraction efficiency across a wide concentration range of sterols; however, this standard does not represent the complex chemical matrix found in a human plasma sample. Interference from this matrix may cause artificially high or low values due to chromatographic, ionization, or mass spectral issues.

To better assess the recovery of sterols from a plasma sample, we added one deuterated internal standard to the autosampler vial prior to transferring the final extract. This addition allowed the recovery of deuterated surrogates in each sample to be determined. We quantified the recovery of four representative compounds that cover the range of oxysterols analyzed. The recovery for (d6) 1,25-hydroxyvitamin D_3, (d6) 27-hydroxycholesterol, (d6) 7α-hydroxycholesterol, and (d6) 4β-hydroxycholesterol ranged from 87.9 to 100.8% (Table 3). These values, combined with solvent spike recoveries, show that this extraction procedure is both thorough and robust with excellent recovery values. Additionally, the final dissolution of the

purified dried extract is done in a single step with no additional rinsing. A second rinse step would cause undesired dilution of the final extract.

With each batch of 50 samples extracted, an aliquot of a commercially obtained, pooled plasma sample was analyzed to monitor and evaluate day-to-day variation in measurements. As seen in Table 2, reproducibility was excellent across extractions done on six different days. The relative standard errors (RSE) for oxysterols ranged between 1.4 to 10.6 for known enzymatically formed oxysterols with higher RSE's of 13.5% and 18.3% for two compounds that are potentially formed through oxidation and may be partially degraded during base hydrolysis, 24-, and 7-oxocholesterol. The RSE's for sterols in pooled plasma have less variability and ranged between 0.6 and 3.9%; however, all sterols reported here are enzymatically formed and none are oxidation products or known to be susceptible to base hydrolysis. Included in Table 2 are data from analysis of the NIST human plasma standard reference material (SRM) for use as a reference [40], and for comparison against the commercially obtained pooled plasma used in this study.

The solvent blank that was included with each batch of 50 samples did not show a response for any compound measured here. Therefore, there was no evidence of carryover, cross-contamination, or isobaric interferences originating from the sample extraction.

The instrument detection limit (IDL) was estimated at ≤ 50 pg on-column for each compound. The method detection limit (MDL) for each compound was estimated at ≤ 1 ng/mL. Detector response was linear over at least four orders of magnitude from the instrument detection limit.

Results from Cooper Institute Cohort. Quantitative results for a representative set of sterols from 200 human plasma samples are shown in Table 2. The data include average, median, standard deviation, and range of concentrations measured. For reference and comparison, the

results from the commercially obtained pooled plasma used as a QA/QC sample and the results from the previously analyzed NIST SRM plasma are included [40]. Lastly, the solvent spike recovery value is provided showing one metric of our quality control scheme. In Table 3, the recoveries of four representative deuterated oxysterol standards are shown.

DISCUSSION

Data. The dataset provided herein includes all compounds that were routinely detected in the 200 samples analyzed from the Cooper Institute. We assayed for approximately 60 compounds, but only a subset of 22 compounds was routinely detected. Not included in these data are values obtained for most known oxidation products, such as the 5/6(α/β)-epoxycholesterols [52] due in part to problems with the primary standard or deuterated analog, which have been subsequently resolved. Table 2 provides values for 25-hydroxyvitamin D_3 and a select group of sterols and oxysterols measured in the 200 samples. These data were acquired using methods described here, but it should be noted that quantitative values for some compounds may vary depending on specific extraction procedures employed. This method combines techniques from previously published work as well as novel aspects developed in our laboratory. The intent of this work was in part to develop a robust extraction procedure that generated values consistent with those in the literature and was capable of a reasonable throughput so it could be applied to large human cohorts. It is optimized towards enzymatically formed sterols with secondary thought given to oxidation products of cholesterol. Investigators wishing to target these oxidation products may consider alternative extraction procedures.

Comparison of the data obtained from the Cooper Institute cohort to that obtained from the NIST SRM and commercially purchased pooled plasma provides insight into the variability observed between sample populations. In the Cooper Institute cohort, the average oxysterol concentrations for the 200 subjects ranged from 1.8 ng/mL for 24,25-epoxycholesterol to 158.7 ng/mL for 7α-hydroxycholesterol. The NIST SRM and the commercially purchased pooled

plasma also showed 24,25-epoxycholesterol to be the least abundant of the oxysterols, with concentration levels of 1.5 and 1.8 ng/mL, respectively. In contrast to the 200 Cooper Institute samples, the most abundant oxysterol was determined to be 27-hydroxycholesterol, at 124.6 ng/mL (NIST) and 131.0 ng/mL (pooled plasma). Average sterol concentrations ranged from 20.8 ng/mL for 24-dihydrolanosterol to 3892 ng/mL for lathosterol. Cholesterol was measured by a non-MS method at an average of 1.84 mg/mL. Average observed sterol concentrations for the NIST SRM and pooled plasma were consistent with that observed in the Cooper Institute samples. The exception was campesterol (rather than lathosterol) as the most abundant sterol at ~2645 ng/mL. Cholesterol levels were lower in the NIST SRM than those in the Cooper Institute samples; the average amount of cholesterol for the NIST SRM was 1.45 mg/mL and the pooled plasma 1.21 mg/mL.

The Cooper Institute samples originate from a largely Caucasian and affluent population. In contrast, the NIST SRM plasma was designed specifically to be representative of the broader US population in age, gender, and ethnicity. The only sample that was not well defined in terms of population was the commercially purchased pooled plasma, which was collected from anonymous donors. The only defined parameter for this sample is the age of the donors, ranging from 18 to 65 years of age. Though the populations showed differences in the measured values for some compounds, such as cholesterol and 7α-hydroxycholesterol (158.7 ng/mL for the Cooper samples, 91.8 ng/mL for the NIST SRM, and 56.9 ng/mL for the pooled plasma), most compounds were present in comparable levels (Table 2). For example, desmosterol levels were 713.4 ng/mL in the Cooper samples, 623.0 ng/mL in the pooled plasma, and 722.2 ng/mL in the NIST SRM. The variation observed between these samples may be attributable to population differences such as the geographic region from which the pools were collected or the diet, age, gender, and/or ethnicity of the subjects.

Knowing the potential variability of sterol levels in different human populations provides an illustration in the nuances of comparing published values in the literature. Clearly the composition of the population can and will play a role in the measured levels of various compounds. This being written, the values we report for the Cooper Institute cohort compare favorably with other values in the literature [52], with the understanding that there can be variation between populations.

The diversity of sterols and secosteroids analyzed using these methods do come with some compromises. The liquid chromatography methods described here are not able to resolve all stereoisomers (e.g., 7α- and 7β-hydroxycholesterol; 4α- and 4β-hydroxycholesterol), thus the values we report for these sterols in the Cooper Institute cohort include both isomers for each respective pair. Furthermore, while reasonable steps are taken to reduce non-enzymatic oxidation of sterols during isolation, we cannot rule out that at least some of the sterols measured here represent non-specific oxidation products. A case in point is 7-oxocholesterol, which is readily detected but of unknown origin. It is likely that more aggressive measures such as the removal of cholesterol would mitigate the formation of oxidation products such as this oxysterol; however, the present method was developed to allow relative comparisons in sterol levels between subjects in large human cohorts. Because all samples were extracted with the same procedure, a relative analysis within the cohort is valid. The absolute value of each compound is reflective of the methods described here. Comparison of mean values for the Cooper Institute cohort to other cohort values that were obtained using different methods of extraction and analysis must be interpreted with care, especially for unresolved isomers and known oxidation products.

FUTURE DIRECTIONS

While the HPLC methods described here are satisfactory for analyzing a wide range of sterols, oxysterols, and secosteroids, we believe further modifications to the methods may

provide increased resolution and efficiency. For example, the dihydroxysterols (e.g., 7α,27-dihydroxycholesterol) and similar compounds are too polar for optimal elution and separation with the methods described here. The starting mobile phase of 70% ACN elutes this group of oxysterols early (around 2 min). Some of the chromatographic signals are broader than those for ring-structure and side-chain oxysterols and some show tailing. To further optimize chromatographic conditions to resolve these polar sterols, we plan on testing more aqueous mobile phases such as those containing 50-60% ACN. The opposite problem is seen with respect to the sterol HPLC program. These compounds, especially the methylated, saturated sterols like 24,25-dihydrolanosterol are highly retained at even 100% MeOH. The shallow two-step isocratic gradient (96% MeOH, 100% MeOH) used here is not optimal and employing a gradient elution may increase resolution and efficiency of separation. We will further attempt to develop an HPLC program that makes use of a less retentive C8 column that may be more appropriate for sterol separation.

As we have discussed here, sterols are neutral molecules and therefore not well suited for ionization with ESI, although APCI yields sufficient sensitivity to measure physiological levels of sterols. Furthermore, the multi-ring structure of sterols does yield unique or useful fragment ions with CID. Recently, several groups have investigated derivatization schemes that “charge-tag” sterols resulting in increases in ionization efficiency and or unique fragments obtained with CID [53-56]. Despite the added steps required to perform this derivatization, the benefits of charge tagging are substantial and worth an increased effort in select situations. We plan to evaluate charge tagging schemes to determine their suitability for the analysis of the broad set of sterols, oxysterols, and secosteroids we measure here.

Table 1. List of sterols, oxysterols, and secosteroids measured using this method. LIPID MAPS numbers can be used to access additional information at lipidmaps.org. The alphabetical identifier corresponds to the chromatographs in Figure 1.

Common Name	LIPID MAPS Number	Elemental Formula	MW	Identifier	RRI*	Source
dehydroergosterol	LMST01031023	$C_{28}H_{42}O$	394.32	A	0.77	AVT
vitamin D2	LMST03010001	$C_{28}H_{44}O$	396.34	B	0.80	AVT
vitamin D3	LMST03020001	$C_{27}H_{46}O$	384.34	C	0.83	AVT
zymosterol	LMST01010066	$C_{27}H_{44}O$	384.34	D	0.87	AVT
desmosterol	LMST01010016	$C_{27}H_{44}O$	384.34	E	0.92	AVT
8(9)-dehydrocholesterol	LMST01010242	$C_{27}H_{44}O$	384.34	F	0.97	AVT
ergosterol	LMST01030093	$C_{28}H_{44}O$	396.34	G	0.98	SIG
7-dehydrocholesterol	LMST01010069	$C_{27}H_{44}O$	384.34	H	1.00	AVT
8(14)-dehydrocholesterol					1.00	AVT
cholestenone (Δ4)	LMST01010015	$C_{27}H_{44}O$	384.34	I	1.00	AVT
cholestenone (Δ5)	LMST01010248	$C_{27}H_{44}O$	384.34	J	1.03	STER
brassicasterol	LMST01030098	$C_{28}H_{46}O$	398.35	K	1.05	SIG
lathosterol	LMST01010089	$C_{27}H_{46}O$	386.35	L†	1.05	SIG
cholesterol	LMST01010001	$C_{27}H_{46}O$	386.35	M†‡	1.06	AVT
14-demethyl-lanosterol	LMST01010176	$C_{29}H_{48}O$	412.37	N	1.07	AVT
lanosterol	LMST01010017	$C_{30}H_{50}O$	426.39	O	1.09	AVT
dihydrocholesterol	LMST01010077	$C_{27}H_{48}O$	388.37	P	1.12	SIG
campesterol	LMST01030097	$C_{28}H_{48}O$	400.37	Q	1.13	SIG
stigmasterol	LMST01040124	$C_{29}H_{48}O$	412.37	R	1.13	AVT
cycloartenol	LMST01100008	$C_{30}H_{50}O$	426.39	S	1.13	STER
β-sitosterol	LMST01040129	$C_{29}H_{50}O$	414.39	T	1.20	SIG
24,25-dihydrolanosterol	LMST01010087	$C_{30}H_{52}O$	428.40	U	1.22	AVT
stigmastanol	LMST01040128	$C_{29}H_{52}O$	416.40	V	1.27	SIG

† Lathosterol and cholesterol coelute in an actual plasma extract

‡ Cholesterol signal shown 0.1x scale

* Relative to cholestenone (Δ4) (I)

BOLD indicates deuterated analog available from Avanti Polar Lipids

AVT = Avanti Polar Lipids (Alabaster, AL)

STER = Seraloids (Newport, RI)

SIG = Sigma-Aldrich (St. Louis, MO)

EMD = EMD Chemicals (Rockland, MA)

LM Common Name 2	LM Number	Elemental Formula	MW	Identifier	RRI**	Source
1α,25-dihydroxy-previtamin D3	LMST03020660	$C_{27}H_{44}O_3$	416.33	b	0.35	SIG
7α,25-dihydroxycholesterol	LMST04030166	$C_{27}H_{46}O_3$	418.34	a	0.33	AVT
7ß,27-dihydroxycholesterol	LMST04030178	$C_{27}H_{46}O_3$	418.34	c	0.38	AVT

Table 2. Results from the measurements of sterols, oxysterols, and secosteroids from a cohort of 200 subjects from the Cooper Institute in Dallas, TX. Data are in ng/mL except for cholesterol which is in mg/dL. NIST SRM, pooled plasma, and spike recovery are included for comparison as well as for QA/QC analysis. Letters in parentheses correspond to chromatographic peak labels in Figure 1. Error values are given in parentheses and represent the relative standard error (RSE).

Oxysterol (ng/mL)*	7αHC (x)	7α,27HC (c)	25OH VD_3 (i)	25HC (l)	24HC (m)	27HC (o)	4βHC (*k*)	24oxoC (n)	24/25EC (r)	7oxoC (*a*)
average (RSE)	158.7 (3.2)	10 (2.4)	24.3 (2.8)	11.8 (2.4)	56.1 (2.1)	151.4 (2.0)	53.1 (2.4)	6.0 (2.2)	1.8 (4.4)	84 (4.5)
median	153.6	9.6	25.6	11.0	53.6	144.1	48.9	5.6	1.5	66.5
range	33-435	2-22.8	0-57.6	2.6-28.2	24-117	60-390	16.7-144	2.6-12.1	0.2-9.1	25.7-360.8
pooled plasma avg (RSE)**	56.86 (10.6)	9.24 (5.3)	9.32 (1.4)	6.1 (3.9)	46.13 (3.3)	124.6 (2.0)	43.9 (3.0)	5.1 (13.5)	1.5 (6.7)	40.54 (18.3)
NIST SRM Plasma Avg	91.8	9.6	20.7	5.7	44.6	131.0	31.4	3.7	1.8	24.0
spike recovery (%) **	104.3	99.6	97.1	106.3	101.4	100.9	104.0	109.0	100.1	104.6

* n=200

** n=6

Sterol (ng/mL)*	Chol (M)‡†	Zymo (D)	Desm (E)	Lano (O)	24-DiHL (U)	7-DHC (H)	Cholestanol (P)	14-DML (N)	Lath	Camp (Q)
average (RSE)	184.0	24.8 (6.5)	713.4 (3.3)	203.2 (6.4)	20.8 (13)	803.2 (2.8)	2913.9 (2.3)	517 (3.6)	3892 (7.1)	3831.4 (3.8)
median	182.5	16.9	692.0	151.2	10.2	744.7	2827.6	456.0	3388	3546.1
range	112-319	0-139	37-1800	35-1480	2.4-347	424-2488	160-6200	14.5-1915	166-14460	808-16400
pooled plasma avg (RSE)**	120.7	19.7 (1.6)	623 (0.8)	101.2 (1.1)	5.5 (1.6)	510 (1.1)	2526 (0.6)	305 (1.1)	3078 (3.9)	2502 (0.7)
NIST SRM Plasma Avg	145.0	32.2	722.2	123.9	8.5	1137.8	2581.1	451.1	2080	2645.6
spike recovery (%) **	n/a	96.9	97.1	94.6	96.0	85.0	95.9	107.3	106.5	111.0

* n=200

** n=6

‡ units of mg/dL

† measured by clinical chemistry assay

Table 3. Recovery of four deuterated surrogate standards.

	Average Recovery (%)*	%RSD	%RSE
(d6) 1,25 VD_3	87.9	25.7	1.8
(d6) 27HC	90.7	18.1	1.3
(d6) 7αHC	100.8	20.3	1.4
(d6) 4βHC	100.3	21.8	1.5

* n=200

Figure 1. Sterol structures. Structures of *A*, cholesterol, *B,* 25-hydroxyvitamin D_3, and *C,* cholesteryl ester with positional numbering system.

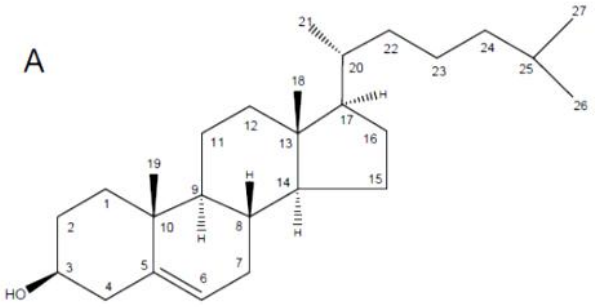

cholesterol

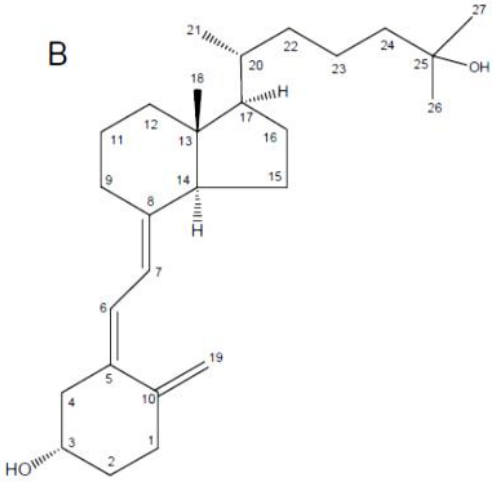

25-hydroxyvitamin D3

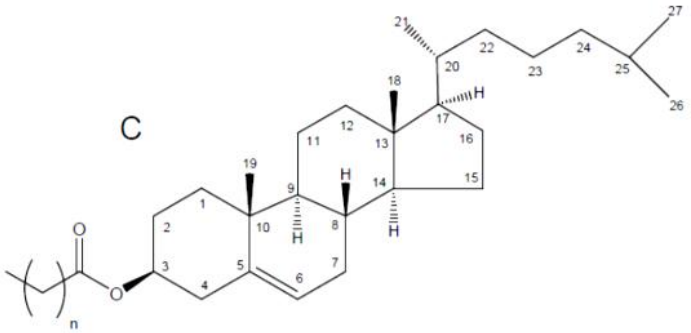

cholesteryl ester

Figure 2. Standard mix and pooled plasma chromatograms. *A-F*, LC-MS chromatograms of standard mixes and extracts of a pooled plasma sample for sterols, oxysterol, and lathosterol.

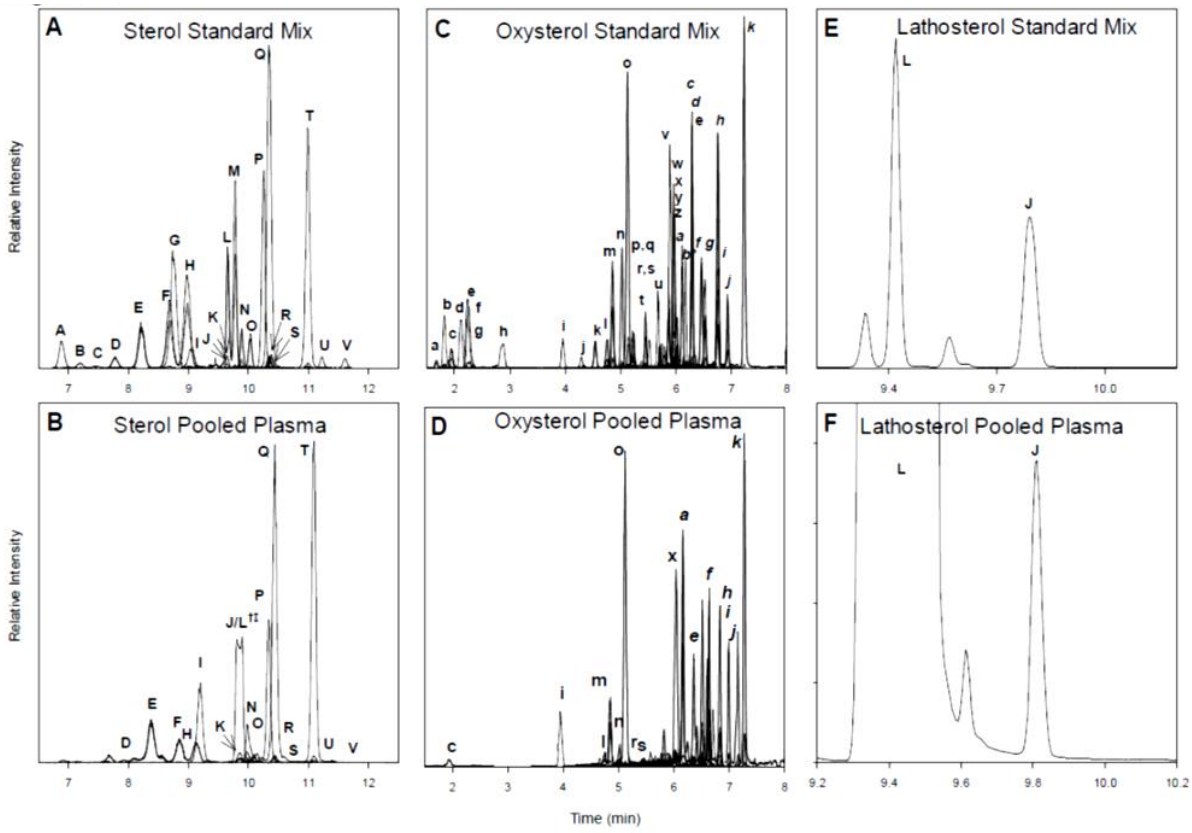
A
Sterol Standard Mix
B
Sterol Pooled Plasma
C
Oxysterol Standard Mix
D
Oxysterol Pooled Plasma
E
Lathosterol Standard Mix
F
Lathosterol Pooled Plasma
Relative Intensity
Time (min)

Figure 3. Sterol mass spectra. *A-C,* ESI product-ion mass spectra of representative oxysterols and the secosteroids 25-hydroxyvitamin D_3. *D,E*, APCI product-ion mass spectra of representative sterols. *F*, EI mass spectrum of derivatized lathosterol. Selected ions are identified and structures are included in each panel for reference.

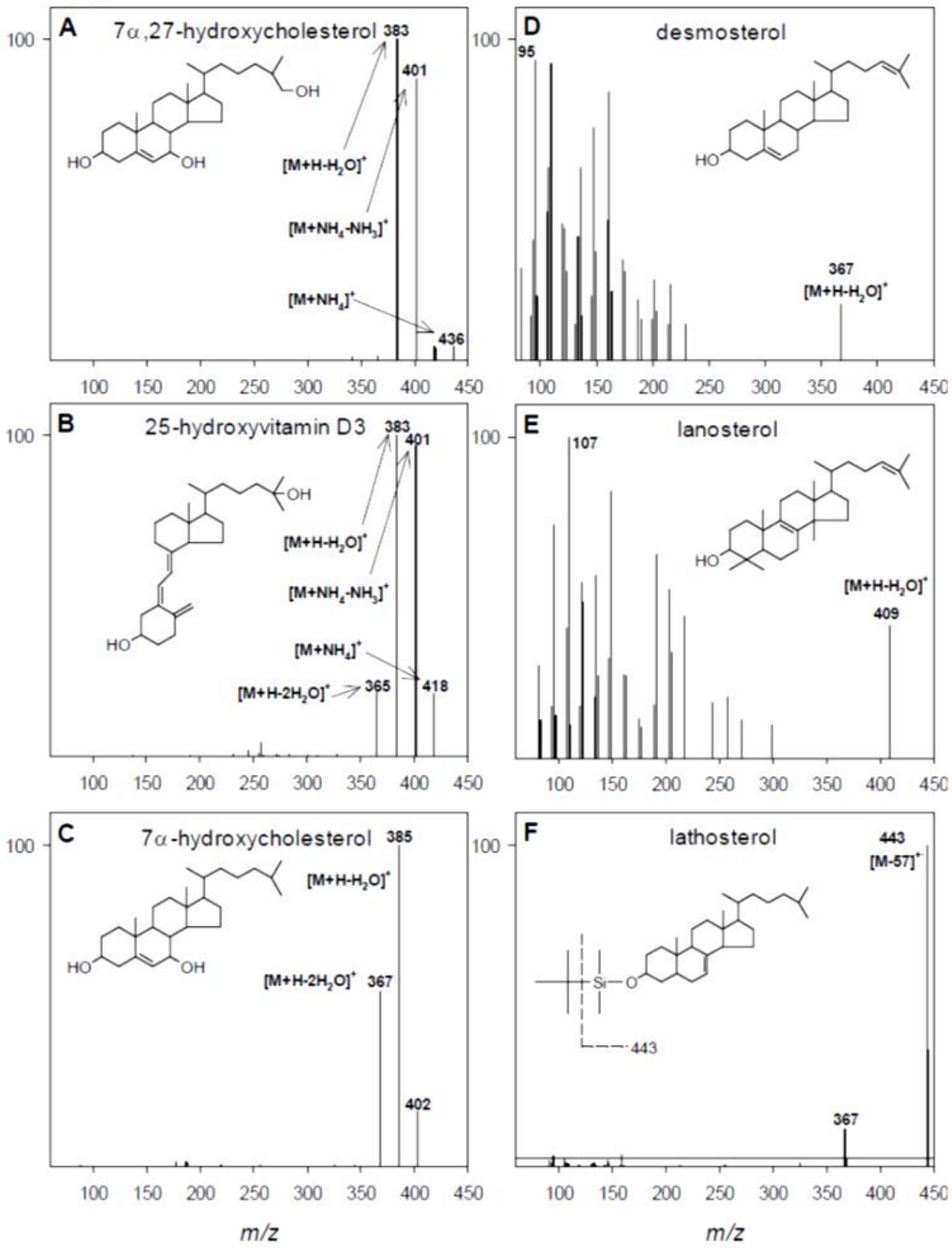
A
7α,27-hydroxycholesterol
383
401
436
[M+H-H2O]+
[M+NH4-NH3]+
[M+NH4]+
HO
OH
OH
B
25-hydroxyvitamin D3
383
401
418
365
[M+H-H2O]+
[M+NH4-NH3]+
[M+NH4]+
[M+H-2H2O]+
HO
OH
C
7α-hydroxycholesterol
385
367
402
[M+H-H2O]+
[M+H-2H2O]+
HO
OH
D
desmosterol
95
367
[M+H-H2O]+
HO
E
lanosterol
107
409
[M+H-H2O]+
HO
F
lathosterol
443
[M-57]+
Si
O
443
367
100
150
200
250
300
350
400
450
m/z

CHAPTER THREE:

CYP7B1: ONE CYTOCHROME P450, TWO HUMAN GENETIC DISEASES, AND MULTIPLE PHYSIOLOGICAL FUNCTIONS

INTRODUCTION

The analytical methods developed in Chapter 1 allow the measurement of several different side-chain oxysterols, including 24*S*-hydroxycholesterol, 25-hydroxycholesterol, and 27-hydroxycholesterol. These sterols are made in extra-hepatic tissues such as the brain, reticuloendothelial system, and lung, and thereafter transported to the liver via lipoproteins for conversion into bile acids and secretion from the tissue. Conversion of side-chain oxysterols into bile acids involves an initial hydroxylation event at carbon 7 and is catalyzed by two different enzymes, the CYP7B1 oxysterol 7α-hydroxylase, and the CYP39A1 oxysterol 7α-hydroxylase. Of these two enzymes, the CYP7B1 protein has been most highly studied and thus prior to initiating sterol measurements in humans, I surveyed the literature on CYP7B1 and wrote the review that follows in this chapter. The CYP39A1 enzyme is a major focus of Chapter 4.

OXYSTEROL 7α-HYDROXYLASE (CYP7B1)

The CYP7B1 cytochrome P450 enzyme hydroxylates carbons 6 and 7 of the B ring of oxysterols and steroids. Hydroxylation reduces the biological activity of these substrates and facilitates their conversion to end-products that are readily excreted from the body. CYP7B1 is expressed in liver, reproductive tract, and brain, and performs different physiological functions in each tissue. Hepatic CYP7B1 activity is crucial for the inactivation of oxysterols and their

subsequent conversion into bile salts. Loss of CYP7B1 activity is associated with liver failure in children. In the reproductive tract, the enzyme metabolizes androgens that antagonize estrogen action; mice without CYP7B1 have abnormal prostates and ovaries. The role of CYP7B1 in the brain is under investigation; recent studies show spastic paraplegia type 5, a progressive neuropathy, is caused by loss-of-function mutations in the human gene.

There are two general types of cytochrome P450 enzymes, those that act on endogenous substrates like lipids and those whose primary function is to act on exogenous substrates like drugs and environmental chemicals. Deciding whether a new P450 acts on endogenous versus exogenous substrates is difficult in the absence of experimental analysis. This was the case for the P450 now known as CYP7B1, whose cDNA was initially isolated from a rat hippocampal library and described in the pages of the *Journal of Biological Chemistry* as a new P450 with 39% sequence identity to cholesterol 7α-hydroxylase (CYP7A1) [57]. The latter enzyme acts on an endogenous substrate (cholesterol) and plays an important role in bile salt synthesis [58], but what role did CYP7B1 play? Subsequent biochemical experiments showed that CYP7B1 also acted on endogenous substrates, hydroxylating dehydroepiandrosterone, pregnenolone, and other steroids [59], as well as two oxysterols, 25-hydroxycholesterol [60] and 27-hydroxycholesterol [61]. Here, we review the biochemistry, physiology, and genetics of CYP7B1, which reveal the enzyme to be a multifunctional P450.

THE CYP7B1 GENE, mRNA, AND ENZYME

The CYP7B1 gene encodes an evolutionarily conserved P450 and is found in the genomes of organisms ranging from the human to the Japanese firebellied newt to the fungus *Aspergillus niger*. The human gene spans ~220 kb on chromosome 8q21.3 and encompasses 6 exons separated by 5 introns (Fig. 1*A*). Transcription is initiated ~200 bp 5' of the initiation codon in exon 1 and produces a mRNA of ~9 kb that has a long (~7 kb) 3'–untranslated sequence [62]. The tissue-specific expression pattern of the CYP7B1 gene differs between species. The

human mRNA is present in many organs with the highest levels detected in the kidney and brain [62]. The mRNA is also widely distributed among different tissues of the rat [63]. Expression is restricted to the liver, lung, kidney, brain, and reproductive tract in the mouse, with the amount of mRNA being highest in the liver and lung. As with several other P450s, the CYP7B1 mRNA, protein, and enzyme activity in liver and kidney are higher in male mice than in female mice, and this sexually dimorphic expression requires androgen receptor signaling [64]. The biological significance of this male–female difference and whether a similar pattern of expression exists in other species are not known.

The human mRNA encodes a 506 amino acid enzyme (E.C. 1.14.13.100), which catalyzes the 6α– or 7α–hydroxylation of several steroids and oxysterols (Fig. 1*B*). NADPH and cytochrome P450 oxidoreductase serve as cofactors in these reactions, and based on the latter requirement CYP7B1 is presumed to be located in the endoplasmic reticulum. An antipeptide antibody raised in a rabbit against amino acids 266–281 of mouse CYP7B1 recognizes a protein of molecular weight ~58,000 on immunoblots [60], which is in good agreement with that (58,359) predicted from conceptual translation of the mouse cDNA. The enzyme has not been purified and kinetically characterized, thus whether steroids are better substrates than oxysterols or whether preferences exist within these two classes remain to be determined. The properties of CYP7B1 isolated from different species may differ as nafimidone (1-(2-naphthoylmethyl)imidazole) selectively inhibits the mouse but not the human enzyme [60]. The three–dimensional structure of CYP7B1 has yet to be solved, but a structure at 2.15Å is available for cholesterol 7α-hydroxylase (PDB 3DAX), which as noted above shares sequence identity and sterol substrate partiality with the enzyme.

PHYSIOLOGICAL ROLES OF CYP7B1

Bile Salt Synthesis — A major metabolic fate of cholesterol is conversion into conjugated bile salts in the liver [58]. Once synthesized, bile salts act in the gut to facilitate solubilization of

hydrophobic nutrients from the diet including fat-soluble vitamins and cholesterol. In the liver, bile salts stimulate bile flow and the excretion of metabolites such as porphyrins that arise from the breakdown of heme. The identification and cDNA cloning of the enzymes that participate in bile salt synthesis began in the late 1980's [65], and inter alia these studies showed that both cholesterol and oxysterols are substrates for bile acid synthesis. The first and rate-limiting step in the cholesterol pathway involved 7α–hydroxylation, a reaction catalyzed by cholesterol 7α-hydroxylase [66]. Björkhem and colleagues later showed that a different enzyme was involved in 7α–hydroxylating oxysterols [67], and the finding that CYP7B1 shared sequence identity with cholesterol 7α-hydroxylase suggested that CYP7B1 might be an oxysterol 7α-hydroxylase. Genetic, pharmacological, and biochemical experiments subsequently confirmed this hypothesis (Table 1) [60, 68].

A majority of mice lacking cholesterol 7α-hydroxylase die from vitamin and caloric deficiencies in the first 18-21 days of life [69]; thereafter, the expression of CYP7B1 is induced in the liver resulting in the synthesis of bile salts and the prevention of further premature death [68]. Adult cholesterol 7α-hydroxylase deficient mice contain ~30% of the normal amount of bile salts suggesting that oxysterols are precursors for ~one–third of the bile salt pool in this species [70]. Cholesterol balance studies support this estimate and indicate that cholesterol 7α-hydroxylase expression is ~30% higher in CYP7B1 knockout mice; this increase in expression produces a normal bile salt pool [64]. Both 25-hydroxycholesterol and 27-hydroxycholesterol accumulate in the sera and tissues of CYP7B1 mutant mice [64], a finding that supports their in vivo roles as enzyme substrates. Unexpectedly, the related side-chain oxysterol, 24*S*-hydroxycholesterol, does not accumulate; this sterol is metabolized to a bile salt precursor by another oxysterol 7α-hydroxylase, CYP39A1 [71].

Steroid Hormone Metabolism — CYP7B1 was initially identified as a steroid 7α-hydroxylase with activity towards pregnenolone, a 21–carbon steroid, and dehydroepiandrosterone, a 19–carbon steroid [59]. This result, the isolation of the cDNA from a hippocampal library [57], and histochemical data [63] suggested that CYP7B1 had a function in the brain (Table 1). Pregnenolone and dehydroepiandrosterone are so-called neurosteroids, an enigmatic class of compounds that are ascribed broad regulatory, functional, and metabolic roles [72], thus one hypothesis currently under investigation is that CYP7B1 inactivates neurosteroids in the brain. There is as yet no evidence that pregnenolone or dehydroepiandrosterone accumulate in CYP7B1 knockout mice, consequently the importance of CYP7B1 in clearing these steroids from the brain and body versus other enzymes that utilize these substrates such as 3β-hydroxysteroid dehydrogenases, is unknown. A case for CYP7B1 action in the central nervous system can be made given the clinical presentation of subjects with spastic paraplegia type 5 (see below), but whether this disease is caused by abnormalities in steroid versus oxysterol metabolism remains to be determined.

Metabolism of Estrogen Receptor Ligands — A third steroid substrate of CYP7B1 is 5α-androstane-3β,17β-diol [63], a 19–carbon steroid that is an agonist for the estrogen receptor [73]. Unlike with other substrates, CYP7B1 prefers to 6α–hydroxylate 5α-androstane-3β,17β-diol (Fig. 1*B*) [74], but the net effect of this hydroxylation is the same as that for 7α–hydroxylation, namely inactivation of the steroid. Loss of CYP7B1 in males derived from one line of knockout mice [63] leads to smaller prostates [75], and to early ovarian failure in female mice [76]. In both sexes, these reproductive tract abnormalities are ascribed to excess 5α-androstane-3β,17β-diol, which is postulated to accumulate in the absence of CYP7B1 and to drive pathologic activation of the estrogen receptor [75, 76].

The oxysterol 27-hydroxycholesterol is a selective estrogen receptor modulator (SERM), antagonizing estrogen-mediated activation of the receptor in the vascular wall [77], and activating the receptor in the absence of estrogen in breast cancer and other cell lines [78]. In agreement with this SERM activity, CYP7B1 knockout mice [64], which accumulate 27-hydroxycholesterol in serum and tissues, show abnormalities in estrogen-mediated gene expression in the vasculature and defects in reendothelialization [77]. It is not yet known whether these phenotypes arise from a failure of CYP7B1 to catabolize 27-hydroxycholesterol locally (i.e., in the vascular wall) or systemically (i.e., in the liver).

Conflicting evidence exists regarding the ability of 7α-hydroxydehydroepiandrosterone, a product of CYP7B1, to selectively activate the estrogen receptor β subtype. One report suggested that this steroid was made in human prostatic cells and therein activated the receptor [79], whereas a second report failed to replicate the receptor activation in human embryonic kidney 293 cells [80]. Both studies relied on in vitro transfection approaches and to date there is no in vivo evidence to suggest a physiological role for 7α-hydroxylated dehydroepiandrosterone in estrogen receptor function.

Immunoglobulin Production — Activation of macrophages via Toll-like receptors induces cholesterol 25-hydroxylase and the subsequent synthesis of 25-hydroxycholesterol [23, 81]. The oxysterol is secreted from the macrophage and suppresses the production of immunoglobulin A by B cells via two mechanisms; suppression of cytokine-mediated B cell proliferation and repression of a gene (the activation-induced cytidine deaminase) that is required for immunoglobulin A synthesis. This immunoregulatory role is supported by the findings that cholesterol 25-hydroxylase knockout mice, which cannot synthesize 25-hydroxycholesterol, have higher than normal levels of immunoglobulin A in their sera and mucosa, whereas CYP7B1 knockout mice, which accumulate the oxysterol [64], have low levels of this immunoglobulin. CYP7B1 expression is induced in the mouse lung and human joint by

proinflammatory stimuli that are released upon activation of macrophages and other cells of the innate immune system [82, 83]. This induction may reflect the need to inactivate 25-hydroxycholesterol produced by macrophages.

GENETICS OF CYP7B1

Liver Failure in Children — As noted above, a role for CYP7B1 in hepatic bile salt synthesis was suggested by studies in the mouse. This function was confirmed with the description of an infant who presented with liver failure arising from an inherited mutation in the CYP7B1 gene [84]. Chemical analyses revealed that serum oxysterols and other bile salt intermediates were markedly elevated in this individual, whereas mature bile salts were lacking. DNA sequencing revealed a homozygous nonsense mutation at codon 388 in exon 5 of the gene (Fig. 2), which produced a truncated protein that lacked enzymatic activity. A second subject with a similar clinical presentation but resulting from a homozygous nonsense mutation at codon 112 in exon 3 of the CYP7B1 gene was reported [85]. The accumulation of oxysterols and other bile salt intermediates in these subjects was thought to have caused irreparable damage to the liver ultimately necessitating transplantation. Together, these results underscored the importance of CYP7B1 in bile salt synthesis and the role of the enzyme in the inactivation of otherwise hepatotoxic oxysterols.

Neuropathy in Adults — Unexpected insight into CYP7B1 came in 2008 from a team of neurologists who reported that the autosomal recessive disorder spastic paraplegia type 5 was also caused by mutations in the CYP7B1 gene [86]. These results were confirmed [87-90], and to date 17 different mutations in >20 unrelated families have been identified in the gene (Fig. 2). The spastic paraplegias are a clinically heterogeneous group of disorders characterized by lower limb spasticity and weakness associated with degeneration of motor neuron axons in the spinal cord [91]. Over 41 spastic paraplegia loci have been mapped in the human genome, and mutations in 17 different genes have now been identified in individuals affected with the various

forms of the disease. Spastic paraplegia type 5 has a variable age of onset, appearing in children as young as 1 and adults as old as 58 years [88]. Most type 5 cases are said to be “pure” in that progressive lower limb spasticity is the only clinical symptom observed; however, in two families, the disease was manifest in “complex” form and presented in association with ataxia, mental retardation, and other neurological symptoms [89].

ONE GENE, TWO DISEASES

How can mutations in the same gene give rise to two diseases with symptoms as diverse as liver failure in newborns and progressive neuropathy in children and adults? These syndromes are not caused by different mutations in the gene as the same lesions are found in subjects with liver failure and spastic paraplegia type 5 (Fig. 2), nor are they caused by varying amounts of residual enzyme activity since complete loss of function mutations (e.g., homozygous nonsense mutations) are found associated with both presentations. A testable hypothesis is that the two diseases result from the accumulation of different CYP7B1 substrates, for example oxysterols in liver failure and steroids or another lipid in spastic paraplegia type 5. An infection in a newborn infant might lead to increased synthesis of the oxysterol 25-hydroxycholesterol [23, 81], which in the absence of catabolism by CYP7B1 could lead to liver damage. Similarly, a different subclinical episode causing increased steroid synthesis might initiate spinal cord damage by an as yet unknown mechanism, which over time would progress to spastic paraplegia type 5.

Differential manifestations of cytochrome P450 deficiency are not unique to CYP7B1. Loss of CYP27A1, a sterol 27-hydroxylase that participates in oxysterol and bile salt synthesis [58], causes liver disease in some infants [92, 93], but a progressive central nervous system neuropathy and other symptoms (cerebrotendinous xanthomatosis) in a majority of affected adults [94]. Different substrates build up in these presentations; bile alcohols accumulate in

children with liver disease whereas the hydrophobic sterol cholestanol accumulates in the myelin of adults.

PERSPECTIVES

There are straightforward questions to be answered by future CYP7B1 research. First, which substrates of the enzyme amass in spastic paraplegia type 5? Second, is infection and a concomitant elevation of 25-hydroxycholesterol a precipitating condition of liver failure in infants with CYP7B1 deficiency? Third, is childhood liver disease a common but unreported symptom in older subjects with spastic paraplegia type 5? Fourth, do CYP7B1 knockout mice display symptoms of neurodegeneration and the accumulation of previously defined or new enzyme substrates in the central nervous system? Fifth, what are the biochemical properties of purified CYP7B1? Sixth, how does the three-dimensional structure of CYP7B1 compare to cholesterol 7α-hydroxylase (CYP7A1) and what features of the enzymes determine their substrate specificities? The years since the identification of CYP7B1 have provided a wealth of information concerning this P450 and there is more still to learn.

Figure 1. CYP7B1 and reactions catalyzed. *A*, schematic of the 506-amino acid enzyme showing regions encoded by the six exons of the gene and the positions marked by *arrows* at which five introns interrupt individual codons. The heme cofactor is covalently bound to Cys^{449}. *B*, 7α-hydroxylation of substrates (*1*, pregnenolone; *2*, dehydroepiandrosterone; *3*, 25-hydroxycholesterol; *4*, 27-hydroxycholesterol) and 6α-hydroxylation of 5α-androstane-3β,17β-diol. *POR*, cytochrome P450 oxidoreductase.

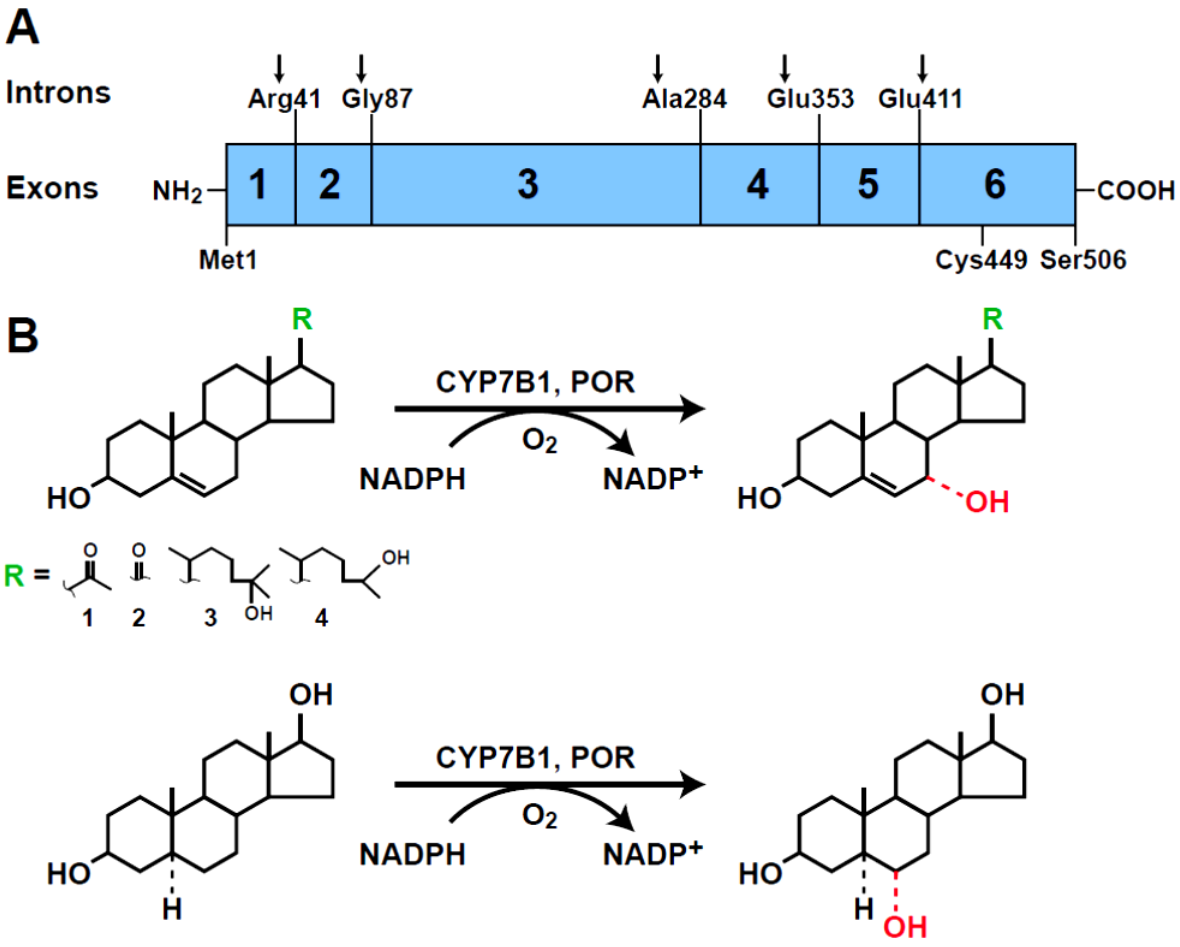
A
Introns
Exons
Arg41
Gly87
Ala284
Glu353
Glu411
NH2
1
2
3
4
5
6
COOH
Met1
Cys449
Ser506
B
R
HO
CYP7B1, POR
O2
NADPH
NADP+
OH
R =
1
2
3
4
H

Figure 2. Mutations in human CYP7B1 gene. Exons are indicated by *shaded boxes* drawn to scale. Introns are indicated by *dashed lines* and are not drawn to scale. Transcript coding regions are shaded *blue*; 5'- and 3'-untranslated regions are *white*. Mutations in subjects with liver failure are shown above the gene; those found in spastic paraplegia type 5 are shown below the gene.

Liver failure in newborns

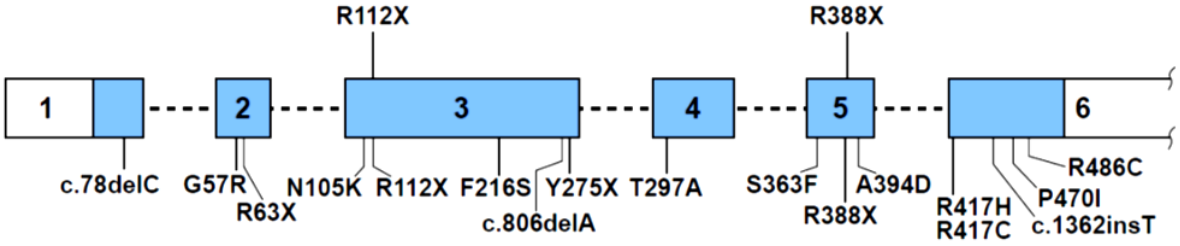

Spastic paraplegia type 5

CHAPTER FOUR:

Environmental, Genetic, and Anatomic Determinants of Serum Sterol Levels

INTRODUCTION

Lipids are an important component of serum and play essential roles in energy metabolism, signaling, and transport. A recent study revealed an unexpectedly large complexity in the serum lipidome, which was found to be composed of hundreds of different molecular species in each of the major classes of lipids [95]. For example, cholesterol and 13 other sterols were detected in concentrations ranging from mg/ml to ng/ml, and over 200 different triglycerides were found. This study analyzed a pooled plasma sample derived from multiple individuals, thus whether the observed complexity reflected functional diversity in the roles played by different lipids, was environmentally driven, or was biologically or medically informative could not be determined.

To address these issues with respect to serum sterols, we developed a comprehensive analytical method that allows quantification of as many as 60 different sterols and secosteroids in small volumes (<200 µl) of human serum [96]. Base hydrolysis to produce free sterols and three types of mass spectrometry are employed in this method together with 17 different deuterated standards and multiple controls to generate an accurate and reproducible profile of serum sterols in an individual. An initial analysis of 200 serum samples documented the usefulness of the approach, confirmed the diversity of sterols observed in the original serum lipidome study, and began to define the ranges and distributions of these sterols in the population [96].

The steady state concentration of a given serum sterol is determined by rates of formation and degradation, the kinetics of movement into and out of cells and tissues, the levels of lipoproteins that transport sterols through the bloodstream, their availability in the diet, and occasionally, the presence of disease. For some sterols, the individual contributions of these variables can be determined from known metabolic pathways, clinical measurements of lipoprotein levels, and nutritional and health information. In other cases, where biosynthetic, catabolic, and transport pathways are unknown, genome-wide association studies can be used to identify loci that are linked to serum sterol levels [97, 98]. Subsequent genetic and functional studies then define the role of the product specified by the identified gene [99, 100].

In the current study, we use the analytical methods of McDonald et al. [96] to measure serum sterols in 3,230 individuals from a clinically well-defined cohort, the Dallas Heart Study [101]. All of the 22 sterols and secosteroids routinely detected in serum showed marked inter-individual variation in their levels. Through further studies, we identify genetic, environmental, and anatomic etiologies for variation in three sterols, 24*S*-hydroxycholesterol, 24,25-epoxycholesterol, and 8-dehydrocholesterol.

MATERIALS AND METHODS

Expression Plasmids

The following expression plasmids were generated in the pcDNA3.1 mammalian expression vector using standard PCR methods. Using QuikChange II site-directed mutagenesis kit methods (Stratagene), pCMV6-CYP39A1, which encodes full-length oxysterol 7α-hydroxylase, CYP39A1, under transcriptional control of the cytomegalovirus (CMV) promoter; pCMV6-CYP39A1-R23P, pCMV6-CYP39A1-R103H, pCMV6-CYP39A1-T288H, pCMV6-CYP39A1-N324K, or pCMV6-CYP39A1-K329Q missense mutations were synthesized. Epoxide hydrolase 2 expression vector pCMV6-EPHX2 was used to synthesize pCMV6-EPHX2-R287Q and

pCMV6-SDR42E1, short-chain dehydrogenase reductase family 42E member 1, was used to synthesize pCMV6-SDR42E1-S10T.

Transfection

For quantitative sterol analysis, human embryonic kidney 293 cells (HEK 293; American Type Culture Collection, Manassas, VA) were plated at a density of 7 x 10^3 cells/dish in 60 mm dishes. Cells were grown and maintained in DMEM with 10% fetal bovine serum. HEK 293 cells were plated two days before the transfection. For transfection, 3.6 μg plasmid DNA per dish (pCMV6, pCMV6-CYP39A1, pCMV6-CYP39A1-R23P, pCMV6-CYP39A1-R103H, pCMV6-CYP39A1-T288H, pCMV6-CYP39A1-N324K, or pCMV6-CYP39A1-K329Q) using Fugene 6 reagent (Roche) was added to 293 cells that were 75-85% confluent and was incubated at 37 ^oC in an 8.8% CO_2 atmosphere and was allowed to remain in contact with the cells for 24 hours. The medium containing the DNA was removed. The cells were washed with phosphate-buffered saline, and 2 ml of fresh medium (Dulbecco's modified Eagle's medium containing 1000 mg glucose/liter, 100 units/ml penicillin and supplemented with 10% fetal calf serum) along with 800 ng 24*S*-hydroxycholesterol, 24,25-epoxycholesterol, 7- or 8-dehydrocholesterol were added, and the mixture was incubated for an additional 4 hours. The medium and cells were then used for HPLC-MS analysis after extraction. The amounts of the substrate and product were calculated using isotope-dilution mass-spectrometry methods.

For immunoblotting, transfection of HEK293 cells with FuGENE6 reagent (Roche Applied Science) was performed as described above. Following substrate addition, triplicate dishes of cells were harvested and washed with DPBS. The resulting cell pellets were resuspended in buffer containing 10 mM HEPES-KOH, pH 7.4, 250 mM sucrose, 1.5 mM $MgCl_2$, 10 mM KCl, 5 mM EDTA, 5 mM EGTA, 5 mM dithiothreitol, 0.1 mM leupeptin, and a protease inhibitor mixture consisting of 1 mM dithiothreitol, 1 mM phenylmethylsulfonyl fluoride, 0.5 mM Pefabloc, 10 μg/ml leupeptin, 5 μg/ml pepstatin A, 25 μg/ml *N*-acetyl-L-leucinyl-L-leucinyl-L-norleucinal, and

10 μg/ml aprotinin. The cell suspension was lysed by passing through a 22.5-gauge needle 30 times, and the resulting lysates were subjected to 1000 x *g* centrifugation for 7 min at 4 ^{o}C. The supernatant of this spin was subjected to centrifugation at 100,000 x *g* for 30 min at 4 ^{o}C to obtain the membrane pellet and cytosolic supernatant fractions. Aliquots of these fractions were fractionated by SDS-PAGE, after which the proteins were transferred to nitrocellulose membranes and subjected to immunoblot analysis. Primary antibodies used for immunoblotting were as follows: a rabbit polyclonal antibody against human CYP39A1 (Sigma-Aldrich).

Real-time PCR

Total RNA was isolated using RNeasy Mini Kit (Qiagen) according to the manufacturer's procedures. mRNA expression was verified by quantitative real-time PCR using specific primers for human genes of interest (e.g., CYP39A1) and the control mRNA ribosomal protein 36B4.

Subjects

DHS2 description (a total of n = 3,230 subjects, including n = 2,485 from the initial cohort (DHS1) and 916 new participants). Of the 2,485 individuals participating at both stages of the study, genotype data were available for 2,109 subjects who had submitted blood samples for genetic analysis (see below).

Genome-wide association methods

The association of each SNP with various analyte levels was tested under an additive model using multiple linear regression including ethnicity, gender, and age as covariates. Sterol and secosteroid levels were logarithm transformed prior to analysis. Genotypes were coded as a numeric variable (0, 1, or 2 alleles). To account for the number of tests performed, P = 5.0 $\times 10^{-6}$ (Bonferroni threshold) was used as a threshold for statistical significance.

To assess the combined effect of multiple SNPs on a given sterol level, joint analysis was done by including all in a linear model as covariates. Further, the number of variant alleles was counted in each individual at given SNP loci and then the cumulative effects of the multiple SNPs were determined.

Genotyping assays

DHS1 participants (n = 3,386) were genotyped using high-density oligonucleotide arrays (Perlegen Sciences, Mountain View, CA). Two genetic screens were performed: The first one included 12,138 nonsynonymous sequence variations from dbSNP and the Perlegen SNP database. The second was based on a candidate-gene approach and included all single-nucleotide variations located within 10 kb of the coding sequence of a set of genes known to be involved in lipid metabolism[1] (a complete list is available on request). SNPs were excluded with a genotype call rate <80% or a significant deviation from Hardy-Weinberg equilibrium ($P < 0.0001$). A total of 9,515 SNPs in the first study and 11,608 in the second study passed our quality control criteria and were used in subsequent analyses.

In addition, several SNPs identified through direct sequencing in the CYP39A1 gene were genotyped in the Dallas Heart Study. Genotypes were determined by using a 5'-nucleotidase assay for CYP39A1 rs41273654, rs7761731, rs17856332, rs2277119 and rs12192544. These were designed and utilized via the TaqMan assay system (Applied Biosystems). The assays were performed on an HT7900 Real-Time PCR system (AB) with TaqMan probes purchased from Applied Biosystems.

Statistical analyses methods

The relationships between 24*S*-hydroxycholesterol levels, white and gray matter volume, and other variables were assessed using multiple regression models, including age, gender,

[1] The genes were selected by a panel of local experts.

ethnicity, body-mass index (BMI), and other covariates where appropriate. A natural log transformation was applied to 24*S*-hydroxycholesterol levels, white and gray matter volume, to achieve a normal distribution.

RESULTS

Fig. *1A* exemplifies the raw data generated in this study and shows the levels of 24*S*-hydroxycholesterol in the 3,230 DHS serum samples analyzed. The mean concentration of this oxysterol in the population was 59.8 ng/ml and the range 10.0 to 314.7 ng/ml. Levels of 24*S*-hydroxycholesterol showed a lognormal distribution with positive skewing (Fig. 1*C*,*D*), suggesting that multiple independent variables affect this trait. Similar distributions characterized all other analytes. Comparisons between the levels of 24*S*-hydroxycholesterol and those of other sterols and secosteroids revealed statistically significant correlations with cholesterol (Fig. 1*B*) and 24-oxocholesterol (r = .53 and .47 respectively). The association with cholesterol explained 3.1% of the observed variance in inter-individual serum 24*S*-hydroxycholesterol levels and most likely reflects the transport of the oxysterol through the bloodstream in cholesterol-rich lipoprotein particles such as LDL and HDL [102]. The relationship with 24-oxocholesterol might indicate a precursor-product relationship between these two sterols. Cholesterol levels were correlated with 17 other sterols (Fig. 2), suggesting that these compounds too reside in lipoproteins. 25-Hydroxycholesterol, 22-hydroxycholesterol, 24-25-epoxycholesterol, and the secosteroids did not correlate with cholesterol and thus may exist free in the circulation or are bound to other carrier proteins as is the case for secosteroids [103]. Additional sterol-sterol correlations were detected among cholesterol biosynthesis intermediates may reflect the common regulation of this pathway by sterol regulatory element binding protein (SREBP) transcription factors (Fig. 3*B*).

A comparison of all possible pairs of analytes revealed numerous statistically significant associations between sterols. Fig. 3*A* shows that the levels of dietary plant sterols such as

sitosterol, campesterol, and stigmasterol correlated with each other as expected given that these sterols are substrates for the ABCG5/ABCG8 transporter, which is responsible both for their absorption from the diet in the gut and for their excretion from the liver [104]. Unexpectedly, serum levels of the cholesterol biosynthetic intermediate 14-desmethyl-lanosterol also correlated with plant sterols. This finding suggests an exogenous dietary origin for serum 14-desmethyl-lanosterol and that this sterol is an ABCG5/ABCG8 substrate. These suggestions are supported by the absence of correlations between 14-desmethyl-lanosterol and those of other intermediates in the cholesterol biosynthetic pathway such as lanosterol and lathosterol (Fig. 3*B*).

To identify genetic determinants contributing to differences in serum sterols and secosteroids, advantage was taken of the fact that 2109 individuals in the DHS2 population have been genotyped for 9,229 non-synonymous (amino acid-changing) sequence variants [105]. Each of these variants was tested for association with serum analyte levels measured in these same individuals. Strong associations ($P \geq 10^{-15}$) between three pairs of sterols and genes were identified, including *CYP39A1* and 24*S*-hydroxycholesterol, *EPHX2* and 24,25-epoxycholesterol, and *SDR42E1* and 8-dehydrocholesterol (Fig. 4).

24S-hydroxycholesterol

For the *CYP39A1* and 24*S*-hydroxycholesterol pair, the variant was a G to A transition that altered codon 103 in the gene from arginine to histidine (R103H). *CYP39A1* maps to chromosome 6p21.1 and encodes a conserved member of the cytochrome P450 family that is expressed in liver and metabolizes 24*S*-hydroxycholesterol to 7α,24-dihydroxycholesterol [71]. The fact that this variant was associated with a higher serum level of the oxysterol implied that R103H was a hypomorphic allele of *CYP39A1*. None of the other sequence variants tested in this genome-wide scan were associated with serum 24*S*-hydroxycholesterol levels (Fig. 4),

including those on chromosome 14 to which *CYP46A1* maps, which specifies the neuronal enzyme (cholesterol 24-hydroxylase) that synthesizes 24*S*-hydroxycholesterol (Fig. 5*A*) [106].

To determine if there were other *CYP39A1* variants that were positively associated with serum 24*S*-hydroxycholesterol levels, the 12 exons of the gene were sequenced in 30 DHS2 individuals with the highest 24*S*-hydroxycholesterol to cholesterol ratios. This resequencing revealed four additional non-synonymous sequence variants: R23P, T288H, N324K, and K329Q (Fig. 5*B*). Each of the five variant alleles in *CYP39A1* was recreated in an expression vector encoding the normal enzyme and the resulting plasmid DNAs were introduced into human embryonic kidney 293 cells. After a 24-h period of expression, 800 ng of 24*S*-hydroxycholesterol was added to the cellular medium and the incubation continued for an additional four h. Conversion of the oxysterol substrate to the 7α-hydroxylated product was then determined by mass spectrometry.

Fig. 5*C* shows averaged results from three separate transfection experiments in which each plasmid was assayed in triplicate dishes. Cells transfected with the vector alone (*Mock*) produced very little 7α,24-dihydroxycholesterol product. Introduction of the normal CYP39A1 cDNA (*WT*) converted approximately 30% of the substrate to product. In contrast, individual sequence variants reduced oxysterol 7α-hydroxylase activity from ~10% (T288H) to 100% (K329Q). The presence of the substitution mutations did not have an obvious effect on overall CYP39A1 mRNA or protein expression as judged by real-time PCR or immunoblotting (Fig. 5*D*), implying that these variants directly reduced enzyme activity.

To assess the unique and combined contributions of the *CYP39A1* alleles to inter-individual variation in serum 24*S*-hydroxycholesterol levels, the DHS2 population was genotyped for the four alleles identified by resequencing (R23P, T288H, N324K and K329Q). Table 1 summarizes the alleles, their frequencies in three major ethnic groups (African American, European American, and Hispanic), and the contributions of each allele to serum oxysterol variation.

Although the presence of each allele gave rise to an increase in serum 24*S*-hydroxycholesterol levels, two (R103H and N324K) made significantly larger contributions than the other three. The R103H allele made the largest contribution, accounting for 8.3% of inter-individual variation in the DHS2 population, while the N324K allele was responsible for 1.95% of the observed variation. Together, the five alleles explained 10.8% of the total variation observed for this trait.

The genotype and ancestry-related contributions of the *CYP39A1* alleles to serum 24*S*-hydroxycholesterol levels were determined next. As shown in Fig. 6*A*, the association between R103H genotype, which contributed the most to inter-individual variation, and this trait reached the highest significance ($P = 9.2 \times 10^{-36}$) of any allele in the whole DHS2 population, and was similarly strongly associated with this variable in African Americans ($P = 1.1 \times 10^{-16}$) and European Americans ($P = 4.6 \times 10^{-19}$) but far less so in Hispanics ($P = 3.7 \times 10^{-3}$). The data of Fig. 6*B* show that the association between N324K genotype and serum 24*S*-hydroxycholesterol level was less strong in the whole population ($P = 5.2 \times 10^{-10}$) and in African Americans and European Americans ($P = 3.7 \times 10^{-3}$ and 2.0×10^{-4}, respectively), but was more strongly associated in Hispanics ($P = 2.9 \times 10^{-7}$). The combined contribution of the five *CYP39A1* alleles to inter-individual variation in serum 24*S*-hydroxycholesterol levels is shown in Fig. 6*C*. Individuals with no variant *CYP39A1* alleles had on average the lowest levels of serum oxysterol whereas those with one or more variant alleles of a possible 10 had progressively higher levels. This genotype-phenotype relationship was highly significant ($P = 1.5 \times 10^{-34}$).

The observation that variant alleles in *CYP39A1* explained only 10.8% of inter-individual variation in serum 24*S*-hydroxycholesterol levels, together with the shape of the distribution curves for this trait (Fig. 1*C*,*D*), suggested that there were other determinants that contributed to the observed variability. Earlier studies in a small number of subjects with cognitive impairment revealed a modestly significant association ($P = 0.03$) between grey matter volume and serum 24*S*-hydroxycholesterol levels [107], and based on indirect measurements, a similar relationship

was detected between the size of the brain and the capacity of the liver to metabolize the oxysterol [108].

To determine whether brain anatomy influenced serum 24*S*-hydroxycholesterol levels in the DHS2, MRI was used to measure total brain, grey matter, and white matter volumes in 2109 participants. These measurements were adjusted for age, race, gender, and cholesterol levels prior to their correlation with oxysterol levels in these individuals. Male and female values were separated in these comparisons to control for the known sexual dimorphism in brain size [109]. Total brain volume was modestly but significantly correlated with oxysterol levels in men and women ($r = 0.21$ in men, $r = 0.16$ in women; $P = 5.5 \times 10^{-5}$ and 2.5×10^{-4}, respectively). Grey matter volume in both females and males was strongly correlated with serum 24*S*-hydroxycholesterol levels (Fig. 7), whereas the association with white matter volume was weaker than that for grey matter but reached statistical significance (Fig. 7). Grey matter volume under lied 1.75% of variance in serum 24*S*-hydroxycholesterol levels after adjustment for white matter volume. White matter was not significantly associated with this trait after accounting for grey matter volume and therefore explained no meaningful variance. Total brain volume explained the same amount of variance (1.75%) as did grey matter volume. We interpret these results to indicate that grey matter volume is directly related to serum 24*S*-hydroxycholesterol levels while white matter is only indirectly associated through correlation to grey matter volume.

24,25-epoxycholesterol

Fig. 8*A* shows the levels of 24,25-epoxycholesterol in the 3,230 DHS serum samples analyzed. The mean concentration of this oxysterol in the population was 1.8 ng/ml and the levels of this sterol ranged from 0.1 to 56.2 ng/ml. Levels of 24,25-epoxycholesterol showed a lognormal distribution with positive skewing (Fig. 8*B*,*C*), suggesting that multiple independent variables affect this trait. To identify genetic determinants contributing to differences in 24,25-

epoxycholesterol levels, 9,229 non-synonymous (amino acid-changing) sequence variants were tested for association with serum 24,25-epoxycholesterol levels. A strong association ($P = 9.5 \times 10^{-25}$) between epoxide hydrolase 2 gene (*EPHX2*) and 24,25-epoxycholesterol was found to exist with no other sequence variants tested in the genome-wide scan found to associate with serum 24,25-epoxycholeseterol levels (Fig. 4).

The variant in *EPHX2* was a G to A transition at nucleotide 860 that resulted in a missense mutation at codon 287 resulting in an arginine to glutamine (R287Q). The variant allele associated with increased levels of 24,25-epoxycholesterol in all ethnicities. As shown in Fig. 8*D*, the association between R287Q genotype, which contributed the most to inter-individual variation, and this trait reached levels of high significance ($P = 9.5 \times 10^{-25}$) of any allele in the whole DHS2 population, and was similarly associated with this variable in European Americans ($P = 8.0 \times 10^{-4}$) and Hispanics ($P = 1.0 \times 10^{-4}$) but more strongly associated in African Americans ($P = 4.5 \times 10^{-15}$).

EPHX2 maps to chromosome 8p12 and encodes a soluble epoxide hydrolase and consists of 19 exons encoding 555 amino acids. The enzyme is ubiquitously expressed and found in tissues such as the liver, kidney, heart, and ovary. The protein is found in both the cytosol and peroxisomes of cells and binds to specific epoxides and converts them to corresponding dihydrodiols. Epoxy lipids are potent vasodilators, can inhibit platelet aggregation, promote fibrinolysis, and have anti-inflammatory properties. Mutations in *EPHX2* have been associated with familial hypercholesterolemia and alternatively spliced variants have been described [110]. The fact that this variant was associated with a higher serum level of 24,25-epoxycholesterol implied that R287Q was a hypomorphic allele of *EPHX2*.

The R287Q variant allele has been recreated in an expression vector encoding the normal enzyme and the plasmid DNAs were introduced into human embryonic kidney 293 cells. After a 24-h period of expression, 1200 ng of 24,25-epoxycholesterol was added to the cellular medium

and the incubation of the substrate continued for an additional 2 h. Conversion of the epoxy sterol to an unknown substrate was then determined by mass spectrometry to measure the levels of 24,25-epoxycholesterol catabolism and determine the functional role of EPHX2 on 24,25-epoxycholesterol.

Fig. 9*A,B* shows the averaged results from three separate transfection experiments in which each plasmid was assayed in triplicate dishes. Cells transfected with the vector alone (*Mock*) showed no metabolism of 24,25-epoxycholesterol. Introduction of the normal EPHX2 cDNA (*WT*) converted approximately 50% of the substrate to product. In contrast, the R287Q sequence variant reduced epoxide hydrolase activity by 25%. An unknown peak suspected to be cholest-5-en-3β,24*S*,25-triol based on its chromatographic retention time and known role of the enzyme, appeared in cells transfected with wild-type EPHX2 and to a lesser degree R287Q EPHX2 (Fig. 9*B*) but not in cells transfected with vector alone (*Mock*). Due to the lack of a deuterated internal standard, we are unable to quantitate the amount synthesized in ng/mL and are only able to calculate a peak area. We can only conclusively say that this peak appears when transfected with EPHX2 cDNA and the conversion of 24,25-epoxycholesterol into cholest-5-en-3β,24*S*,25-triol occurs more rapidly in cells transfected with *WT EPHX2* and is retarded in R287Q *EPHX2* transfected cells.

8-dehydrocholesterol

Our attention first came to focus on 8-dehydrocholesterol when observing sterol 7-dehydrocholesterol, a well characterized sterol. 7-dehydrocholesterol is an intermediate in the Kandutsch-Russell pathway of cholesterol biosynthesis and in the skin, kidney, and liver is the precursor to activated vitamin D_3. Mutations in *DHCR7* result in Smith-Lemli-Opitz and a buildup of 7 dehydrocholesterol is a hallmark of this disease. Fig. 10*A* shows the raw data of levels of 7-dehydrocholesterol in the 3,230 DHS serum samples analyzed. The mean concentration of this sterol in the population was 642.4 ng/ml and range from 7.4 ng/ml to 21.1

µg/ml. Levels of 7-dehydrocholesterol showed a lognormal distribution with positive skewing (Fig. 10*C*,*D*), suggesting that multiple independent variables affect this trait. Comparisons between the levels of 7-dehydrocholesterol and those of other sterols and secosteroids revealed statistically significant correlations with 8-dehydrocholesterol (r = .65) (Fig. 10*D*).

Fig. 11*A* shows the levels of 8-dehydrocholesterol in the 3,230 DHS serum samples analyzed. The mean concentration of this sterol in the population was 765.2 ng/ml and the range 142.4 ng/ml to 11.8 µg/ml. Levels of 8-dehydrocholesterol like most sterols measured, also showed a lognormal distribution with positive skewing (Fig. 11*B,C*), suggesting that multiple independent variables affect this trait. Genetic determinants that contribute to differences in 8-dehydrocholesterol levels were identified by testing the association of 9,229 non-synonymous sequence variants with serum 8-dehydrocholesterol levels [105]. A strong association ($P = 1.5 \times 10^{-15}$) between short-chain dehydrogenase/reductase family 42E member 1 (*SDR42E1*) and 8-dehydrocholesterol was found to exist with no other sequence variants tested in the genome-wide scan found to associate with serum 8-dehydrocholesterol levels (Fig. 4).

The variant in *SDR42E1* was a C to G transversion that resulted in a missense mutation at codon 10 in the gene resulting in a serine to threonine (S10T) amino acid substitution. *SDR42E1* maps to chromosome 16q23.3 and is a member of the short chain dehydrogenase/reductase family and consists of 12 exons encoding a 393 amino acid protein. There is no known biological role or function of SDR42E1 and no known mutations in *SDR42E1* have been described. The fact that this variant was associated with a lower serum level of 8-dehydrocholesterol implies that S10T was a hypermorphic allele of *SDR42E1*. The variant allele associated with decreased levels of 8-dehydrocholesterol in all ethnic groups. As shown in Fig. 11*D*, the association between S10T genotype, which contributed the most to inter-individual variation, and this trait reached levels of high significance in the DHS2 population, and was similarly associated with this variable in European Americans ($P = 3.8 \times 10^{-3}$) and Hispanics

($P = 2.3 \times 10^{-3}$) but more strongly associated with decreased levels of 8-dehydrocholesterol in African Americans ($P = 8.4 \times 10^{-13}$).

To determine if there were other *SDR42E1* variants that were associated with serum 8-dehydrocholesterol levels, the 2 exons of the gene were sequenced in 10 DHS2 individuals with the lowest 8-dehydrocholesterol to cholesterol ratios. This resequencing revealed four additional non-synonymous sequence variants: Q30X, R87Q, N91S, and K96E. To determine if there were other *SDR42E1* variants that were negatively associated with serum 8-dehydrocholesterol levels, the entire DHS2 population (n = 3230) were regenotyped through the Illumina Exome Chip which contains ~250,000 SNPs. This regenotyping revealed two additional non-synonymous sequence variants in *SDR42E1*: K96E ($P = 4.8 \times 10^{-59}$) that was associated with decreased levels of 8-dehydrocholesterol and Q30X ($P = 3.95 \times 10^{-12}$), a non-sense mutation associated with increased levels of 8-dehydrocholesterol.

The combined contribution of the *SDR42E1* alleles to inter-individual variation in serum 24*S*-hydroxycholesterol levels is shown in Fig. 12. Individuals who had no variant *SDR42E1* alleles associated with decreased levels of 8-dehydrocholesterol had on average the highest levels of serum sterol whereas those with one or more variant alleles of a possible 5 had progressively lower levels (Fig. 12*A*). This genotype-phenotype relationship was highly significant ($P = 3.0 \times 10^{-50}$). Individuals who had no variant *SDR42E1* alleles associated with increased levels of 8-dehydrocholesterol (Fig. 12*B*) had on average the lowest levels of serum sterol whereas those with one or two variant alleles had on average the highest levels of serum sterol. This genotype-phenotype relationship was significant ($P = 3.0 \times 10^{-10}$).

The S10T missense mutation has been recreated in an expression vector encoding the normal enzyme and the plasmid DNAs were introduced into human embryonic kidney 293 cells. After a 24-h period of expression, 350 ng of either 8-dehydrocholesterol or 7-dehydrocholesterol was added to the cellular medium and the incubation continued for an additional 4 h.

Conversion of the sterol was then determined by mass spectrometry to determine the enzymatic role of SDR42E1 on 7- or 8-dehydrocholesterol levels.

Fig. 13 shows averaged results from three separate transfection experiments in which each plasmid was assayed in triplicate dishes. Cells transfected with the vector alone (*Mock*) showed no metabolism of 7-dehydrocholesterol when added as substrate. Introduction of the normal SDR42E1 cDNA (*WT*) and S10T sequence variant showed no changes in metabolism of 7-dehydrocholesterol compared to *Mock* (Fig. 13*A*). Cells transfected with the vector alone (*Mock*) showed no metabolism of 8-dehydrocholesterol when added as substrate. Introduction of the normal SDR42E1 cDNA (*WT*) and S10T sequence variant showed no changes in metabolism of 7-dehydrocholesterol compared to *Mock* (Fig. 13*B*). Fig. 13*C* shows cells transfected with empty vector, SDR42E1 cDNA (*WT*) and S10T sequence variant with no addition of either 7- or 8-dehydrocholesterol as substrate to determine the endogenous levels of these sterols in human embryonic kidney 293 cells.

DISCUSSION

The data in this paper provide evidence that genetic determinants of at least two sterols, one known (*CYP39A1* and 24*S*-hydroxycholesterol) and one unknown (*EPHX2* and 24,25-epoxycholesterol), have been identified with work continuing to elucidate a biochemical relationship between sterol 8-dehydrocholesterol and *SDR42E1*.

With respect to 24*S*-hydroxycholesterol and *CYP39A1*, our findings show that inter-individual differences in the levels of this oxysterol vary over a 30-fold range and arise in part from disparities in serum cholesterol levels, genetic variation in the CYP39A1 oxysterol 7α-hydroxylase, and the volume of grey matter in the brain. These observations are consistent with a metabolic pathway in which 24*S*-hydroxycholesterol is formed in the brain, exported into the blood stream, and there associates with circulating cholesterol-rich lipoproteins. Clearance of

these lipoproteins by the liver delivers the oxysterol to the catabolic CYP39A1 enzyme, resulting in the formation of 7α,24-dihydroxycholesterol, an intermediate in bile acid synthesis.

In total, we identified five variant alleles in the CYP39A1 oxysterol 7α-hydroxylase gene that correlated with increased levels of 24*S*-hydroxycholesterol. These alleles displayed an additive effect with respect to increasing 24*S*-hydroxycholesterol levels when multiple alleles were inherited. This effect was observed in African American, European American, and Hispanic ethnic groups, with different allele combinations more prevalent in different ethnic groups. No phenotypic consequences as a result of the inheritance of these alleles or of increased levels of 24*S*-hydroxycholesterol have yet been identified in this patient cohort. Four out of five SNPs were detected in homozygous form and one allele, K329Q, which caused complete loss of function in CYP39A1 enzyme activity as judged by transfection analysis, was detected only in heterozygous form. The allele frequency of K392Q is too low in the population (.00137) to determine whether the absence of homozygosity is detrimental.

Inter-individual differences in human serum 24,25-epoxycholesterol levels vary over a 500-fold range and arise in part from genetic variation in epoxide hydrolase 2. This epoxysterol arises from a shunt pathway that diverges from the cholesterol biosynthetic pathways [9]. Oxysterols such as 24,25-epoxycholesterol inhibit SREBPs that regulate cholesterol synthesis and are also activating ligands for LXRs [111]. Prior to this work, the catabolism of 24,25-epoxycholesterol had not been defined. The current studies show that 24,25-epoxycholesterol is metabolized to cholest-5-en-3β,24*S*,25-triol in an EPHX2-dependent manner. The role of cholest-5-en-3β,24*S*,25-triol in biology remains to be determined.

Inter-individual differences in serum 8-dehydrocholesterol levels vary over an 80-fold range and arise in part from disparities in cholesterol levels, 7-dehydrocholesterol levels, and genetic variation in the SDR42E1 short-chain dehydrogenase/reductase family 42E member 1.

Transfecting SDR42E1 expression vectors into cultured cells did not affect the metabolism of 7- or 8-dehydrocholesterol suggesting either that the observed genetic linkage to *SDR42E1* and these sterols is either indirect or that the encoded protein requires one or more partners to act on these substrates. The fact that variation in *SDR42E1* correlated with serum 8-dehydrocholesterol levels but not 7-dehydrocholesterol levels suggests that this enzyme may not be involved in the isomerization of these two related sterols.

Subsequent regenotyping data has revealed two additional non-synonymous sequence variants in *SRD42E1* that are negatively and positively associated with inter-individual variation in 8-dehydrocholesterol; we are currently performing transfection experiments to assess the effects of these SNPs on SRD42E1 activity. The high level of significance at which these two variants are associated with 8-dehydrocholesterol levels and the lack of biochemical effect associated with the S10T mutation may suggest that the latter variant is benign but in genetic disequilibrium with the former variants.

Many questions remain to be answered by future sterol research. First, are there any phenotypic consequences arising from alterations in *CYP39A1* and the subsequent increased levels of 24*S*-hydroxycholesterol? Second, as no human mutations were identified in cholesterol 24-hydroxylase encoded by *CYP46A1* in the population analyzed here, will expansion of the population size identify mutations or do mutations result in such severe phenotypic consequences that there is selection against them? Third, what are the biological functions if any of cholest-5-en-3β,24*S*,25-triol? What are the phenotypic consequences that result from mutations in *EPHX2*? Fourth, how is 8-dehydrocholesterol formed? Is there a metabolic relationship between 7- and 8-dehydrocholesterol? Is this conversion dependent upon SDR42E1? Why do we not see a common gene that associates with both 7- and 8-dehydrocholesterol if this reaction proceeds through one reaction catalyzed by a single

enzyme? Lastly, what other genetic variants exist that result in an increases or decreases in sterol levels?

Table 1. Association of variant alleles to 24*S*-hydroxycholesterol levels normalized to cholesterol.

Association with 24*S*-Hydroxycholesterol Normalized to Cholesterol

				MAF					Adjusted		
SNP	Chr.	Pos*	AA change	Afr. Am.	Eur. Am.	Hispanic	Effect	Beta	P-value	P-value**	Partial R^2
rs41273654	6	46671763	K/Q	0.21	0.65	0.11	+	0.1765	0.0076	0.0038	0.36%
rs7761731	6	46671776	N/K	36.20	73.41	60.43	+	0.0505	5.18×10^{-10}	8.25×10^{-10}	1.95%
rs17856332	6	46701183	Y/H	0.49	1.55	1.60	+	0.0199	0.6278	0.2718	0.01%
rs2277119	6	46717864	R/H	21.97	21.19	13.89	+	0.1208	9.17×10^{-10}	3.04×10^{-10}	8.32%
rs12192544	6	46728211	R/P	5.18	23.37	14.00	+	0.0199	0.1051	0.6681	0.13%

***NCBI36/hg18**

****After controlling for the other 4 SNPs**

Figure 1. Raw data, distribution, and association between cholesterol and 24*S*-hydroxycholesterol levels. *A*, Levels of 24*S*-hydroxycholesterol show and *C* - D, lognormal distribution of 24*S*-hydroxycholesterol normalized to cholesterol in 3,320 Dallas Heart Study individuals. *B*, Relationship between cholesterol and 24*S*-hydroxycholesterol. The solid line, fitted by least squares, summarizes the relationship. r denotes Spearman's rank correlation coefficient. Logarithmic scale is used for the horizontal and vertical axes.

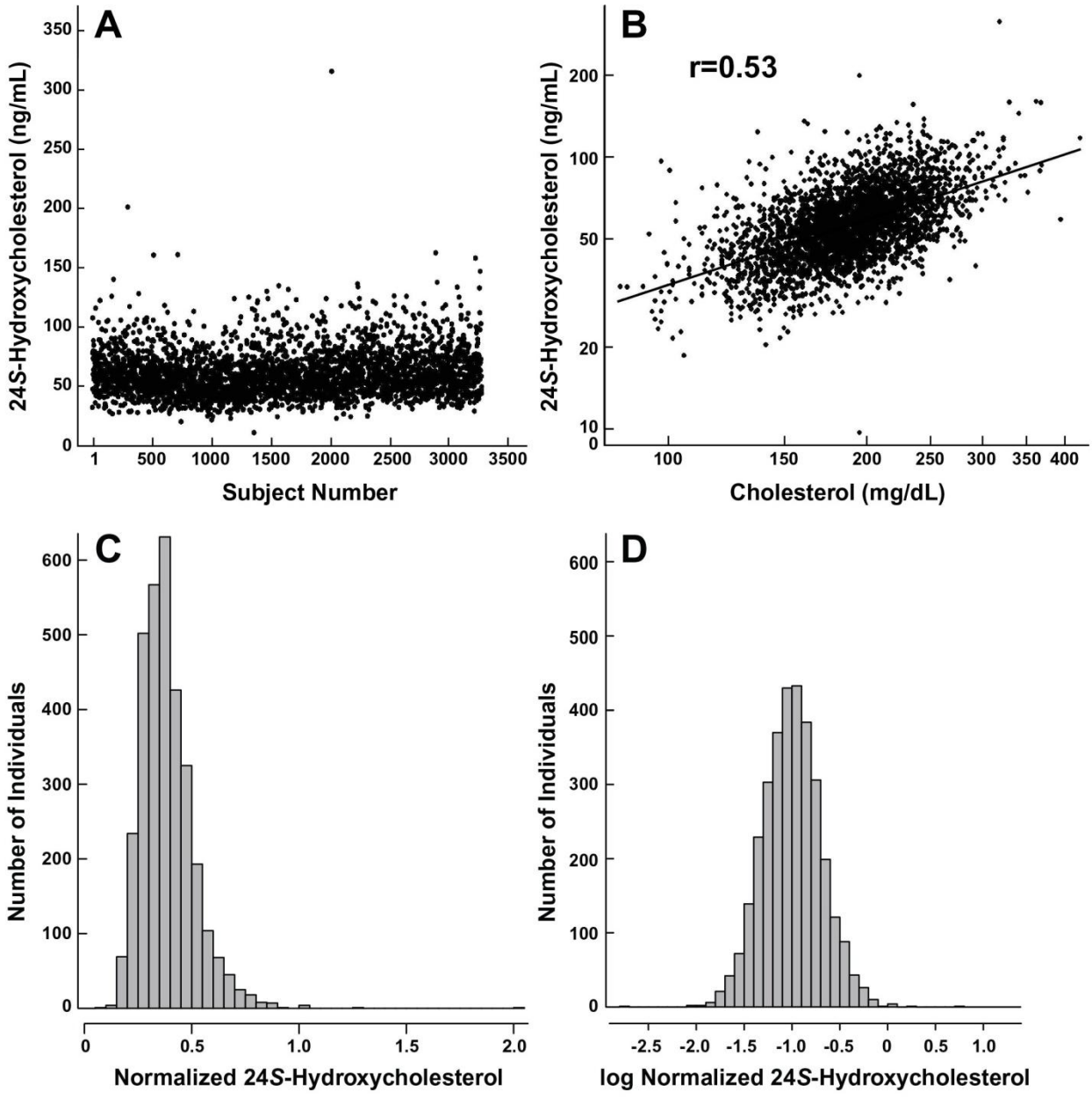
A
24S-Hydroxycholesterol (ng/mL)
Subject Number
B
r=0.53
24S-Hydroxycholesterol (ng/mL)
Cholesterol (mg/dL)
C
Number of Individuals
Normalized 24S-Hydroxycholesterol
D
Number of Individuals
log Normalized 24S-Hydroxycholesterol

Figure 2. Sterol-sterol correlation coefficients. Empty boxes represent no correlation. Shaded boxes represent negative correlations and all else represents positive correlations. A correlation coefficient ≥ │.04 │ is significant.

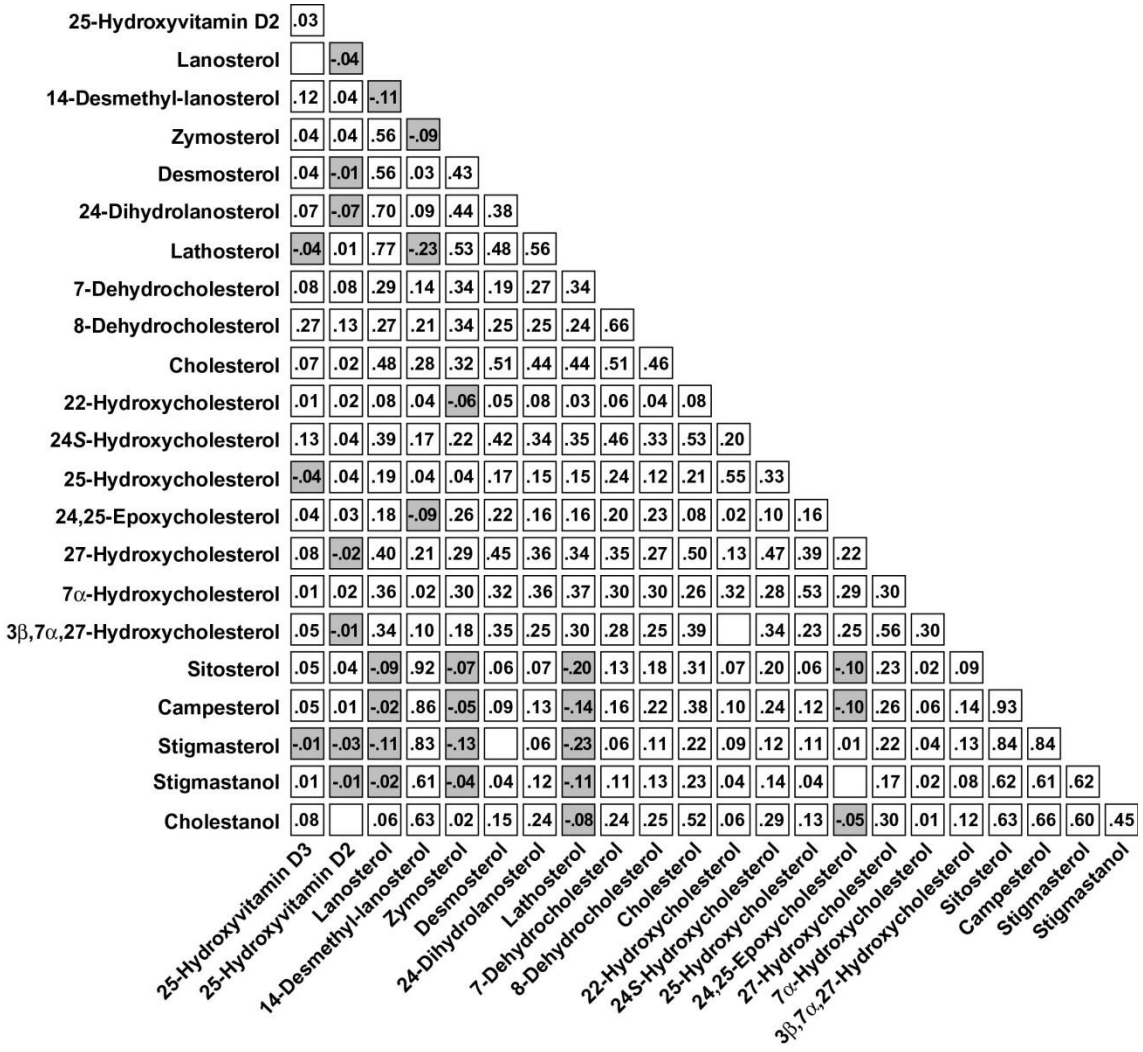
25-Hydroxyvitamin D2 .03
Lanosterol -.04
14-Desmethyl-lanosterol .12 .04 -.11
Zymosterol .04 .04 .56 -.09
Desmosterol .04 -.01 .56 .03 .43
24-Dihydrolanosterol .07 -.07 .70 .09 .44 .38
Lathosterol -.04 .01 .77 -.23 .53 .48 .56
7-Dehydrocholesterol .08 .08 .29 .14 .34 .19 .27 .34
8-Dehydrocholesterol .27 .13 .27 .21 .34 .25 .25 .24 .66
Cholesterol .07 .02 .48 .28 .32 .51 .44 .44 .51 .46
22-Hydroxycholesterol .01 .02 .08 .04 -.06 .05 .08 .03 .06 .04 .08
24S-Hydroxycholesterol .13 .04 .39 .17 .22 .42 .34 .35 .46 .33 .53 .20
25-Hydroxycholesterol -.04 .04 .19 .04 .04 .17 .15 .15 .24 .12 .21 .55 .33
24,25-Epoxycholesterol .04 .03 .18 -.09 .26 .22 .16 .16 .20 .23 .08 .02 .10 .16
27-Hydroxycholesterol .08 -.02 .40 .21 .29 .45 .36 .34 .35 .27 .50 .13 .47 .39 .22
7α-Hydroxycholesterol .01 .02 .36 .02 .30 .32 .36 .37 .30 .30 .26 .32 .28 .53 .29 .30
3β,7α,27-Hydroxycholesterol .05 -.01 .34 .10 .18 .35 .25 .30 .28 .25 .39 .34 .23 .25 .56 .30
Sitosterol .05 .04 -.09 .92 -.07 .06 .07 -.20 .13 .18 .31 .07 .20 .06 -.10 .23 .02 .09
Campesterol .05 .01 -.02 .86 -.05 .09 .13 -.14 .16 .22 .38 .10 .24 .12 -.10 .26 .06 .14 .93
Stigmasterol -.01 -.03 -.11 .83 -.13 .06 -.23 .06 .11 .22 .09 .12 .11 .01 .22 .04 .13 .84 .84
Stigmastanol .01 -.01 -.02 .61 -.04 .04 .12 -.11 .11 .13 .23 .04 .14 .04 .17 .02 .08 .62 .61 .62
Cholestanol .08 .06 .63 .02 .15 .24 -.08 .24 .25 .52 .06 .29 .13 -.05 .30 .01 .12 .63 .66 .60 .45
25-Hydroxyvitamin D3
25-Hydroxyvitamin D2
Lanosterol
14-Desmethyl-lanosterol
Zymosterol
Desmosterol
24-Dihydrolanosterol
Lathosterol
7-Dehydrocholesterol
8-Dehydrocholesterol
Cholesterol
22-Hydroxycholesterol
24S-Hydroxycholesterol
25-Hydroxycholesterol
24,25-Epoxycholesterol
27-Hydroxycholesterol
7α-Hydroxycholesterol
3β,7α,27-Hydroxycholesterol
Sitosterol
Campesterol
Stigmasterol
Stigmastanol

Figure 3. Relationship between sterols in the Dallas Heart Study. *A,* shows the correlation plot of sterols regulated by *ABCG5/ABCG8* with 25-hydroxy-vitamin D_3 as a negative control. *B,* shows correlation of cholesterol biosynthetic intermediates with 14-desmethyl-lanosterol as a negative control.

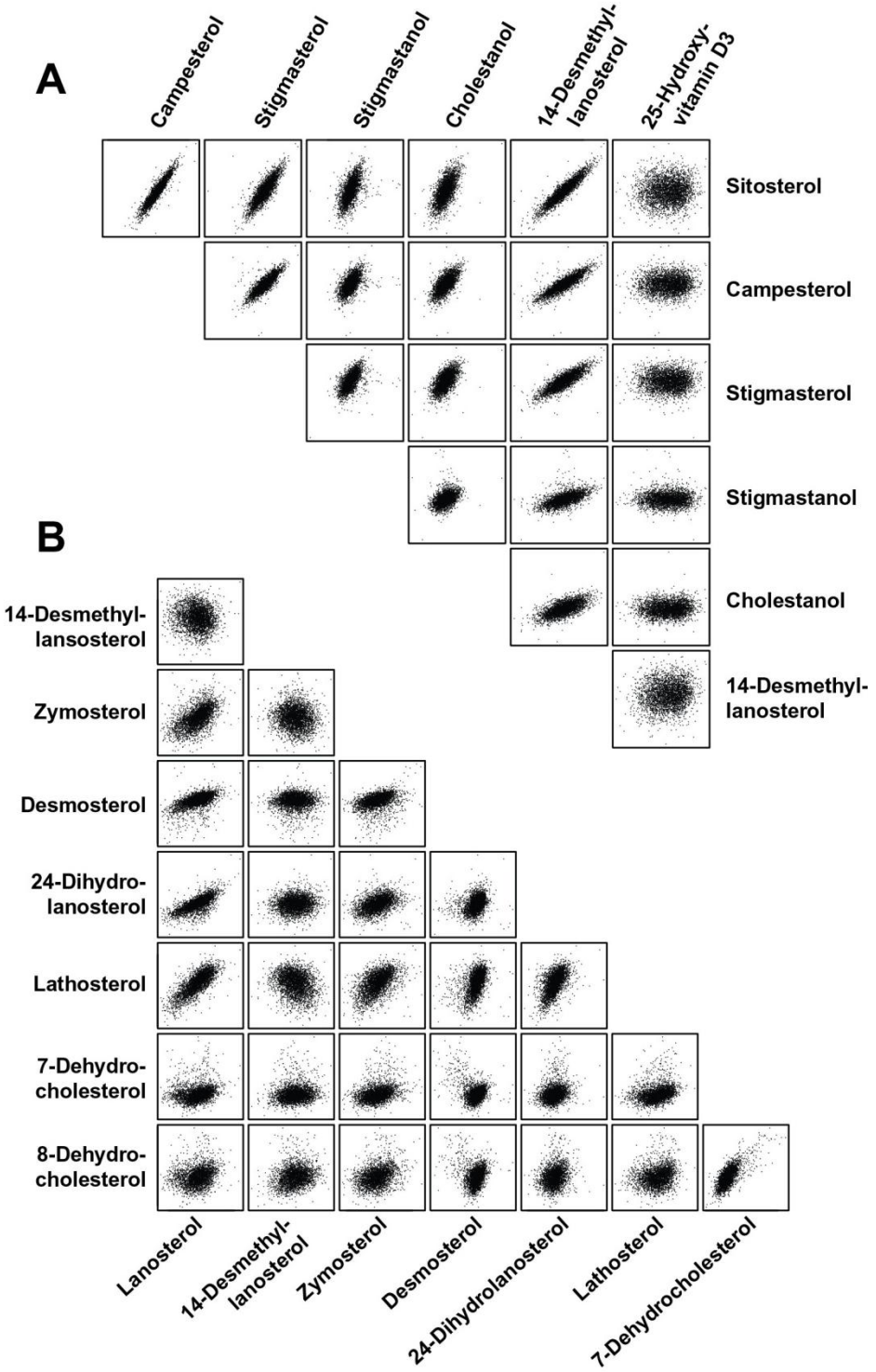
A
Campesterol
Stigmasterol
Stigmastanol
Cholestanol
14-Desmethyl-lanosterol
25-Hydroxy-vitamin D3
Sitosterol
Campesterol
Stigmasterol
Stigmastanol
Cholestanol
14-Desmethyl-lanosterol
B
14-Desmethyl-lansosterol
Zymosterol
Desmosterol
24-Dihydro-lanosterol
Lathosterol
7-Dehydro-cholesterol
8-Dehydro-cholesterol
Lanosterol
14-Desmethyl-lanosterol
Zymosterol
Desmosterol
24-Dihydrolanosterol
Lathosterol
7-Dehydrocholesterol

Figure 4. Genome-wide scan of 24*S*-hydroxycholesterol, 24,25-epoxycholesterol, and 8-dehydrocholesterol levels measured by mass-spectrometry in the Dallas Heart Study. Manhattan plot of *P* values. The dashed line denotes the Bonferroni-corrected significance threshold ($P = 5.4 \times 10^{-6}$).

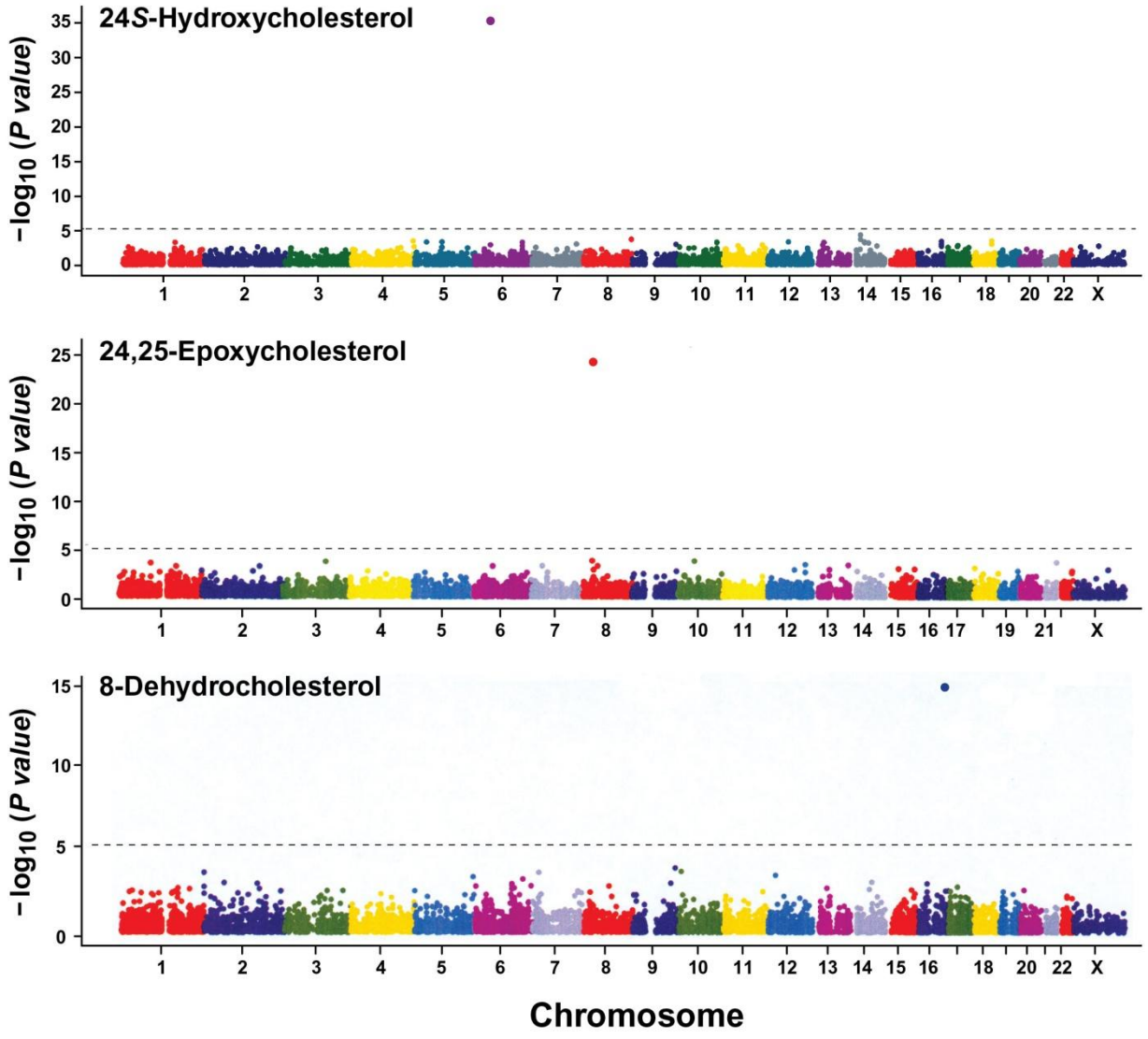
24S-Hydroxycholesterol
24,25-Epoxycholesterol
8-Dehydrocholesterol
−log10 (P value)
Chromosome

Figure 5. Association between sequence variants in *CYP39A1* (rs12192544, rs2277119, rs17856332, rs7761731, and rs41273654) and 24*S*-hydroxycholesterol levels. *A*, Steps and enzymes involved in the synthesis of 24*S*-hydroxycholesterol and 7α,24-dihydroxycholesterol. *B*, CYP39A1 is encoded by 12 exons. Mutations are found in exons 1, 2, 7 and 8. *C*, Transfection of *CYP39A1* mutant cDNA in to human embryonic 293 cells shows decreased enzymatic function as measured by conversion of 24*S*-hydroxycholesterol in to 7α,24-dihydroxycholesterol with no change in protein level. (* = P ≤ .05), (*** = P ≤ .001), (R103H from SNP analysis, R23P, T288H, N324K, and K329Q from sequencing of 30 individuals).

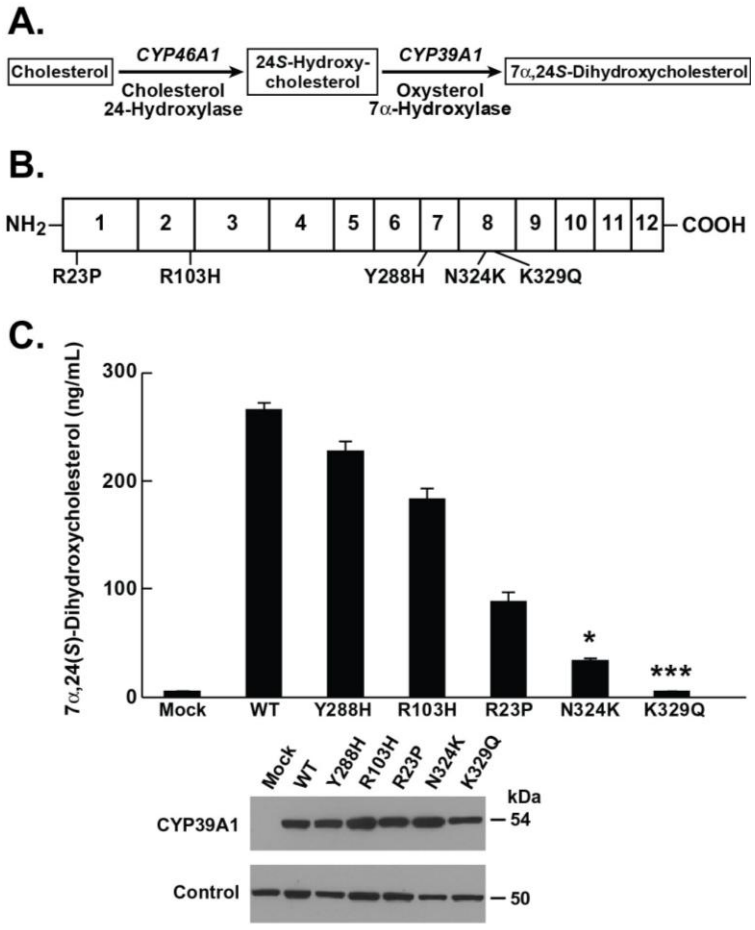
A.
Cholesterol
CYP46A1
Cholesterol 24-Hydroxylase
24S-Hydroxy-cholesterol
CYP39A1
Oxysterol 7α-Hydroxylase
7α,24S-Dihydroxycholesterol
B.
NH2
1
2
3
4
5
6
7
8
9
10
11
12
COOH
R23P
R103H
Y288H
N324K
K329Q
C.
7α,24(S)-Dihydroxycholesterol (ng/mL)
300
200
100
0
*
***
Mock
WT
Y288H
R103H
R23P
N324K
K329Q
Mock
WT
Y288H
R103H
R23P
N324K
K329Q
kDa
CYP39A1
54
Control
50

Figure 6. Association between sequence variants and 24*S*-hydroxycholesterol levels stratified by ethnicity. *A*-*B*, Median 24*S*-hydroxycholesterol levels normalized to cholesterol for individuals by *CYP39A1* genotype (*A*, rs2277119 and *B*, rs7761731; y-axis is in the log scale). *C*, Median 24*S*-hydroxycholesterol levels normalized to cholesterol for individuals by the presence of variants in *CYP39A1*. Logarithmic scale is used for all vertical axes.

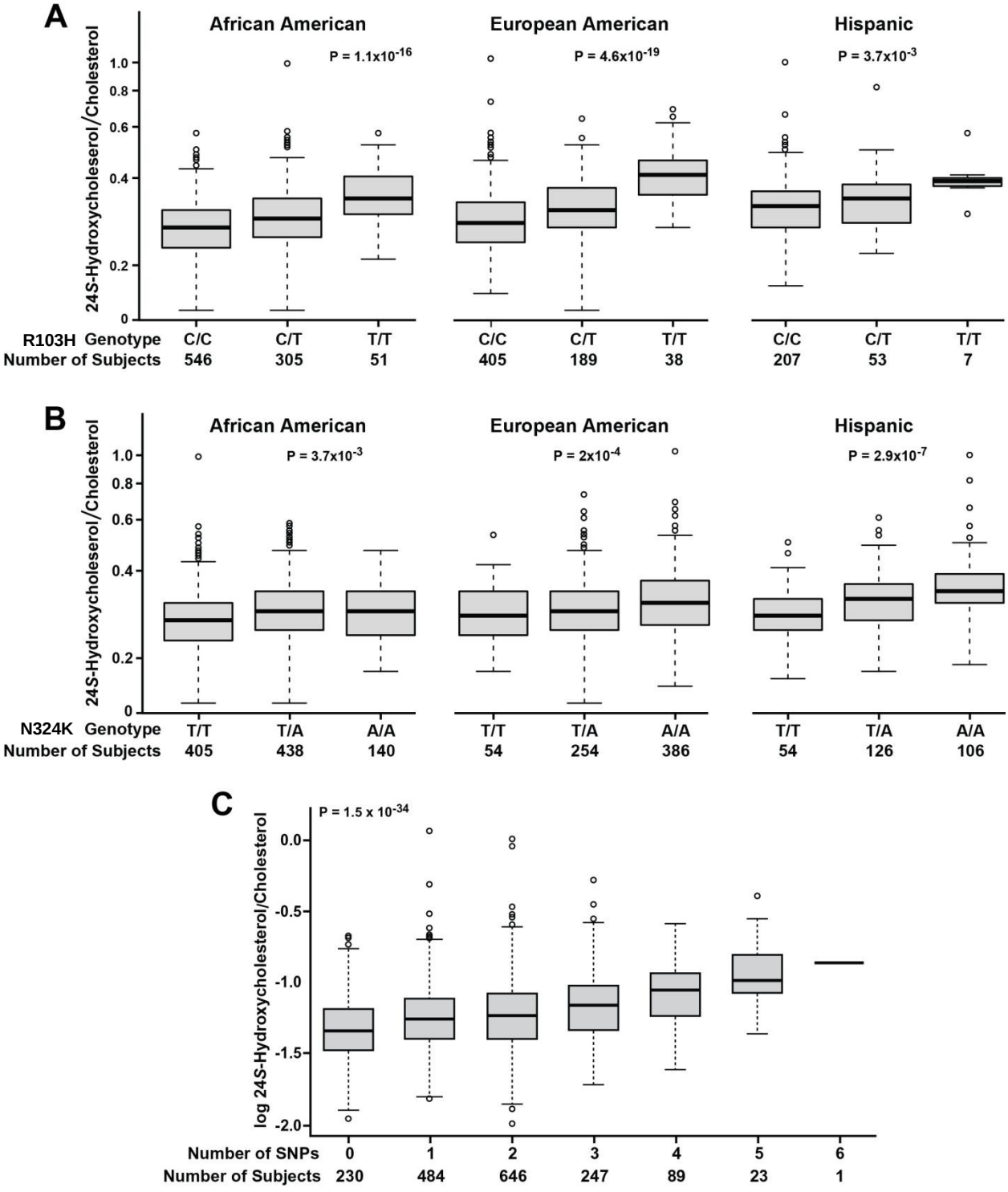
A
African American
European American
Hispanic
P = 1.1x10-16
P = 4.6x10-19
P = 3.7x10-3
24S-Hydroxycholesterol/Cholesterol
1.0
0.8
0.6
0.4
0.2
0
R103H Genotype C/C C/T T/T C/C C/T T/T C/C C/T T/T
Number of Subjects 546 305 51 405 189 38 207 53 7
B
African American
European American
Hispanic
P = 3.7x10-3
P = 2x10-4
P = 2.9x10-7
24S-Hydroxycholesterol/Cholesterol
1.0
0.8
0.6
0.4
0.2
0
N324K Genotype T/T T/A A/A T/T T/A A/A T/T T/A A/A
Number of Subjects 405 438 140 54 254 386 54 126 106
C
P = 1.5 x 10-34
log 24S-Hydroxycholesterol/Cholesterol
0.0
-0.5
-1.0
-1.5
-2.0
Number of SNPs 0 1 2 3 4 5 6
Number of Subjects 230 484 646 247 89 23 1

Figure 7. Relationship between grey and white matter and 24*S*-hydroxycholesterol levels normalized to cholesterol stratified by gender. The logarithmic scale is used for the horizontal and vertical axes. The solid line, fitted by least squares, summarizes the relationship. r denotes Spearman's rank correlation coefficient.

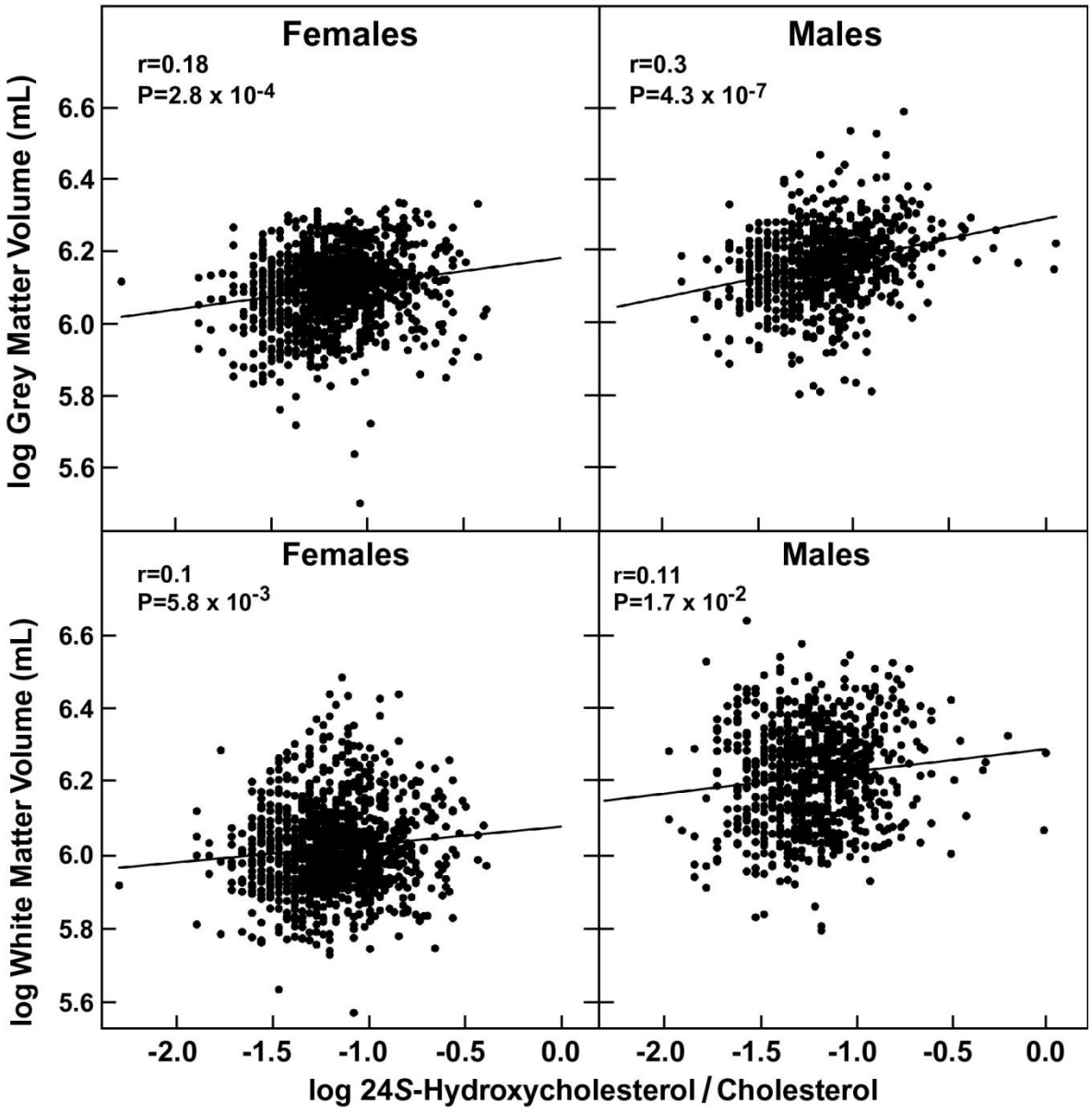
Females
r=0.18
P=2.8 x 10-4
Males
r=0.3
P=4.3 x 10-7
Females
r=0.1
P=5.8 x 10-3
Males
r=0.11
P=1.7 x 10-2
log Grey Matter Volume (mL)
log White Matter Volume (mL)
6.6
6.4
6.2
6.0
5.8
5.6
-2.0
-1.5
-1.0
-0.5
0.0
log 24S-Hydroxycholesterol / Cholesterol

Figure 8. Raw data, distribution, and association between sequence variant (rs751141) and 24,25-epoxycholesterol levels. *A*, Levels of 24,25-epoxycholesterol and *B* - *C*, lognormal distribution of 24,25-epoxycholesterol in 3,320 Dallas Heart Study individuals. *D*, Median 24,25-epoxycholesterol levels and *EPHX2* rs751141 genotypes in African Americans, European Americans and Hispanics. Associations between 24,25-epoxycholesterol levels and *EPHX2* rs751141 genotypes were tested using ANOVA with age, gender, and BMI as covariates. Logarithmic scale is used for the y-axis.

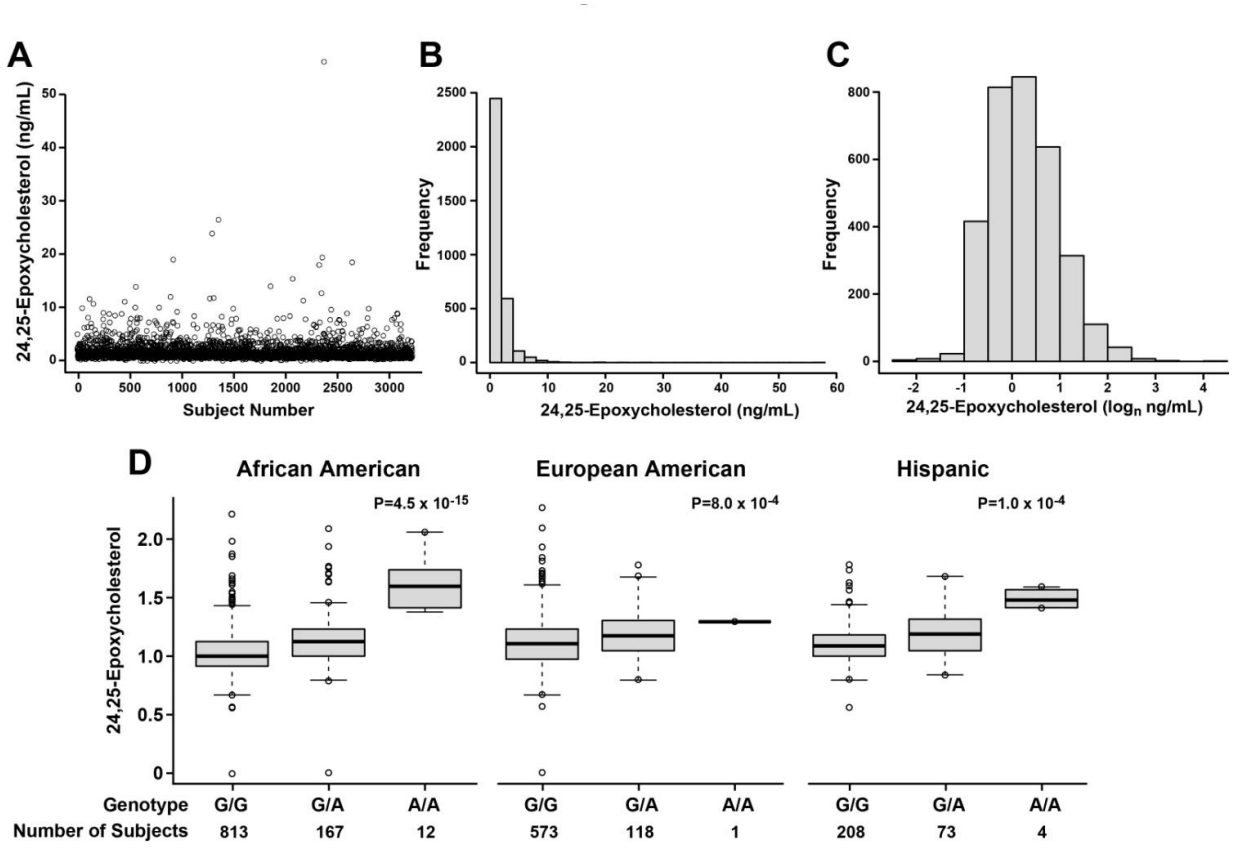
A
24,25-Epoxycholesterol (ng/mL)
Subject Number
B
Frequency
24,25-Epoxycholesterol (ng/mL)
C
Frequency
24,25-Epoxycholesterol (log$_n$ ng/mL)
D
African American
European American
Hispanic
P=4.5 x 10^{-15}
P=8.0 x 10^{-4}
P=1.0 x 10^{-4}
24,25-Epoxycholesterol
Genotype G/G G/A A/A G/G G/A A/A G/G G/A A/A
Number of Subjects 813 167 12 573 118 1 208 73 4

Figure 9. Rates of 24,25-epoxycholesterol metabolism in human embryonic kidney 293 cells transfected with *EPHX2* wild-type and mutant cDNA. *A* - *B*, There was no conversion of 24,25-epoxycholesterol into cholest-5-en-3β,24*S*,25-triol in cells transfected with empty vector. 50% of 24,25-epoxycholesterol was metabolized in *EPHX2* wild-type (*WT*) with 33% of 24,25-epoxycholesterol converted in *EPHX2* mutant (*R287Q*) into cholest-5-en-3β,24*S*,25-triol.

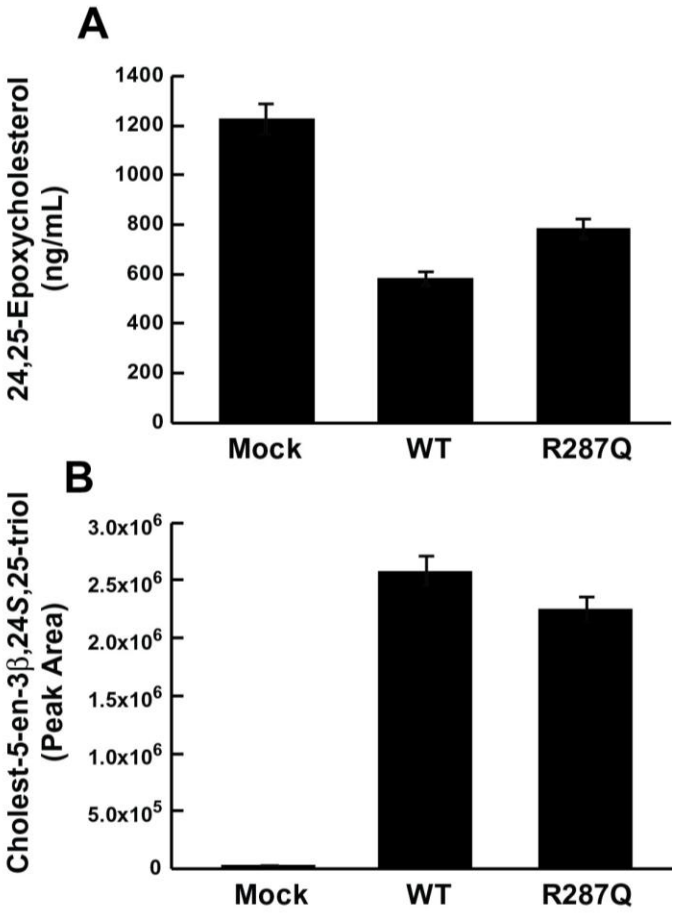
A
24,25-Epoxycholesterol (ng/mL)
1400
1200
1000
800
600
400
200
0
Mock
WT
R287Q
B
Cholest-5-en-3β,24S,25-triol (Peak Area)
3.0x10^6
2.5x10^6
2.0x10^6
1.5x10^6
1.0x10^6
5.0x10^5
0
Mock
WT
R287Q

Figure 10. Raw data and distribution of 7-dehydrocholesterol and association between 7-dehydrocholesterol and 8-dehydrocholesterol levels. *A*, Levels of 7-dehydrocholesterol show and *C* - *D*, lognormal distribution of 7-dehydrocholesterol in 3,320 Dallas Heart Study individuals. *B*, Relationship between 7-dehydrocholesterol and 8-dehydrocholesterol. r denotes Spearman's rank correlation coefficient. Logarithmic scale is used for the horizontal and vertical axes.

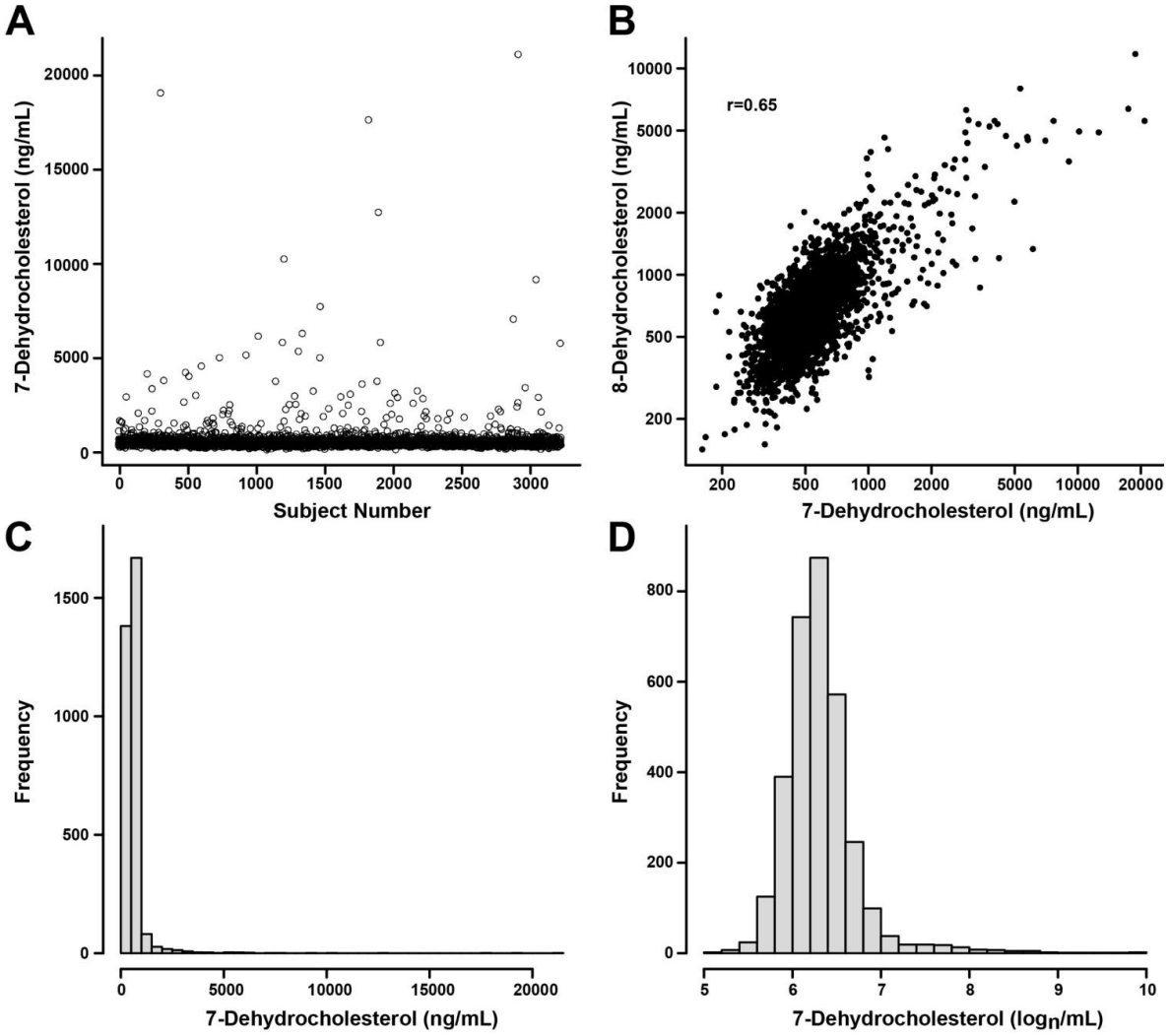
A
7-Dehydrocholesterol (ng/mL)
20000
15000
10000
5000
0
0
500
1000
1500
2000
2500
3000
Subject Number
B
8-Dehydrocholesterol (ng/mL)
r=0.65
10000
5000
2000
1000
500
200
200
500
1000
2000
5000
10000
20000
7-Dehydrocholesterol (ng/mL)
C
Frequency
1500
1000
500
0
0
5000
10000
15000
20000
7-Dehydrocholesterol (ng/mL)
D
Frequency
800
600
400
200
0
5
6
7
8
9
10
7-Dehydrocholesterol (log$_n$/mL)

Figure 11. Raw data, distribution, and association between sequence variant (rs6564956) and 8-dehydrocholesterol levels. *A*, Levels of 8-dehydrocholesterol and *B* - *C*, lognormal distribution of 8-dehydrocholesterol in 3,320 Dallas Heart Study individuals. *D*, Median 8-dehydrocholesterol levels and *SDR42E1* rs6564956 genotypes in African Americans, European Americans and Hispanics. Associations between 8-dehydrocholesterol levels and *SDR42E1* rs6564956 genotypes were tested using ANOVA with age, gender, and BMI as covariates. Logarithmic scale is used for the y-axis.

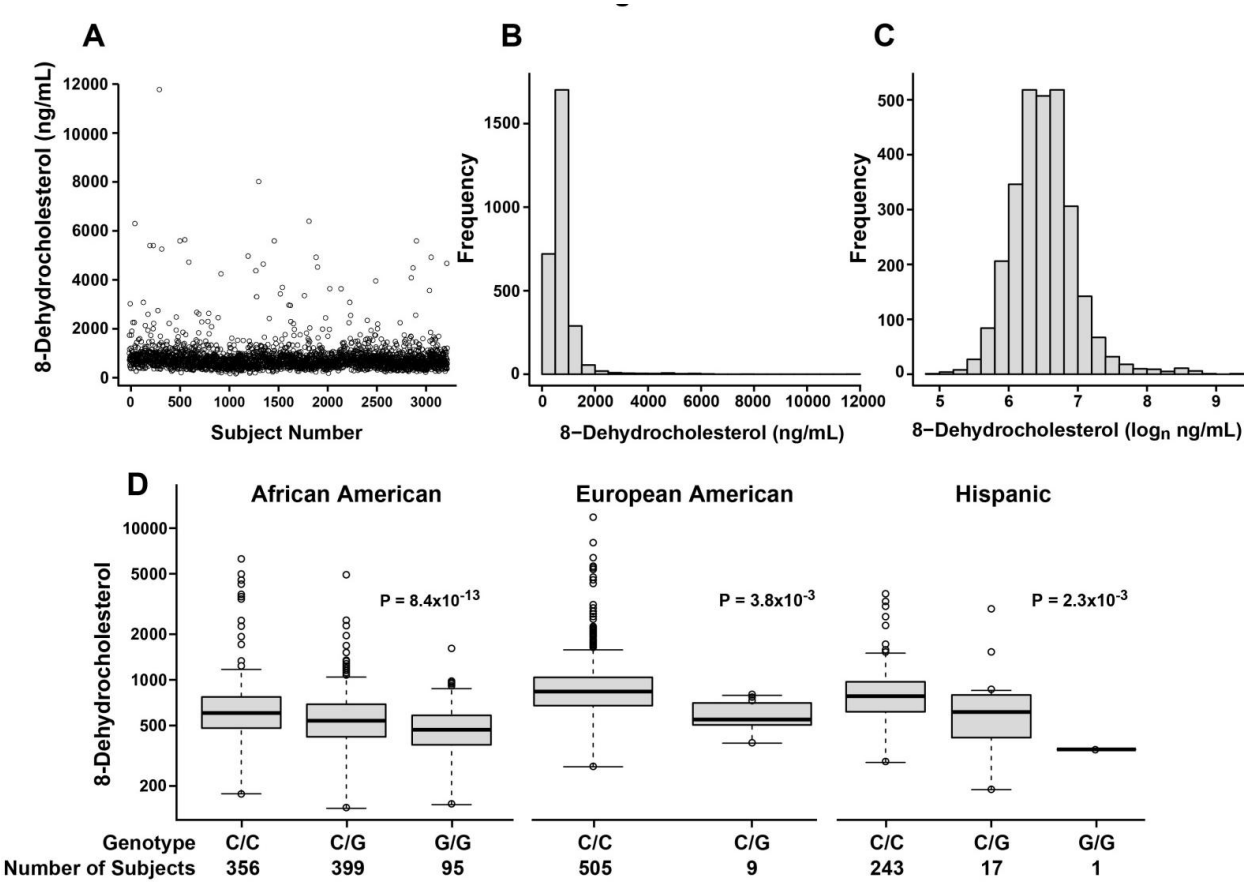
A
8-Dehydrocholesterol (ng/mL)
Subject Number
B
Frequency
8−Dehydrocholesterol (ng/mL)
C
Frequency
8−Dehydrocholesterol (log$_n$ ng/mL)
D
African American
European American
Hispanic
8-Dehydrocholesterol
P = 8.4x10^{-13}
P = 3.8x10^{-3}
P = 2.3x10^{-3}
Genotype C/C C/G G/G C/C C/G C/C C/G G/G
Number of Subjects 356 399 95 505 9 243 17 1

Figure 12. Association between sequence variants in *SDR42E1* and 8-dehydrocholesterol levels. *A*, Median 8-dehydrocholesterol levels for individuals in the Dallas Heart Study with the presence of variants rs16956174, rs79313103 and rs6564956 in *SDR42E1*. *B*, Median 8-dehydrocholesterol levels for individuals in the Dallas Heart Study with the presence of variants rs80065483 and rs11542462 in *SDR42E1*. Logarithmic scale is used for all vertical axes.

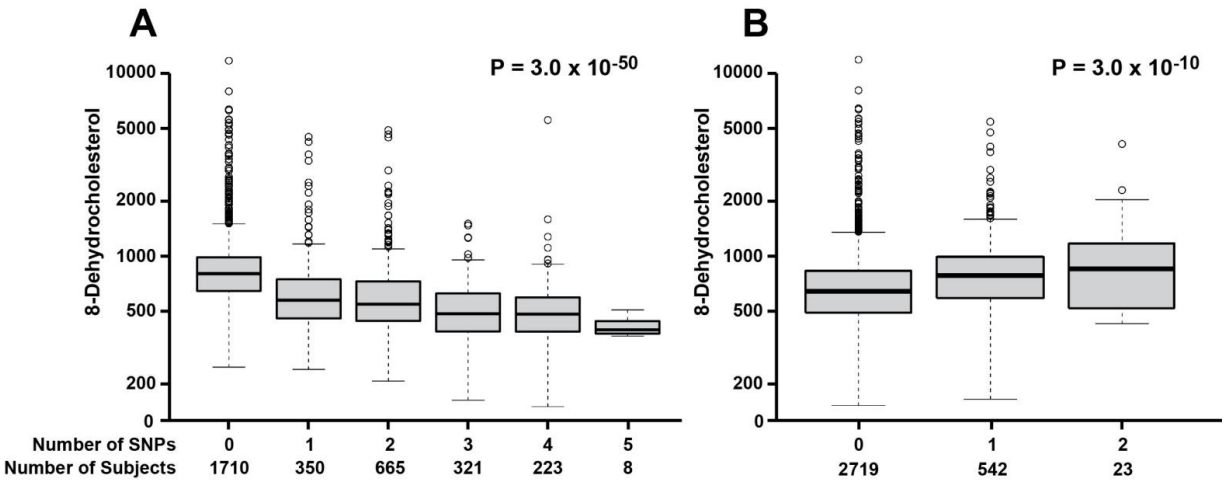
A
P = 3.0 x 10-50
8-Dehydrocholesterol
10000
5000
2000
1000
500
200
0
Number of SNPs 0 1 2 3 4 5
Number of Subjects 1710 350 665 321 223 8
B
P = 3.0 x 10-10
8-Dehydrocholesterol
10000
5000
2000
1000
500
200
0
0 1 2
2719 542 23

Figure 13. Rates of 7- and 8-dehydrocholesterol metabolism in human embryonic kidney 293 cells transfected with *SDR42E1* wild-type and mutant cDNA. *A* - *B*, There was no metabolism of 7- or 8-dehydrocholesterol in cells transfected with *SDR42E1* wild-type (*WT*) or *SDR42E1* mutant (*R287Q*) cDNA when either 7-dehydrocholesterol (*A*) or 8-dehydrocholesterol (*B*) was added as substrate compared to endogenous levels of 7- and 8-dehydrocholesterol (*C*) in which no exogenous substrate was added.

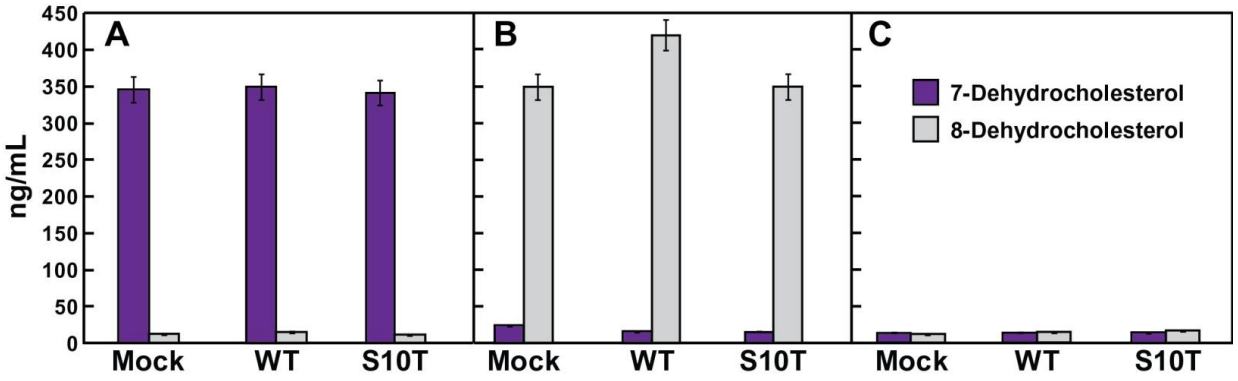
A
B
C
ng/mL
450
400
350
300
250
200
150
100
50
0
Mock
WT
S10T
Mock
WT
S10T
Mock
WT
S10T
7-Dehydrocholesterol
8-Dehydrocholesterol

CHAPTER FIVE:

Concluding Remarks

Cholesterol precursors, plant sterols, and oxysterols have considerable potential as biomarkers in disorders of sterol metabolism and intestinal sterol absorption [112]. In an effort to understand the biological roles of sterols in humans, we have developed a novel approach to measure sterols in small amounts of human serum [113]. These methods can be applied to other biological fluids and tissues such as brain, liver, and breast. Our long-term goal is to use this approach to learn about the biochemistry of sterol metabolism. This work provides an in-depth sterol profile in human serum that reveals inherent variation of sterol levels suggestive of genetic regulation. Sterol analysis of the analyzed sample was challenging due to the complexity of the medium composed of many proteins and lipids, the existence of free and esterified sterols, and the wide differences in polarity between sterols that further complicates the purification process. Nevertheless, we were able to quantitatively measure the 22 sterols that appear to be commonly found in a majority of human sera.

The results presented here provide strong evidence for the methodology we developed and for the detectability of sterols in general using LC-MS. A comparison of all possible pairs of analytes revealed numerous statistically-significant associations between sterols. The levels of dietary plant sterols such as sitosterol, campesterol, stigmastanol, and stigmasterol correlated with each other as expected given that these sterols are substrates for the ABCG5/ABCG8 transporter [114, 115]. An unexpected finding in this comparison revealed that serum levels of the cholesterol biosynthetic intermediate 14-desmethyl-lanosterol also correlated with plant sterols. This finding suggests an exogenous dietary origin for serum 14-desmethyl-lanosterol and that this sterol is an ABCG5/ABCG8 substrate. These suggestions are supported by the

absence of correlations between 14-desmethyl-lanosterol and those of other intermediates in the cholesterol biosynthetic pathway. This finding provides the identification of a novel biomarker of an old disease, sitosterolemia, which arises from mutations in either *ABCG5* or *ABCG8* and is characterized by the cytotoxic build-up of neutral sterols [116].

Many other interesting associations were made as a result of this comprehensive sterolomic profile of human serum. A negative correlation was found between sterols 14-desmethyl-lanosterol (r = -.28), 4β-hydroxycholesterol (r = -.28), 27-hydroxycholesterol (r = -.1), cholestanol (r = -.19), sitosterol (r = -.24), campesterol (r = -.23), stigmasterol (r = -.24), stigmastanol (r = -.19), and as previously shown, 25-hydroxyvitamin D_3 (r = -.26) with BMI [117, 118]. BMI was positively correlated with several sterols, including lathosterol (r = .22), lanosterol (r = .11), and 7-dehydrocholesterol (r = .15). A positive correlation was found to exist between levels of 24,25-epoxycholesterol (r =.11) and 7- and 8-dehydrocholesterol (r = .21 and r = .15) and age, whereas in contrast a negative correlation was found between 22-hydroxycholesterol (r = -.08), lathosterol (r = -.12), lanosterol (r = -.12), 24*S*-hydroxycholesterol (r = -.17) and age [119, 120]. Many sterols showed differences in levels that were gender-dependent, including 7α-hydroxycholesterol (r = .14), 3β,7α,27-hydroxycholesterol (r = .21), 25-hydroxycholesterol (r = .12), 27-hydroxycholesterol (r = .37), 24,25-epoxycholesterol (r = .14), desmosterol (r = .22), and 14-desmethyl-lanosterol (r = .1) [121, 122]. Finally, 25-hydroxyvitamin D_3 (r = .35), 25-hydroxyvitamin D_2 (r = .11), 24*S*-hydroxycholesterol (r = .19), 4β-hydroxycholesterol (r = -.13), 24-oxocholesterol (r = .12), 24,25-epoxycholesterol (r = .19), zymosterol (r = .17), desmosterol (r = .15), lanosterol (r = .14), 24,25-dihydrolanosterol (r = .1), 7- and 8-dehydrocholesterol (r = .11 and r = .4), 14-desmethyl-lanosterol (r = -.1), campesterol (r = -.11), sitosterol (r = -.1), stigmasterol (r = -.21), and lathosterol (r = .11), all showed significant differences in serum levels between different ethnic groups [123].

The results presented here also provide strong evidence for the biochemical roles of enzymes in sterol metabolism. In total, we identified five variant alleles in the *CYP39A1* oxysterol 7α-hydroxylase gene that correlated with increased levels of 24*S*-hydroxycholesterol. These alleles displayed an additive effect with respect to increasing 24*S*-hydroxycholesterol levels when multiple alleles were inherited. This effect was observed in all ethnicities, with different allele combinations more prevalent in different ethnic groups. No phenotypic consequences as a result of the inheritance of these alleles or of increased levels of 24*S*-hydroxycholesterol have yet been identified. Four out of five SNPs were detected in homozygous form and one allele, K329Q, which caused complete loss of function in CYP39A1 enzyme activity as judged by transfection analysis, was detected only in heterozygous form. The allele frequency of K392Q is too low in the population (.0011 in Hispanics, .0021 in African Americans, and .0065 in European Americans) to determine whether the absence of homozygosity reflects lethality.

Linkage analysis revealed a SNP in high linkage to increased levels of 24,25-epoxycholesterol. This variant allele in *EPHX2* was shown to modestly decrease the conversion of 24,25-epoxycholesterol into the product, cholest-5-en-3β,24*S*,25-triol as determined by mass spectrometry analysis of purified cell and medium extracts. A remarkable aspect of the current data is that the cholest-5-en-3β,24*S*,25-triol is present only when an EPHX2 cDNA is transfected into human embryonic kidney 293 cells and is otherwise undetectable in mock-transfected cells. This result implies that EPHX2 has a direct role in the catabolism of 24,25-epoxycholesterol and is consistent with the known biological function of the epoxide hydrolase 2 enzyme. We hypothesize that EPHX2 converts the epoxide group at carbons 24 and 25 to hydroxyl groups forming cholest-5-en-3β,24*S*,25-triol, a vicinal diol structure that would appear chromatographically in the triol region. It will be interesting to determine the role of this cholest-

5-en-3β,24*S*,25-triol metabolite and to determine if the presence of the variant allele results in phenotypic consequences.

Further pursuit of the role of *SDR42E1* in 8-dehydrocholesterol metabolism is ongoing in the lab. We have performed *in-vitro* experiments in which human embryonic kidney 293 cells were transfected with vector alone, wild-type SDR42E1 cDNA, or SDR42E1 cDNA with the S10T variant allele and observed no changes in the metabolism of exogenously added 7- or 8-dehydrocholesterol. The biological role, function, and origin of 8-dehydrocholesterol and SDR42E1 are currently unknown. Based on the build-up of both 7- and 8-dehydrocholesterol in Smith-Lemli-Opitz patients, there may be an enzyme responsible for the conversion of 7-dehydrocholesterol into 8-dehydrocholesterol and SDR42E1 may assist this reaction. After repeated transfection experiments with the SRD42E1 cDNA yielded no evidence of isomerism between 7- and 8-dehydrocholesterol, we are currently screening for other cDNAs/proteins that may catalyze the conversion of 7-dehydrocholesterol into 8-dehydrocholesterol or vice versa.

There were no additional variants identified through direct sequencing or regenotyping of the Dallas Heart Study individuals in *EPHX2* that associate with levels of 24,25-epoxycholesterol. Additional variants were identified in *SDR42E1* and these were shown to associate with both decreased and increased levels of 8-dehydrocholesterol. Variants that maintained levels of high significance after all other SNPs were adjusted for will be studied further to determine the functional role of *SDR42E1* in 8-dehydrocholesterol metabolism.

The present work describes the identification of genetic determinants of 24*S*-hydroxycholesterol, 24,25-epoxycholesterol, and 8-dehdyrocholesterol levels. At present, no phenotype has been identified that is a result of inheritance of these variant alleles and no mutations were identified in cholesterol 24-hydroxylase, the neuron specific enzyme that hydroxylates cholesterol at C_{24} in the brain. With access to a small cohort (n = 200) characterized for intellectual disabilities, we are expanding our search to identify human genetic

mutations in *CYP46A1* in individuals with decreased levels of 24*S*-hydroxycholesterol. A specific effect of EPHX2 on 24,25-epoxycholesterol metabolism is seen in cultured human embryonic kidney 293 cells, consistent with the function of the enzyme in conversion of epoxides to diols. Further studies will address the apparent EPHX2 enzymatic specificity on the metabolism of 24,25-epoxycholesterol and determine the mechanism by which 24,25-epoxycholesterol is inactivated. While genetic determinants of 8-dehydrocholesterol levels were identified, there has not been a functional role of SDR42E1 in cultured human embryonic kidney 293 cells that explains this genetic relationship. Further studies will address SDR42E1 enzymatic specificity on 8-dehydrocholesterol levels and determine the molecular mechanism by which 8-dehydrocholesterol is formed, shedding light on its endogenous activity.

APPENDIX A:

Method Details

A.1 Abstract

Method Details. Although numerous biological functions of sterols have been described, many more are yet to be discovered. The incorporation of sterolomics through translational research is a field with potential. The elucidation of new functions for sterols will require both advances in biology and the development of more sophisticated and sensitive analytical techniques for the identification and quantitation of sterols *in situ*. The extraction and analysis procedures outlined here represent a comprehensive method measuring ~60 sterols in a single extraction. The method combines previously published methods/concepts, with original and *de novo* improvements.

Studies have shown that plastics are incompatible with many organic solvents and can leach plasticizers into the extracts [124]. These contaminating compounds can interfere with the extraction procedure, foul instrumentation, and complicate data analysis. For this reason, the use of plastics in each step of the extraction procedure was minimized. We used glass, PTFE, and stainless steel vessels whenever possible. Plastic pipette tips were specifically used for transferring an aliquot of the final extract. This was done as a matter of practicality (to maintain throughput) and to reduce the possibility of cross-contamination. Trace-level cross contamination was of great concern due to the complexity of the plasma samples analyzed (containing ≥ 0.5 mg/mL of lipids). The plastic tips were used only with water or water/methanol systems, and not in the steps involving more aggressive solvents. It is important to note that

safety concerns associated with analyzing human samples outweigh any complications resulting from the minimal use of plastics during our extraction procedure.

The formation of oxidation products, derived primarily from cholesterol, has been established as a common occurrence in the extraction and processing of biological samples [7, 8, 43]. To minimize oxidation and purge volatile contaminants, extraction solvents were sparged with N_2 for 10 minutes. BHT was included in the initial DCM/MeOH solution (3 mL) at 50 µg/mL. The presence of atmospheric oxygen in the glass extraction tubes was minimized by purging with N_2 prior to both hydrolysis and derivatization. Lastly, we used amino-propyl SPE columns to enrich sterols prior to analysis; this choice produces far less oxidation compared to the use of silica columns [8, 43]. Other options such as working in an inert environment or with deactivated glassware may reduce oxidation, but would be prohibitive when working with large sample sets.

The extraction of sterols from plasma requires their separation from associated proteins, solubilization, and isolation from other lipids and aqueous-soluble components of plasma. There are numerous published procedures for performing protein precipitation, most involving the precipitation of proteins using a cold organic solvent such as ACN, MeOH, EtOH, or acetone followed by centrifugation of the sample. While these methods are effective at removing proteins from solution, most sterols are packaged in lipoproteins and will precipitate with proteins. To precipitate proteins and solubilize sterols and other lipids in a single step, we used a 1:1 mixture of DCM:MeOH. DCM was used due in part to its similar properties to $CHCl_3$. In contrast to $CHCl_3$; however, DCM is more stable (no phosgene formation), considerably less toxic. Plasma (200 µL) was added in a drop-wise manner to 3 mL of the 1:1 mixture of DCM:MeOH while sonicating the solution at 30 °C. Following the addition of the plasma to the DCM:MeOH, the sample tube was flushed with N_2 and placed in a 30 °C ultrasonic bath for 10 min. This method encouraged dissolution of lipids and minimized protein aggregation by

maintaining a homogenous solution. In other published methods, the extract is then split into two-phases by the addition of H_2O and proteins pelleted by centrifugation. A protein disk forms at the interface of the aqueous and organic layers. Care must be taken in subsequent isolation of the organic layer. The slightest agitation of the sample can cause dissociation of the pelleted protein resulting in insoluble protein being carried through subsequent extraction steps. Our method skips the addition of H_2O to the sample; instead, following a 10 min incubation in an ultrasonic bath, proteins are pelleted by centrifugation at room temperature. Centrifugation at room temperature is important to maintain solubility of the extract and minimize day-to-day variation in extraction efficiency between sample batches. Using our method, the proteins and other insoluble materials are pelleted at the bottom of the tube ensuring maximum removal of protein and solubilization of lipids (sterols) in a single step.

The use of DCM for extraction also allows for an *in situ*, low temperature hydrolysis. We found that adding an aliquot of base (KOH) directly to the extract (~ 6 mL 1:1 DCM:MeOH + 200 µL plasma) efficiently hydrolyzed steryl esters to free sterols after a 1.5 hr incubation at 35 °C. The extraction must be done using DCM, not $CHCl_3$, as the latter will react with KOH to form dichlorocarbene, a reactive product that can degrade and/or modify sterols [125]. Other saponification methods involve adding an alcoholic base solution directly to a dried extract followed by heating at elevated temperatures (60-100°C) for 1 to 2 hours. These conditions are harsh, cause degradation of some sterol compounds, and add additional steps to the extraction procedure. With our method, sterols are subsequently separated from base- and aqueous-soluble compounds through the addition of 4.5 mL of DPBS to form a two-layer system. Following vortexing and centrifugation of the sample, a clean interface is formed without a protein disk or emulsion. This phasing allows for removal of the lower, sterol-containing layer, with minimal carryover of insoluble material.

The SPE procedure described here is simple and robust in effecting separation of sterols from other compounds. The hydrolysis step results in the removal of fatty acyl chains from major lipid classes (triglycerides, phospholipids, sphingolipids, cholesteryl esters). Saponification generates significant amounts of fatty acids at levels much greater than those of free sterols, oxysterols, and secosteroids, and that must be removed to eliminate complications in downstream analyses. To this end, non-polar, neutral compounds are eluted first from the SPE column using hexane. Sterols, including polar dihydroxy sterols, are then eluted using 23:1 $CHCl_3$:MeOH. This solvent combination does not elute fatty acids; which are highly retained on NH_2 stationary phases of the column and require stronger elution solvents such as MeOH with 5% acetic acid. Biotage SPE columns were the only ones tested that had a consistent, even flow rate of 1-2 drops per/sec without the use of a vacuum manifold. This trait facilitated the processing of large numbers of samples with consistent results. An inconsistent flow rate often leads to the drying of the column, and increased variation observed within and between sample sets. In our experience, there are drawbacks to using a standard silica column versus a NH_2 column. Silica is very hydroscopic and its chromatographic behavior can be affected by minor changes in exposure to water. Silica columns can be affected by ambient humidity and/or storage conditions once removed from a hermetically sealed package, and as noted above oxidation of sterols occurred more frequently with silica-based SPE.

Solubilization of the final, SPE-purified extract is a crucial step and must be done with careful attention. Cholesterol is the most abundant compound in the final extract and is present at levels more than 1000X higher than the next most abundant sterol. Cholesterol has low solubility in solvents typically used for reverse-phase chromatography, such as ACN or MeOH. This insolubility increases when an aqueous component is added to the solvent system. We have empirically determined that in most cases, samples arising from extraction of 200 µL of plasma will dissolve in 400 µL of 37 °C, 90% MeOH followed by a 5 min incubation in a 30 °C

ultrasonic bath. For plasma samples with elevated cholesterol levels (> 300 mg/mL), an additional centrifugation step may be necessary to remove insoluble material. To this end, the vial inserts from incompletely dissolved samples were placed in a typical snap-cap microcentrifuge tube and centrifuged at 6000 rpm using a bench-top microcentrifuge at 25 °C. The maximum centrifuge speed for this step is 6000 rpm; use of higher speeds will occasionally cause the vial inserts to break. This step is an alternative to sample filtration and is well suited to small sample volumes, uses the existing glass vial insert, and does not require an additional sample transfer step. Following centrifugation, the vial insert containing the pelleted material is placed back into the original autosampler vial. In our experience, the pelleted material does not resuspend, even after a priming cycle of an auto injector syringe. We recommend acquiring several high-quality, fine-point tweezers to use in transferring the vial inserts between the autosampler vial and the microfuge tube.

Derivatization reactions using MTBSTFA have significant advantages over reactions involving other derivatization reagents. The reaction is fast and efficient, and the derivatized products are stable for extended periods of time (≥ 4 weeks). In addition, no precipitate is formed in reaction with atmospheric water. The formation of a precipitate can quickly foul samples as well as auto injector syringes. An additional benefit of using MTBSTFA is that the mass spectrum of a MTBSTFA-derivatized sterol such as lathosterol, shows an almost exclusive ion at M-57 (loss of *t*-butyl group). This single, high-mass fragment increases detectability by putting the majority of the signal intensity into one ion, and when coupled with SIM offers superior sensitivity over previous derivatization schemes. Using neat MTBSTFA with 1% TBDMCS, however, does not effectively derivatize sterols; a proton-accepting solvent is required for the reaction to go to completion. A previous method described the use of NH_4I dissolved in toluene as the proton-accepting solvent used in conjunction with MTBSTFA [126]. We were unable to dissolve NH_4I in toluene, even with gentle heating and sonication. Instead

we determined that NH_4I was soluble in pyridine, which in turn was a suitable solvent for performing derivatizations.

Throughout this extraction procedure, exceptional care was given to minimizing sample loss during extraction and sample transfer. Due to the complexity of the sample, numerous sample transfer steps are involved and each presents an opportunity for loss. By including a second wash or rinse, we ensured that little if any sample was lost at this early step. Other steps, like using the same pipette at each transfer, also minimize loss. While this level of detail increased extraction time and required extra glassware, it is critical to maximize sample recovery so that trace level analytes such as 25-hydroxycholesterol, 7α,27-dihydroxycholesterol, and zymosterol are effectively measured.

Compounds that contain a carbonyl functional group can be susceptible to base hydrolysis. For example, previous work has shown 7-oxocholesterol to be one such compound [127]. In this study, our intent was to measure 7α-hydroxycholestenone, however; even under the mild extraction conditions described, the matrix spike recovery for this compound was approximately 25%. Attempts to minimize degradation included reducing hydrolysis time, concentration of base, and temperature. While the recovery of this compound increased with these alterations, the milder hydrolysis conditions led to matrix interference problems with other compounds. As 7α-hydroxycholestenone has a carbonyl group at the 3 position (Figure 1*A*), it cannot be esterified and therefore circulates as a free sterol. Should an investigator want to measure this compound specifically it can be done by eliminating the hydrolysis step thereby removing the source of degradation?

The sterol analysis method previously published by our laboratory [8] used a single chromatographic column, solvent program, and ion source (ESI). We have since determined that for optimal resolution and detection of oxysterols, secosteroids, and sterols, the use of two HPLC columns, gradient programs, and ion sources (ESI and APCI) are necessary. The

polarity differences between mono- and di-hydroxylated sterols and sterols were too great to be effectively separated with a single HPLC method. This polarity difference also played an important role in choosing the appropriate ion source; less polar sterols showed a significant increase in signal intensity when ionized with APCI.

Due to one of the HPLC's being configured for standard pressure (400 Bar max), the use of UPLC columns was not feasible; however, the advent of "core-shell technology" by several HPLC column vendors offered an opportunity to gain efficiency and resolution while maintaining pressures compatible with standard HPLC. These columns proved to be a key component for resolving the numerous sterol and oxysterol isomers with a reasonable run time. Although columns from different vendors are fundamentally the same, we found that the Kinetex column from Phenomenex was superior at resolving oxysterols, especially for separating the isobaric group of oxysterols consisting of 22-, 24-, 25-, and 27 hydroxycholesterol. Likewise, the Poroshell column from Agilent was superior at separating some pairs of sterols such as zymosterol and desmosterol. The HPLC used for oxysterol analysis is capable of UPLC pressures, so the 430 Bar max pressure developed by this method is well within capabilities. The sterol method developed a maximum of 355 Bar on the standard pressure HPLC. While the system performed as expected, we noted a marked increase in maintenance on the HPLCs, especially piston seal life time. The lower pressure HPLC system was not equipped with the same seal wash feature as the high pressure system. The seal wash dissipates heat generated when pumping solvents at higher pressures, which helped increase seal lifetime. Both HPLCs were plumbed with stainless steel tubing up to the column to handle the increased pressure. We also note that although the pumps were rated to 400 Bar, the injection module was only rated to 350 Bar. We ensured that all injector fittings (including the ball seat) were properly tightened and the injector performed at or slightly above its rating without leaking. Column life for the sterol analysis was 1200-1500 samples before observed loss of performance. Column

life for oxysterol analysis is shorter, but still acceptable at up to 1000 sample injections; this reduction may be due to the larger sample injection volume (30 µL for oxysterols versus 5 µL for sterols), which places 6× more cholesterol on the column (already in massive excess). Column temperatures were determined empirically and it was found that sub-ambient conditions gave maximum resolution for oxysterols. This result may be due to the reduction in heat generated by the increased solvent flow over the smaller particles at increased pressures. For sterols, an above ambient (30 ^{o}C) temperature was determined to increase the elution of highly-retained sterols from the column at earlier times.

To achieve optimal chromatographic resolution of oxysterols, it was imperative that the final dried sample be reconstituted in 90% MeOH. We tested numerous combinations of solvents, including mixtures of ACN, DCM, MeOH, and H_20, and found that 90% MeOH yielded the best results and solubilized nearly every sample; only the most cholesterol-rich samples required that insoluble material be removed by centrifugation (as described above). Less than 10% aqueous MeOH resulted in decreased chromatographic performance.

Our mass spectrometer settings, parameters, and MRM pairs for oxysterol analysis with ESI are specific to the AB Sciex platform and Turbo V source. Colleagues with mass spectrometers from different vendors report different optimal MRM pairs using ESI. The key difference is the observation of the ammonium adduct. The Turbo V source is gentle when used at mild settings (50 °C source); the labile ammonium adduct remains intact and can be used as the molecular adduct ion in MRM and the fragment ion arises from loss of water. Ionization sources from other manufacturers appear to be harsher and result in in-source decay and fragmentation of the ammonium adduct before transfer into the MS. As a result, the $[M+H-H_20]^+$ ion becomes the pseudo-molecular ion and with no logical fragment ion to complete the MRM transition, detectability is significantly decreased. The only way to complete the MRM transition is the use of either an $[M+H-2H_2O]^+$ ion or an ion at *m/z* 81, 95, or 109, depending on

the instrument, sterol, and collision energy. In contrast to oxysterol analysis, the implementation of our MS method with respect to sterol analysis translates more easily to APCI compared to ESI. The physical characteristics of APCI make it more consistent between instrument platforms. In comparison to ESI, APCI almost exclusively generates an $[M+H-H_2O]^+$ ion as the pseudo molecular ion and with a high energy CID, uses an ion at m/z 81, 95, or 109 to complete the MRM transition. Regardless of compound or instrument, the user should optimize each analyte for their specific platform.

Because ionization of oxysterols by ESI requires the formation of ammonium adducts, ammonium acetate must be added to the mobile phase (1:1 ACN:IPA). Ammonium acetate; however, is not soluble in ACN and thus must first be dissolved in either water or IPA prior to mixing with ACN. In a previous methods paper [8], we reported that use of ACN caused a decrease in mass spectral signal intensity; however, these data were based on infusion experiments with standards dissolved in 99:1 ACN:H_2O with 5 mM NH_4OAc. In the oxysterol method described here, we determined that ACN was necessary to resolve some pairs of isomeric compounds. While we did not perform a detailed comparison, under the conditions described above we were able to detect all expected oxysterols. One possible explanation for the inter-method differences is that we now use more efficient columns and a more sensitive mass spectrometer (API 5000) than was used in our previous work. Another possible explanation is that the use of ACN in combination with IPA and MeOH may not cause decreased signal intensity. Regardless, the method described here has sufficient detectability for oxysterols and a positive influence on chromatographic resolution.

Cholesterol is approximately 1000 times more abundant than the next most abundant sterol. As described in detail in the manuscript, this abundance presents numerous analytical challenges. Furthermore, this excess requires a separate assay to accurately measure cholesterol levels. This assay would encompass taking another aliquot, performing an

analytical dilution with standards and assaying the additional sample with either GC- or LC-MS. Because we already use three instruments to profile the sterols, we chose not to implement an additional method just for the measurement of cholesterol. Cholesterol in plasma is routinely and reliably measured in clinical chemistry laboratories and in a prior study we determined that having the cholesterol assayed by an external commercial laboratory yields results consistent with MS measurements [128].

APPENDIX B:

Oxysterol Method File

Oxysterol Data Acquisition File

File Name: DHS 14-PP 100510.wiff
File Path: \\Mgone\deptdata\Jeff McDonald\DHS\LC_GC Data\100510DHS14 O\
Original Name: 100510\DHS 14-PP 100510.wiff
Software Version: Analyst 1.5.1

Log Information from Devices at Start of acquisition:
Integrated System Shimadzu Controller CBM20A
Serial# L20234651864
ROM Version 1.20
Pressure Units bar
Time from start =0.0000 min Pump Shimadzu LC20ADXR
Serial# L20434600250
ROM Version 1.21
Time from start =0.0000 min Pump Shimadzu LC20ADXR
Serial# L20434600244
ROM Version 1.21
Time from start =0.0000 min Pump Shimadzu LC20ADXR
Serial# L20434600239
ROM Version 1.21
Time from start =0.0000 min AutoSampler Shimadzu SIL20ACXR
Serial# L20454600194
ROM Version 1.20
Time from start =0.0000 min Column Oven Shimadzu CTO20AC
Serial# L20214650436
ROM Version 1.07
Time from start =0.0000 min
Time from start =0.0000 min Injection Volume used 25.00 µl
Time from start =0.0167 min Mass Spectrometer API 5000
Config Table Version 01
Firmware Version M401402 B4T0301 M3L1417 B3T0300
Component Name Triple Quadrupole LC/MS/MS Mass Spectrometer
Component ID API 5000

Manufacturer	AB Sciex Instruments
Model	1011122-AG
Serial Number	AG21530801H

Time from start =0.0167 min	Mass Spectrometer API 5000
Start of Run - Detailed Status	
Vacuum Status	At Pressure
Vacuum Gauge (10e-5 Torr)	1.8
Backing Pump	Ok
Interface Turbo Pump	Normal
Analyzer Turbo Pump	Normal
Sample Introduction Status	Ready
Source/Ion Path Electronics	On
Source Type	Turbo Spray
Source Temperature (at setpoint)	50.0 C
Source Exhaust Pump	Ok
Interface Heater	Ready

Time from start =0.0167 min	Mass Spectrometer API 5000
End of Run - Detailed Status	
Vacuum Status	At Pressure
Vacuum Gauge (10e-5 Torr)	1.8
Backing Pump	Ok
Interface Turbo Pump	Normal
Analyzer Turbo Pump	Normal
Sample Introduction Status	Ready
Source/Ion Path Electronics	On
Source Type	Turbo Spray
Source Temperature (at setpoint)	50.0 C
Source Exhaust Pump	Ok
Interface Heater	Ready
Time from start =12.5167 min	

Acquisition Info

Acquisition Method:	\Oxysterol Finalx7.dam
Acquisition Path:	D:\Analyst Data\Projects\Oxy Sterols\Acquisition Methods\
First Sample Started:	Wednesday, October 06, 2010 2:50:50 AM
Last Sample Finished:	Wednesday, October 06, 2010 2:50:50 AM
Sample Acq Time:	Wednesday, October 06, 2010 2:50:50 AM
Sample Acq Duration:	12min0sec
Number of Scans:	0
Periods in File:	1
Batch Name:	\DHS 14 100510.dab
Batch Path:	D:\Analyst Data\Projects\Oxy Sterols\Batch\
Submitted by:	API5000\Administrator()
Logged-on User:	API5000\Administrator
Synchronization Mode:	LC Sync
Auto-Equilibration:	Off
Comment:	
Software Version:	Analyst 1.5.1
Set Name:	SET1
Sample Name	DHS 14-PP 100510

Sample ID
Sample Comments:
Autosampler Vial: 52
Rack Code: 1.5mL Standard
Rack Position: 1
Plate Code: 1.5mL Standard
Plate Position 1

Shimadzu LC Method Properties
Shimadzu LC system Equlibration time = 0.00 min
Shimadzu LC system Injection Volume = 25.00 ul
Shimadzu LC Method Parameters
Pumps
=====
Pump A Model: LC-20ADXR 70%ACN with 5mM ammonium acetate
Pump B Model: LC-20ADXR 1:1 IPA:ACN with 5mM ammonium acetate
Pump C Model: LC-20ADXR
Pump D Model: LC-20ADXR
Column: Phenomenex Kinetex 2.6um C18 150x2.1mm
Pumping Mode: Ternary Flow
Total Flow: 0.5000 mL/min.
Pump B Conc: 0.0 %
Pump C Conc: 0.0 %
B Curve: 0
C Curve: 0
Pump D Flow: 0.0000 mL/min.
Pressure Range (Pump A/B/C): 0 - 660 Bars
Pressure Range (Pump D): 0 - 660 Bars
Autosampler
==========
Model: SIL-20ACXR
Rinsing Volume: 200 uL
Needle Stroke: 52 mm.
Rinsing Speed: 35 uL/sec.
Sampling Speed: 5.0 uL/sec.
Purge Time: 2.0 min.
Rinse Dip Time: 1 sec.
Rinse Mode: Before aspiration
Cooler Enabled: Yes
Cooler Temperature: 25 deg. C
Control Vial Needle Stroke: 52 mm
Pump Method: Rinse Pump Then Port
Rinse Time: 2 sec
Oven
====
Model: CTO-20AC
Temperature Control: Enabled
Temperature: 18 deg. C
Max. Temperature: 85 deg. C
Left Valve Position (FCV-12AH): 0
Right Valve Position (FCV-12AH): 0

System Controller
==========
Model: CBM-20A
Power: On
Event 1: Off
Event 2: Off
Event 3: Off
Event 4: Off
Time Program
==========

Time	Module	Events	Parameter
0.01	Autosampler	Inject	
0.02	Pumps	Pump B Conc.	0.0
7.00	Pumps	Pump B Conc.	100
10.00	Pumps	Pump B Conc.	100
10.25	Pumps	Pump B Conc.	0.0
12.00	Pumps	Pump B Conc.	0.0
12.01	System Controller	Stop	

Quantitation Information:

Sample Type:	Unknown
Dilution Factor:	1.000000

Custom Data:

Quantitation Table:

Peak Name	Concentration
d6 1,25 D3	8.000000
d6 25 D3	12.000000
d6 25D2	10.000000
d7 22r	11.900000
d6 25 OHC	7.200000
d6 27 OHC	57.900000
d7 7b	80.400000
d7 7OXO	32.400000
d7 6a	39.208000
d7 4b	20.300000
d7 5/6a	10.400000
1,25 D3	8.000000
3,7,25	12.000000
3,7,27	9.000000
1,25 D2	9.600000
3b27d57o	6.600000
3b16a27	7.100000
3b17a20a	23.000000
25 D3	12.000000
25 D2	10.800000
22r OHC	11.900000
25 OHC	7.100000
24(r/s) OHC	31.800000
24 OXO	16.100000

27 OHC	57.600000
8(14) 3,15aOHC	7.632000
20	8.400000
24/25 EPC	4.300000
3b,5a,6b	15.600000
8(14) 3OH,15OXO	7.656000
AN 3,15OXO	4.992000
8(14) 3,15bOHC	6.996000
3oxo7a	4.200000
3o7o	8.600000
7(a,b)	80.600000
1a,D2	1.600000
1a,D3	3.200000
3b5a6o	24.000000
7OXO	32.000000
3,15(a,b)OHC	3.750000
6oxo anol	10.000000
19	16.500000
6a	40.600000
5/6b	10.300000
5a	16.000000
5/6a	10.500000
4b	20.300000

Period 1:

Scans in Period: 720
Relative Start Time: 0.00 msec
Experiments in Period: 1

Period 1 Experiment 1:

Scan Type: MRM (MRM)
Scheduled MRM: Yes
Polarity: Positive
Scan Mode: N/A
Ion Source: Turbo Spray
MRM detection window: 80 sec
Target Scan Time: 1.0000 sec
Resolution Q1: Low
Resolution Q3: Unit
Intensity Thres.: 0.00 cps
Settling Time: 0.0000 msec
MR Pause: 5.0070 msec
MCA: No
Step Size: 0.00 Da

Q1 Mass (Da)	Q3 Mass (Da)	Time (min)	Param	Start	Stop	ID
440.301	405.300	1.90	DP	60.00	60.00	d6 1,25 D3
			CE	14.00	14.00	

Q1 Mass (Da)	Q3 Mass (Da)	Time (min)	Param	Start	Stop	ID

434.301	399.300	1.92	DP	60.00	60.00	1,25 D3
			CE	14.00	14.00	
Q1 Mass (Da)	Q3 Mass (Da)	Time (min)	Param	Start	Stop	ID
401.306	383.300	1.94	DP	100.00	100.00	3,7,25
			CE	18.00	18.00	
Q1 Mass (Da)	Q3 Mass (Da)	Time (min)	Param	Start	Stop	ID
401.305	383.300	2.07	DP	100.00	100.00	3,7,27
			CE	18.00	18.00	
Q1 Mass (Da)	Q3 Mass (Da)	Time (min)	Param	Start	Stop	ID
446.401	411.400	2.25	DP	65.00	65.00	1,25 D2
			CE	15.00	15.00	
Q1 Mass (Da)	Q3 Mass (Da)	Time (min)	Param	Start	Stop	ID
434.302	417.300	2.37	DP	62.00	62.00	3b27d57o
			CE	16.00	16.00	
Q1 Mass (Da)	Q3 Mass (Da)	Time (min)	Param	Start	Stop	ID
436.302	401.301	2.39	DP	60.00	60.00	3b16a27
			CE	15.00	15.00	
Q1 Mass (Da)	Q3 Mass (Da)	Time (min)	Param	Start	Stop	ID
436.301	401.302	3.01	DP	60.00	60.00	3b17a20a
			CE	12.00	12.00	
Q1 Mass (Da)	Q3 Mass (Da)	Time (min)	Param	Start	Stop	ID
407.304	389.300	4.08	DP	85.00	85.00	d6 25 D3
			CE	12.00	12.00	
Q1 Mass (Da)	Q3 Mass (Da)	Time (min)	Param	Start	Stop	ID
401.304	383.300	4.10	DP	85.00	85.00	25 D3
			CE	12.00	12.00	
Q1 Mass (Da)	Q3 Mass (Da)	Time (min)	Param	Start	Stop	ID
419.301	401.300	4.40	DP	85.00	85.00	d6 25D2
			CE	12.00	12.00	
Q1 Mass (Da)	Q3 Mass (Da)	Time (min)	Param	Start	Stop	ID
413.309	395.300	4.43	DP	85.00	85.00	25 D2
			CE	12.00	12.00	
Q1 Mass (Da)	Q3 Mass (Da)	Time (min)	Param	Start	Stop	ID
427.302	392.300	4.66	DP	60.00	60.00	d7 22r
			CE	13.00	13.00	
Q1 Mass (Da)	Q3 Mass (Da)	Time (min)	Param	Start	Stop	ID
420.306	367.300	4.68	DP	60.00	60.00	22r OHC
			CE	18.00	18.00	
Q1 Mass (Da)	Q3 Mass (Da)	Time (min)	Param	Start	Stop	ID
426.302	373.300	4.87	DP	60.00	60.00	d6 25 OHC

			CE	18.00	18.00	
Q1 Mass (Da)	Q3 Mass (Da)	Time (min)	Param	Start	Stop	ID
420.307	367.300	4.89	DP	60.00	60.00	25 OHC
			CE	18.00	18.00	
Q1 Mass (Da)	Q3 Mass (Da)	Time (min)	Param	Start	Stop	ID
420.305	385.300	4.98	DP	60.00	60.00	24(r/s) OHC
			CE	13.00	13.00	
Q1 Mass (Da)	Q3 Mass (Da)	Time (min)	Param	Start	Stop	ID
418.302	383.300	5.14	DP	60.00	60.00	24 OXO
			CE	14.00	14.00	
Q1 Mass (Da)	Q3 Mass (Da)	Time (min)	Param	Start	Stop	ID
426.301	391.300	5.24	DP	60.00	60.00	d6 27 OHC
			CE	14.00	14.00	
Q1 Mass (Da)	Q3 Mass (Da)	Time (min)	Param	Start	Stop	ID
420.304	385.300	5.26	DP	60.00	60.00	27 OHC
			CE	14.00	14.00	
Q1 Mass (Da)	Q3 Mass (Da)	Time (min)	Param	Start	Stop	ID
385.304	367.300	5.28	DP	100.00	100.00	8(14)
3,15aOHC						
			CE	18.00	18.00	
Q1 Mass (Da)	Q3 Mass (Da)	Time (min)	Param	Start	Stop	ID
385.301	367.300	5.30	DP	65.00	65.00	20
			CE	12.00	12.00	
Q1 Mass (Da)	Q3 Mass (Da)	Time (min)	Param	Start	Stop	ID
418.304	383.300	5.35	DP	60.00	60.00	24/25 EPC
			CE	14.00	14.00	
Q1 Mass (Da)	Q3 Mass (Da)	Time (min)	Param	Start	Stop	ID
438.301	403.300	5.37	DP	65.00	65.00	3b,5a,6b
			CE	15.00	15.00	
Q1 Mass (Da)	Q3 Mass (Da)	Time (min)	Param	Start	Stop	ID
401.303	383.300	5.63	DP	100.00	100.00	8(14)
3OH,15OXO						
			CE	26.00	26.00	
Q1 Mass (Da)	Q3 Mass (Da)	Time (min)	Param	Start	Stop	ID
420.303	403.300	5.85	DP	100.00	100.00	AN 3,15OXO
			CE	15.00	15.00	
Q1 Mass (Da)	Q3 Mass (Da)	Time (min)	Param	Start	Stop	ID
385.303	367.300	5.90	DP	100.00	100.00	8(14)
3,15bOHC						

			CE	18.00	18.00	
Q1 Mass (Da)	Q3 Mass (Da)	Time (min)	Param	Start	Stop	ID
401.302	383.300	6.02	DP	80.00	80.00	3oxo7a
			CE	23.00	23.00	
Q1 Mass (Da)	Q3 Mass (Da)	Time (min)	Param	Start	Stop	ID
418.301	401.300	6.09	DP	65.00	65.00	3o7o
			CE	12.00	12.00	
Q1 Mass (Da)	Q3 Mass (Da)	Time (min)	Param	Start	Stop	ID
392.301	374.300	6.11	DP	100.00	100.00	d7 7b
			CE	20.00	20.00	
Q1 Mass (Da)	Q3 Mass (Da)	Time (min)	Param	Start	Stop	ID
385.302	367.300	6.13	DP	100.00	100.00	7(a,b)
			CE	20.00	20.00	
Q1 Mass (Da)	Q3 Mass (Da)	Time (min)	Param	Start	Stop	ID
430.301	413.300	6.14	DP	65.00	65.00	1a,D2
			CE	10.00	10.00	
Q1 Mass (Da)	Q3 Mass (Da)	Time (min)	Param	Start	Stop	ID
418.303	401.300	6.16	DP	55.00	55.00	1a,D3
			CE	12.00	12.00	
Q1 Mass (Da)	Q3 Mass (Da)	Time (min)	Param	Start	Stop	ID
436.303	401.303	6.20	DP	60.00	60.00	3b5a6o
			CE	15.00	15.00	
Q1 Mass (Da)	Q3 Mass (Da)	Time (min)	Param	Start	Stop	ID
408.309	390.300	6.24	DP	80.00	80.00	d7 7OXO
			CE	30.00	30.00	
Q1 Mass (Da)	Q3 Mass (Da)	Time (min)	Param	Start	Stop	ID
401.301	383.300	6.26	DP	80.00	80.00	7OXO
			CE	30.00	30.00	
Q1 Mass (Da)	Q3 Mass (Da)	Time (min)	Param	Start	Stop	ID
422.301	369.300	6.31	DP	100.00	100.00	3,15(a,b)OHC
			CE	16.00	16.00	
Q1 Mass (Da)	Q3 Mass (Da)	Time (min)	Param	Start	Stop	ID
420.309	403.300	6.43	DP	100.00	100.00	6oxo anol
			CE	15.00	15.00	
Q1 Mass (Da)	Q3 Mass (Da)	Time (min)	Param	Start	Stop	ID
420.301	403.300	6.50	DP	60.00	60.00	19
			CE	12.00	12.00	
Q1 Mass (Da)	Q3 Mass (Da)	Time (min)	Param	Start	Stop	ID
429.201	376.300	6.61	DP	75.00	75.00	d7 6a

			CE	18.00	18.00	
Q1 Mass (Da)	Q3 Mass (Da)	Time (min)	Param	Start	Stop	ID
422.302	369.300	6.63	DP	75.00	75.00	6a
			CE	18.00	18.00	
Q1 Mass (Da)	Q3 Mass (Da)	Time (min)	Param	Start	Stop	ID
420.310	385.300	6.83	DP	60.00	60.00	5/6b
			CE	15.00	15.00	
Q1 Mass (Da)	Q3 Mass (Da)	Time (min)	Param	Start	Stop	ID
422.303	369.300	6.89	DP	75.00	75.00	5a
			CE	18.00	18.00	
Q1 Mass (Da)	Q3 Mass (Da)	Time (min)	Param	Start	Stop	ID
427.309	392.300	7.00	DP	60.00	60.00	d6 5/6a
			CE	15.00	15.00	
Q1 Mass (Da)	Q3 Mass (Da)	Time (min)	Param	Start	Stop	ID
420.309	385.300	6.98	DP	60.00	60.00	5/6a
			CE	15.00	15.00	
Q1 Mass (Da)	Q3 Mass (Da)	Time (min)	Param	Start	Stop	ID
427.301	392.300	7.33	DP	60.00	60.00	d7 4b
			CE	15.00	15.00	
Q1 Mass (Da)	Q3 Mass (Da)	Time (min)	Param	Start	Stop	ID
420.302	385.300	7.35	DP	60.00	60.00	4b
			CE	15.00	15.00	

Parameter Table (Period 1 Experiment 1)

CUR:	25.00
GS1:	65.00
GS2:	30.00
IS:	5500.00
TEM:	50.00
ihe:	ON
CAD:	4.00
EP	10.00
CXP	14.00

Resolution tables

Quad 1 Positive Low

Last Modification Date Time: October 06, 2010 02:50:51

Mass (Da)	Offset Value
59.050	0.050
175.133	0.235
500.380	0.753
616.464	0.945
906.673	1.470
1196.883	2.045

Quad 3 Positive Unit
Last Modification Date Time: March 18, 2010 14:07:25

IE3 -0.500

Mass (Da)	Offset Value
59.050	0.032
175.133	0.145
500.380	0.438
616.464	0.556
906.673	0.888
1196.883	1.285

Calibration tables
Quad 1 Positive Unit Resolution
Last Modification Date Time: March 18, 2010 14:05:07

Mass (Da)	Dac Value
59.050	2501
175.133	7490
500.380	21469
616.464	26452
906.673	38886
1196.883	51306

Quad 3 Positive Unit Resolution
Last Modification Date Time: March 18, 2010 14:09:45

Mass (Da)	Dac Value
59.050	2520
175.133	7548
500.380	21642
616.464	26668
906.673	39215
1196.883	51742

Instrument Parameters:
Detector Parameters (Positive):
CEM 2000.0
DF -200.0

Keyed Text:
File was created with the software version: Analyst 1.5.1

APPENDIX C

Sterol Method File

Sterol Data Acquisition File

File Name: DHS 14 PP 100610.wiff
File Path: D:\Analyst Data\Projects\API Instrument\Data\100610DHS 14 S\
Original Name: 100610\DHS 14 PP 100610.wiff
Software Version: Analyst 1.5.1

Log Information from Devices at Start of acquisition:

AutoSampler	CTC PAL	0	CTC
Loop Volume 1 (user entered)		10 µL	
Loop Volume 2 (user entered)		20 µL	
Vendor Driver Ver		1.3.0.40	
Device FW Ver		2.3.6	
Actual Injection Volume	15.000 µL		

Time from start =0.0000 min		Integrated System	Shimadzu
Controller SCL10Avp			
Serial#	C21014153233		
ROM Version	5.42		
Pressure Units	bar		
Time from start =0.0000 min		Pump	Shimadzu
LC10ADvp			
Serial#	C20963502186		
ROM Version	5.26		
Time from start =0.0000 min		Pump	Shimadzu
LC10ADvp			
Serial#	C20964153586		
ROM Version	5.27		
Time from start =0.0000 min		Pump	Shimadzu
LC10ADvp			
Serial#	C20964153587		
ROM Version	5.27		
Time from start =0.0000 min		Column Oven	Shimadzu
CTO10ASvp			
Serial#	C21044250574		
ROM Version	5.27		
Time from start =0.0000 min			

Time from start =0.0000 min		Mass Spectrometer	4000 Q TRAP
Config Table Version	10		
Firmware Version	M401402 B4T0301 M3L1417 B3T0300		

Component Name	Linear Ion Trap Quadrupole LC/MS/MS Mass Spectrometer
Component ID	4000 Q TRAP
Manufacturer	AB Sciex Instruments
Model	1004229-N
Serial Number	U01030402

Time from start =0.0000 min		Mass Spectrometer	4000 Q TRAP
Start of Run - Detailed Status			
Vacuum Status	At Pressure		
Vacuum Gauge (10e-5 Torr)	3.7		
Backing Pump	Ok		
Interface Turbo Pump	Normal		
Analyzer Turbo Pump	Normal		
Sample Introduction Status	Ready		
Source/Ion Path Electronics	On		
Source Type	Heated Nebulizer		
Source Temperature (at setpoint)	380.0 C		
Source Exhaust Pump	Ok		
Interface Heater	Ready		

Time from start =0.0167 min		Mass Spectrometer	4000 Q TRAP
End of Run - Detailed Status			
Vacuum Status	At Pressure		
Vacuum Gauge (10e-5 Torr)	3.7		
Backing Pump	Ok		
Interface Turbo Pump	Normal		
Analyzer Turbo Pump	Normal		
Sample Introduction Status	Ready		
Source/Ion Path Electronics	On		
Source Type	Heated Nebulizer		
Source Temperature (at setpoint)	380.0 C		
Source Exhaust Pump	Ok		
Interface Heater	Ready		

Time from start =16.5833 min

Acquisition Info

Acquisition Method:	\Sterol APCI 032310 Sched X2.dam
Acquisition Path:	D:\Analyst Data\Projects\Sterols\2009_07_02\Acquisition Methods\
First Sample Started:	Thursday, October 07, 2010 8:40:04 AM
Last Sample Finished:	Thursday, October 07, 2010 8:40:04 AM
Sample Acq Time:	Thursday, October 07, 2010 8:40:04 AM
Sample Acq Duration:	16min0sec
Number of Scans:	0
Periods in File:	1
Batch Name:	\100610 DHS 14a S.dab
Batch Path:	D:\Analyst Data\Projects\Sterols\2009_07_02\Batch\
Submitted by:	QTRAP\Administrator()
Logged-on User:	QTRAP\Administrator
Synchronization Mode:	LC Sync
Auto-Equilibration:	Off
Comment:	

Software Version:	Analyst 1.5.1
Set Name:	SET1
Sample Name	DHS 14 PP 100610
Sample ID	
Sample Comments:	
Autosampler Vial:	52
Rack Code:	Stk1-01
Rack Position:	1
Plate Code:	VT54
Plate Position	1

CTC PAL Autosampler Method Properties

Loop Volume1 (µl):	10
Loop Volume2 (µl):	20
Injection Volume (µl):	15.000

Method Description:

Syringe: 100ul

01Analyst LC-Inj

Air Volume (µl)	5
Pre Clean with Solvent 1 ()	0
Pre Clean with Solvent 2 ()	0
Pre Clean with Sample ()	0
Filling Speed (µl/s)	10
Filling Strokes ()	1
inject to	LC Vlv1
Injection Speed (µl/s)	10
Pre Inject Delay (ms)	500
Post Inject Delay (ms)	500
Post Clean with Solvent 1 ()	1
Post Clean with Solvent 2 ()	1
Valve Clean with Solvent 1 ()	1
Valve Clean with Solvent 2 ()	1
Replicate Count ()	1
Analysis Time (s) ()	0

Shimadzu LC Method Properties

Shimadzu LC system Equlibration time = 0.00 min
Shimadzu LC Method Parameters
Pumps
=====
Pump A Model: LC-10ADvp 96% MeOH (0.1% acetic acid)
Pump B Model: LC-10ADvp 100% MeOH (0.1% acetic acid)
Pump C Model: LC-10ADvp
Column: Agilent Poroshell 2.7um C18 150x2mm
Pumping Mode: Ternary Flow
Total Flow: 0.400 mL/min.
Pump B Conc: 40.0 %
Pump C Conc: 0.0 %

B Curve: 0
C Curve: 0
Pressure Range: 0 - 400 Bars
Oven
====
Model: CTO-10ASvp
Temperature Control: Enabled
Temperature: 32 deg. C
Max. Temperature: 85 deg. C
System Controller
==========
Model: SCL-10Avp
Power: On
Event 1: Off
Event 2: Off
Event 3: Off
Event 4: Off
Time Program
==========

Time	Module	Events	Parameter
0.51	Pumps	Pump B Conc.	40
8.00	Pumps	Pump B Conc.	50
8.25	Pumps	Pump B Conc.	100
3.00	Pumps	Pump B Conc.	100
3.25	Pumps	Pump B Conc.	40
6.00	System Controller	Stop	

Quantitation Information:

Sample Type:	Unknown
Dilution Factor:	1.000000

Custom Data:

Quantitation Table:

Peak Name	Mass (ng)
d5 Zym	55.000000
d6 Des	181.440000
d4 Lath	519.000000
d7 Chol	207.672000
d6 14DML	122.400000
d Sito	608.640000
DeHerg	133.000000
VD2	64.000000
VD3	17.000000
Zym	57.000000
Des	181.000000
8_9D	2625.000000
Erg	14.000000
7DA	492.000000
x4 3one	560.000000

Lath	100.000000
Brassi	427.000000
x5 3one A	10.000000
x5 3one B	10.000000
Chol	212.000000
14DML	133.000000
Lan	95.000000
Canol	1079.000000
Camp	52.000000
Stig	1295.000000
Cycloart	100.000000
Sito	616.000000
24DiHL	20.000000
Stiganol	196.700000

Period 1:

Scans in Period:	800	
Relative Start Time:		0.00 msec
Experiments in Period:		1

Period 1 Experiment 1:

Scan Type:	MRM (MRM)	
Scheduled MRM:	Yes	
Polarity:	Positive	
Scan Mode:	N/A	
Ion Source:	Heated Nebulizer	
MRM detection window:		80 sec
Target Scan Time:	1.2000 sec	
Resolution Q1:	Low	
Resolution Q3:	Unit	
Intensity Thres.:	0.00 cps	
Settling Time:	0.0000 msec	
MR Pause:	5.0070 msec	
MCA:	No	
Step Size:	0.00 Da	

Q1 Mass (Da)	Q3 Mass (Da)	Time (min)	Param	ID
377.301	157.200	6.88	DP 80.00	DeHerg
			CE 36.00	
			CXP 12.00	
Q1 Mass (Da)	Q3 Mass (Da)	Time (min)	Param	ID
397.302	91.100	7.20	DP 80.00	VD2
			CE 90.00	
			CXP 4.00	
Q1 Mass (Da)	Q3 Mass (Da)	Time (min)	Param	ID
385.302	367.300	7.45	DP 80.00	VD3
			CE 20.00	

			CXP 12.00	
Q1 Mass (Da)	Q3 Mass (Da)	Time (min)	Param	ID
372.301	95.100	7.71	DP 80.00 CE 48.00 CXP 6.00	d5 Zym
Q1 Mass (Da)	Q3 Mass (Da)	Time (min)	Param	ID
367.301	95.100	7.79	DP 80.00 CE 48.00 CXP 6.00	Zym
Q1 Mass (Da)	Q3 Mass (Da)	Time (min)	Param	ID
373.301	81.200	8.10	DP 80.00 CE 55.00 CXP 4.00	d6 Des
Q1 Mass (Da)	Q3 Mass (Da)	Time (min)	Param	ID
367.302	81.200	8.20	DP 80.00 CE 55.00 CXP 4.00	Des
Q1 Mass (Da)	Q3 Mass (Da)	Time (min)	Param	ID
367.303	81.200	8.70	DP 80.00 CE 55.00 CXP 4.00	8_9D
Q1 Mass (Da)	Q3 Mass (Da)	Time (min)	Param	ID
379.300	81.300	8.70	DP 80.00 CE 50.00 CXP 4.00	Erg
Q1 Mass (Da)	Q3 Mass (Da)	Time (min)	Param	ID
367.304	159.200	9.00	DP 80.00 CE 30.00 CXP 4.00	7DA
Q1 Mass (Da)	Q3 Mass (Da)	Time (min)	Param	ID
385.301	109.100	9.05	DP 100.00 CE 37.00 CXP 12.00	x4 3one
Q1 Mass (Da)	Q3 Mass (Da)	Time (min)	Param	ID
373.302	81.200	9.63	DP 80.00 CE 50.00 CXP 4.00	d4 Lath
Q1 Mass (Da)	Q3 Mass (Da)	Time (min)	Param	ID
369.401	81.200	9.65	DP 80.00 CE 50.00 CXP 4.00	Lath

Q1 Mass (Da)	Q3 Mass (Da)	Time (min)	Param	ID
381.301	81.300	9.65	DP 80.00 CE 62.00 CXP 4.00	Brassi
Q1 Mass (Da)	Q3 Mass (Da)	Time (min)	Param	ID
376.401	161.200	9.72	DP 80.00 CE 30.00 CXP 12.00	d7 Chol 30.00 12.00
Q1 Mass (Da)	Q3 Mass (Da)	Time (min)	Param	ID
385.308	109.300	9.73	DP 80.00 CE 5.00 CXP 13.00	x5 3one A
Q1 Mass (Da)	Q3 Mass (Da)	Time (min)	Param	ID
383.303	95.300	9.74	DP 100.00 CE 50.00 CXP 6.00	x5 3one B
Q1 Mass (Da)	Q3 Mass (Da)	Time (min)	Param	ID
369.402	161.200	9.78	DP 80.00 CE 30.00 CXP 12.00	Chol
Q1 Mass (Da)	Q3 Mass (Da)	Time (min)	Param	ID
401.401	81.300	9.87	DP 80.00 CE 60.00 CXP 4.00	d6 14DML
Q1 Mass (Da)	Q3 Mass (Da)	Time (min)	Param	ID
395.301	81.300	9.90	DP 80.00 CE 60.00 CXP 4.00	14DML
Q1 Mass (Da)	Q3 Mass (Da)	Time (min)	Param	ID
409.302	95.300	10.04	DP 80.00 CE 49.00 CXP 6.00	Lan
Q1 Mass (Da)	Q3 Mass (Da)	Time (min)	Param	ID
371.401	95.200	10.25	DP 80.00 CE 42.00 CXP 6.00	Canol
Q1 Mass (Da)	Q3 Mass (Da)	Time (min)	Param	ID
383.401	81.100	10.36	DP 80.00 CE 65.00 CXP 4.00	Camp
Q1 Mass (Da)	Q3 Mass (Da)	Time (min)	Param	ID
395.302	83.100	10.36	DP 80.00	Stig

			CE 40.00 CXP4.00	
Q1 Mass (Da) 409.303	Q3 Mass (Da) 81.300	Time (min) 10.40	Param DP 80.00 CE 60.00 CXP 12.00	ID Cycloart
Q1 Mass (Da) 404.401	Q3 Mass (Da) 161.200	Time (min) 10.94	Param DP 80.00 CE 35.00 CXP 12.00	ID d Sito
Q1 Mass (Da) 397.303	Q3 Mass (Da) 161.200	Time (min) 10.99	Param DP 80.00 CE 35.00 CXP 12.00	ID Sito
Q1 Mass (Da) 411.401	Q3 Mass (Da) 95.100	Time (min) 11.24	Param DP 90.00 CE 57.00 CXP 6.00	ID 24DiHL
Q1 Mass (Da) 399.301	Q3 Mass (Da) 95.500	Time (min) 11.62	ParamStop DP 80.00 CE 50.00 CXP 6.00	ID Stiganol

Parameter Table(Period 1 Experiment 1)

GS1:	40.00
GS2:	0.00
CAD:	4.00
CUR:	16.00
TEM:	380.00
ihe:	ON
NC:	5.00
EP	10.00

Resolution tables

Quad 1 Positive Low

Last Modification Date Time: October 07, 2010 08:40:04

Mass (Da)	Offset Value
59.050	0.018
175.133	0.098
616.464	0.369
906.673	0.543
1254.925	0.747
1545.134	0.918
2008.469	1.204
2242.637	1.347

Quad 3 Positive Unit
Last Modification Date Time: September 11, 2009 10:11:23

IE3 -0.500

Mass (Da)	Offset Value
59.050	0.025
175.133	0.045
616.464	0.094
906.673	0.130
1254.925	0.161
1545.134	0.184
2010.469	0.235
2242.637	0.265

Calibration tables
Quad 1 Positive Unit Resolution
Last Modification Date Time: August 27, 2010 15:04:40

Mass (Da)	Dac Value
59.050	1096
175.133	3299
616.464	11681
906.673	17193
1254.925	23808
1545.134	29320
2010.469	38162
2242.637	42572

Quad 3 Positive Unit Resolution
Last Modification Date Time: March 19, 2010 11:52:26

Mass (Da)	Dac Value
59.050	1108
175.133	3333
616.464	11802
906.673	17371
1254.925	24053
1545.134	29623
2010.469	38553
2242.637	43010

Instrument Parameters:
Detector Parameters (Positive):
CEM 2100.0

Keyed Text:
File was created with the software version: Analyst 1.5.1

APPENDIX D

Lathosterol Method File

INSTRUMENT CONTROL PARAMETERS: GCMS

C:\MSDCHEM\1\METHODS\LATH SIM.M
Thu Sep 16 22:32:41 2010

Control Information

Sample Inlet : GC
Injection Source : GC ALS
Mass Spectrometer : Enabled

Oven
Equilibration Time 0.25 min
Oven Program On
200 °C for 0 min
then 20 °C/min to 325 °C for 5.75 min
Run Time 12 min

Front Injector
Syringe Size 10 µL
Injection Volume 1 µL
Injection Repetitions 1
Injection Delay 0 sec
Solvent A Washes (PreInj) 2
Solvent A Washes (PostInj) 2
Solvent A Volume 8 µL
Solvent B Washes (PreInj) 2
Solvent B Washes (PostInj) 2
Solvent B Volume 8 µL
Sample Washes 0
Sample Wash Volume 8 µL
Sample Pumps 1
Dwell Time (PreInj) 0 min
Dwell Time (PostInj) 0 min
Solvent Wash Draw Speed 300 µL/min
Solvent Wash Dispense Speed 6000 µL/min
Sample Wash Draw Speed 300 µL/min
Sample Wash Dispense Speed 6000 µL/min

Injection Dispense Speed 6000 µL/min
Viscosity Delay 0 sec
Sample Depth -2 mm

Sample Overlap
Prepare sample before end of GC run 0.25 min

Front SS Inlet H2
Mode Splitless
Heater On 280 °C
Pressure On 36.337 psi
Total Flow On 21.22 mL/min
Septum Purge Flow On 10 mL/min
Septum Purge Flow Mode Switched
Gas Saver On 15 mL/min After 2 min
Purge Flow to Split Vent 10 mL/min at 0.5 min

Thermal Aux 2 (MSD Transfer Line)
Heater On
Temperature Program On
300 °C for 0 min
Run Time 12 min

Column #1
DB-5ms: 939.41594
DB-5ms
325 °C: 40 m x 180 µm x 0.18 µm
In: Front SS Inlet H2
Out: Vacuum

(Initial) 200 °C
Pressure 36.337 psi
Flow 1.2201 mL/min
Average Velocity 55 cm/sec
Holdup Time 1.2121 min
Flow Program On
1.2201 mL/min for 0.5 min
Run Time 12 min

Signals
Test Plot Save Off
50 Hz
Test Plot Save Off
50 Hz
Test Plot Save Off
50 Hz

Test Plot Save Off
50 Hz

MS ACQUISITION PARAMETERS

General Information
------- -----------

Tune File : atune.u
Acquistion Mode : SIM

MS Information
-- -----------

Solvent Delay : 5.00 min

EMV Mode : Gain Factor
Gain Factor : 15.00
Resulting EM Voltage : 2647

[Sim Parameters]

GROUP 1
Group ID : 1
Resolution : High
Plot 1 Ion : 443.40
Plot 2 Ion : 443.4
Ions/Dwell In Group (Mass, Dwell) (Mass, Dwell) (Mass, Dwell)
(443.40, 100) (445.40, 100) (447.40, 100)

[MSZones]

MS Source : 230 C maximum 250 C
MS Quad : 150 C maximum 200 C

END OF MS ACQUISITION PARAMETERS

TUNE PARAMETERS for SN: US91742661

Trace Ion Detection is OFF.

EMISSION : 34.610
ENERGY : 69.922
REPELLER : 34.814
IONFOCUS : 90.157

ENTRANCE_LE : 22.000
EMVOLTS : 2188.235
Actual EMV : 2647.06
GAIN FACTOR : 15.00
AMUGAIN : 2125.000
AMUOFFSET : 121.813
FILAMENT : 1.000
DCPOLARITY : 1.000
ENTLENSOFFS : 19.075
MASSGAIN : -515.000
MASSOFFSET : -38.000

END OF TUNE PARAMETERS

END OF INSTRUMENT CONTROL PARAMETERS

APPENDIX E

Standard Concentrations, recipes, and deuterated analog pairs

Deuterated Cocktail Mix	**20uL to each sample and to RRF mix**			
	ng/uL		To each sample tube prior to addition of sample:	20 uL deuterated cocktail
d 1,25VD3	0.40			
d 25D2	0.50		Te each vial insert prior to transfer of final extract:	20 uL deuterated internal standard
d 25D3	0.60			
d 22r	0.59		RRF	20 uL deuterated cocktail
d 25	0.36			20 uL primary standard cocktail
d 27	2.89			20 uL secondary standard cocktail
d 7o	1.62			20 uL deuterated internal standard
d 7b	4.02			370uL 88% MeOH
d 4b	1.02			
d 5/6a	0.52		Ergosterol RRF*	20 uL deuterated cocktail
d Zymosterol	2.75			20uL ergosterol standard
d Desmosterol	9.07			410 uL 88% MeOH
d Lath	25.95			
d 14DML	6.12		*We have not been able to obtain a pure ergosterol standard. The commercially available	
d Sitosterol	30.43		ergosterol standard we tested showed it to contain small amounts of other sterols. Therefore,	
d Cholesterol	10.38		we prepared a separate RRF standard so as not to skew RRF values for other sterols. Also,	
			we did not include ergosterol in the primary standard mix used for matrix spike as we would have	
			biased the values of some sterols.	
Internal Standard	**20uL to vial insert prior to adding final extract**			
	ng/mL			
d6a	1.96			

Primary Standard Mix	**20uL to RRF Std and to matrix spike**	
	ng/uL	deuterated Surrogate
1α,25-dihydroxy-previtamin D3	0.4	d6 1,25 D3
7α,25-dihydroxycholesterol	0.6	d6 1,25 D3
7ß,27-dihydroxycholesterol	0.448	d6 1,25 D3
1α,25-dihydroxyvitamin D 2	0.48	d6 1,25 D3
3β,27-dihydroxy-5-cholesten-7-one	0.33	d6 1,25 D3
7α,26-dihydroxycholest-4-en-3-one	0.54	d6 1,25 D3
16α,27-dihydroxycholesterol	0.357	d6 1,25 D3
(20R)-17α,20-dihydroxycholesterol	1.152	d6 1,25 D3
25-hydroxyvitamin D_3	0.6	d6 25 D3
25-hydroxyvitamin D2	0.54	d6 25 D2
22R-hydroxycholesterol	0.5936	d6 22r
25-hydroxy-cholesterol	0.3536	d6 25
24S-hydroxy-cholesterol	1.59	d6 27
24-oxocholesterol	0.8032	d6 27
27-hydroxy-cholesterol	2.88	d6 27
24(S),25-epoxycholesterol	0.21312	d6 22r
3-oxo-7α-hydroxycholesterol	0.21	d7 7b
7α-hydroxy-cholesterol	4.032	d7 7b
1α-hydroxyvitamin D2	0.08	d7 7b
1a-hydroxyvitamin D3	0.16	d7 7b
7-oxocholesterol	1.6	d7 7oxo
6α-hydroxycholestanol	2.03	d7 6a
4β-hydroxy-cholesterol	1.0128	d7 4b
dehydroergosterol	6.66	d5 zym
vitamin D2	3.2	d5 zym
vitamin D3	0.825	d5 zym
zymosterol	2.85	d5 zym
desmosterol	9.04	d6 des
8(9)-dehydrocholesterol	12.3	d6 des
7-dehydrocholesterol	28	d6 des
cholestenone (Δ4)	0.675	d6 des
brassicasterol	5	d6 des
lathosterol	21.35	d4 lath
cholesterol	10.591	d7 chol
14-demethyl-lanosterol	6.625	d6 des
lanosterol	4.74	d6 des
dihydrocholesterol	53.97	d6 des
campesterol	64.75	d6 des
stigmasterol	5	d5 zum
cycloartenol	2.6025	d6 des
β-sitosterol	30.8	d sito
24,25-dihydrolanosterol	1.02	d5 zym
stigmastanol	9.835	d5 zym

Secondary Standard Mix	**20 uL to RRF Std and to matrix spike**	
	ng/uL	deuterated Surrogate
15α-hydroxycholestene	0.3816	d6 22r
20-hydroxycholesterol	0.42	d6 22r
5a,6b-dihydroxycholestanol	0.78	d7 7b
15-ketocholestene	0.3828	d7 7b
15-ketocholestane	0.2496	d7 7b
7-oxo-cholestenone	0.43	d7 7b
cholestan-6-oxo-3,5-diol	1.8	d7 7b
15ß-hydroxycholestane	0.1875	d7 7b
15α-hydroxycholestane	0.3498	d7 7b
6-ketocholestanol	0.518	d7 7b
19-hydroxycholesterol	0.9	d7 7b
5,6β-epoxy-cholesterol	0.514	d7 5/6a
5α-hydroxycholesterol	0.8	d7 4b
5,6α-epoxy-cholesterol	0.524	d7 5/6a

Ergosterol Std	**20 uL to Ergosterol RRF standard**	
	ng/uL	
Ergosterol	131.25	d6 des

BIBLIOGRAPHY

1. Goedeke, L. and C. Fernandez-Hernando, *Regulation of cholesterol homeostasis.* Cell Mol Life Sci, 2012. **69**(6): p. 915-30.
2. Waterham, H.R., *Defects of cholesterol biosynthesis.* FEBS Lett, 2006. **580**(23): p. 5442-9.
3. Nes, W.D., *Biosynthesis of cholesterol and other sterols.* Chem Rev, 2011. **111**(10): p. 6423-51.
4. Brown, M.S. and J.L. Goldstein, *Multivalent feedback regulation of HMG CoA reductase, a control mechanism coordinating isoprenoid synthesis and cell growth.* J Lipid Res, 1980. **21**(5): p. 505-17.
5. Lund, E., et al., *Determination of serum levels of unesterified lathosterol by isotope dilution-mass spectrometry.* Scand J Clin Lab Invest, 1989. **49**(2): p. 165-71.
6. Lund, E.G. and U. Diczfalusy, *Quantitation of receptor ligands by mass spectrometry.* Methods Enzymol, 2003. **364**: p. 24-37.
7. Griffiths, W.J. and Y. Wang, *Sterol lipidomics in health and disease: Methodologies and applications.* European Journal of Lipid Science and Technology, 2009. **111**(1): p. 14-38.
8. McDonald, J.G., et al., *Extraction and Analysis of Sterols in Biological Matrices by High Performance Liquid Chromatography Electrospray Ionization Mass Spectrometry*, in *Methods in Enzymology*. 2007, Academic Press. p. 145-170.
9. Gill, S., R. Chow, and A.J. Brown, *Sterol regulators of cholesterol homeostasis and beyond: the oxysterol hypothesis revisited and revised.* Prog Lipid Res, 2008. **47**(6): p. 391-404.
10. Dzeletovic, S., et al., *Determination of cholesterol oxidation products in human plasma by isotope dilution-mass spectrometry.* Anal Biochem, 1995. **225**(1): p. 73-80.
11. Shan, H., et al., *Chromatographic behavior of oxygenated derivatives of cholesterol.* Steroids, 2003. **68**(3): p. 221-33.
12. Byrdwell, W.C., *Dual parallel mass spectrometry for lipid and vitamin D analysis.* J Chromatogr A, 2010. **1217**(25): p. 3992-4003.
13. Brown, M.S. and J.L. Goldstein, *Cholesterol feedback: from Schoenheimer's bottle to Scap's MELADL.* J Lipid Res, 2009. **50 Suppl**: p. S15-27.
14. Horton, J.D., *Sterol regulatory element-binding proteins: transcriptional activators of lipid synthesis.* Biochem Soc Trans, 2002. **30**(Pt 6): p. 1091-5.

15. van der Velde, A.E., *Reverse cholesterol transport: from classical view to new insights.* World J Gastroenterol, 2010. **16**(47): p. 5908-15.

16. Pikuleva, I.A., *Cholesterol-metabolizing cytochromes P450.* Drug Metab Dispos, 2006. **34**(4): p. 513-20.

17. Russell, D.W., *Oxysterol biosynthetic enzymes.* Biochim Biophys Acta, 2000. **1529**(1-3): p. 126-35.

18. Lund, E.G., J.M. Guileyardo, and D.W. Russell, *cDNA cloning of cholesterol 24-hydroxylase, a mediator of cholesterol homeostasis in the brain.* Proc Natl Acad Sci U S A, 1999. **96**(13): p. 7238-43.

19. Russell, D.W., et al., *Cholesterol 24-hydroxylase: an enzyme of cholesterol turnover in the brain.* Annu Rev Biochem, 2009. **78**: p. 1017-40.

20. Shea, H.C., et al., *Analysis of HSD3B7 knockout mice reveals that a 3alpha-hydroxyl stereochemistry is required for bile acid function.* Proc Natl Acad Sci U S A, 2007. **104**(28): p. 11526-33.

21. Cheng, J.B., et al., *Molecular genetics of 3beta-hydroxy-Delta5-C27-steroid oxidoreductase deficiency in 16 patients with loss of bile acid synthesis and liver disease.* J Clin Endocrinol Metab, 2003. **88**(4): p. 1833-41.

22. Cao, G., J.L. Goldstein, and M.S. Brown, *Complementation of mutation in acyl-CoA:cholesterol acyltransferase (ACAT) fails to restore sterol regulation in ACAT-defective sterol-resistant hamster cells.* J Biol Chem, 1996. **271**(24): p. 14642-8.

23. Bauman, D.R., et al., *25-Hydroxycholesterol secreted by macrophages in response to Toll-like receptor activation suppresses immunoglobulin A production.* . Proc. Natl. Acad. Sci. U.S.A., 2009. **106**: p. in press.

24. McDonald, J.G. and D.W. Russell, *Editorial: 25-Hydroxycholesterol: a new life in immunology.* J Leukoc Biol, 2010. **88**(6): p. 1071-2.

25. Victor, R.G., et al., *The Dallas Heart Study: a population-based probability sample for the multidisciplinary study of ethnic differences in cardiovascular health.* Am J Cardiol, 2004. **93**(12): p. 1473-80.

26. Yang, C., et al., *Sterol intermediates from cholesterol biosynthetic pathway as liver X receptor ligands.* J Biol Chem, 2006. **281**(38): p. 27816-26.

27. Haas, D., et al., *Smith-Lemli-Opitz syndrome with a classical phenotype, oesophageal achalasia and borderline plasma sterol concentrations.* J Inherit Metab Dis, 2005. **28**(6): p. 1191-6.

28. Brown, M.S. and J.L. Goldstein, *Cholesterol feedback: from Schoenheimer's bottle to Scap's MELADL.* Journal of Lipid Research, 2009. **50**(Supplement): p. S15-S27.

29. McLean, K.J., M. Hans, and A.W. Munro, *Cholesterol, an essential molecule: diverse roles involving cytochrome P450 enzymes.* Biochem Soc Trans, 2012. **40**(3): p. 587-93.

30. Russell, D.W., *THE ENZYMES, REGULATION, AND GENETICS OF BILE ACID SYNTHESIS.* Annual Review of Biochemistry, 2003. **72**(1): p. 137-174.

31. Bjorkhem, I., et al., *Cholesterol homeostasis in human brain: turnover of 24S-hydroxycholesterol and evidence for a cerebral origin of most of this oxysterol in the circulation.* J Lipid Res, 1998. **39**(8): p. 1594-600.

32. Bjorkhem, I., et al., *From brain to bile. Evidence that conjugation and omega-hydroxylation are important for elimination of 24S-hydroxycholesterol (cerebrosterol) in humans.* J Biol Chem, 2001. **276**(40): p. 37004-10.

33. Goldstein, J.L. and M.S. Brown, *Regulation of the mevalonate pathway.* Nature, 1990. **343**(6257): p. 425-30.

34. Horton, J.D., J.L. Goldstein, and M.S. Brown, *SREBPs: transcriptional mediators of lipid homeostasis.* Cold Spring Harb Symp Quant Biol, 2002. **67**: p. 491-8.

35. Yang, T., et al., *Crucial step in cholesterol homeostasis: sterols promote binding of SCAP to INSIG-1, a membrane protein that facilitates retention of SREBPs in ER.* Cell, 2002. **110**(4): p. 489-500.

36. Horton, J.D., J.L. Goldstein, and M.S. Brown, *SREBPs: activators of the complete program of cholesterol and fatty acid synthesis in the liver.* J Clin Invest, 2002. **109**(9): p. 1125-31.

37. Wang, Y., et al., *Molecular characterization of proprotein convertase subtilisin/kexin type 9-mediated degradation of the LDLR.* J Lipid Res, 2012. **53**(9): p. 1932-43.

38. Molho-Pessach, V., et al., *Homozygosity mapping identifies a bile acid biosynthetic defect in an adult with cirrhosis of unknown etiology.* Hepatology, 2012. **55**(4): p. 1139-45.

39. Rios, J.J., et al., *Deletion of GPIHBP1 causing severe chylomicronemia.* J Inherit Metab Dis, 2012. **35**(3): p. 531-40.

40. Li, Y., et al., *Genetic variant in PNPLA3 is associated with nonalcoholic fatty liver disease in China.* Hepatology, 2012. **55**(1): p. 327-8.

41. Huang, Y., J.C. Cohen, and H.H. Hobbs, *Expression and characterization of a PNPLA3 protein isoform (I148M) associated with nonalcoholic fatty liver disease.* J Biol Chem, 2011. **286**(43): p. 37085-93.

42. Cohen, J.C., J.D. Horton, and H.H. Hobbs, *Human fatty liver disease: old questions and new insights.* Science, 2011. **332**(6037): p. 1519-23.

43. Dzeletovic, S., et al., *Determination of Cholesterol Oxidation Products in Human Plasma by Isotope Dilution-Mass Spectrometry.* Analytical Biochemistry, 1995. **225**(1): p. 73-80.

44. Ramirez, R., et al., *Hepatic triglyceride content in individuals with reduced intestinal cholesterol absorption due to variants in Nieman Pick C1-like 1.* Hepatology, 2011. **54**(2): p. 736-7.

45. Yoder, J.A., et al., *Increased cave dwelling reduces the ability of cave crickets to resist dehydration.* J Comp Physiol B, 2011. **181**(5): p. 595-601.

46. Kozlitina, J., et al., *Dissociation between APOC3 variants, hepatic triglyceride content and insulin resistance.* Hepatology, 2011. **53**(2): p. 467-74.

47. Wang, J., et al., *Sequences in the nonconsensus nucleotide-binding domain of ABCG5/ABCG8 required for sterol transport.* J Biol Chem, 2011. **286**(9): p. 7308-14.

48. Musunuru, K., et al., *Exome sequencing, ANGPTL3 mutations, and familial combined hypolipidemia.* N Engl J Med, 2010. **363**(23): p. 2220-7.

49. Browning, J.D., J.C. Cohen, and H.H. Hobbs, *Patatin-like phospholipase domain-containing 3 and the pathogenesis and progression of pediatric nonalcoholic fatty liver disease.* Hepatology, 2010. **52**(4): p. 1189-92.

50. Rios, J., et al., *Identification by whole-genome resequencing of gene defect responsible for severe hypercholesterolemia.* Hum Mol Genet, 2010. **19**(22): p. 4313-8.

51. Yoder, J.A., et al., *The pheromone of the cave cricket, Hadenoecus cumberlandicus, causes cricket aggregation but does not attract the co-distributed predatory spider, Meta ovalis.* J Insect Sci, 2010. **10**: p. 47.

52. Huang, Y., et al., *A feed-forward loop amplifies nutritional regulation of PNPLA3.* Proc Natl Acad Sci U S A, 2010. **107**(17): p. 7892-7.

53. He, S., et al., *A sequence variation (I148M) in PNPLA3 associated with nonalcoholic fatty liver disease disrupts triglyceride hydrolysis.* J Biol Chem, 2010. **285**(9): p. 6706-15.

54. Lakoski, S.G., et al., *Indices of cholesterol metabolism and relative responsiveness to ezetimibe and simvastatin.* J Clin Endocrinol Metab, 2010. **95**(2): p. 800-9.

55. Honda, A., et al., *Highly sensitive analysis of sterol profiles in human serum by LC-ESI-MS/MS.* Journal of Lipid Research, 2008. **49**(9): p. 2063-2073.

56. Lakoski, S.G., et al., *Genetic and metabolic determinants of plasma PCSK9 levels.* J Clin Endocrinol Metab, 2009. **94**(7): p. 2537-43.

57. Stapleton, G., et al., *A novel cytochrome P450 expressed primarily in brain.* J. Biol. Chem., 1995. **270**: p. 29739-29745.

58. Russell, D.W., *The enzymes, regulation, and genetics of bile acid synthesis.* Annu. Rev. Biochem., 2003. **72**: p. 137-174.

59. Rose, K.A., et al., *Cyp7b, a novel brain cytochrome P450, catalyzes the synthesis of neurosteroids 7α-hyroxy DHEA and 7α-hydroxypregnenolone.* Proc. Natl. Acad. Sci. U.S.A., 1997. **94**: p. 4925-4930.

60. Schwarz, M., et al., *Identification and characterization of a mouse oxysterol 7α-hydroxylase cDNA.* J. Biol. Chem., 1997. **272**: p. 23995-24001.

61. Martin, K.O., et al., *7α-Hydroxylation of 27-hydroxycholesterol: biologic role in the regulation of cholesterol synthesis.* J. Lipid Res., 1997. **38**: p. 1053-1058.

62. Wu, Z., et al., *Structure and functions of human oxysterol 7alpha-hydroxylase cDNAs and gene CYP7B1.* J. Lipid Res., 1999. **40**: p. 2195-2203.

63. Rose, K.A., et al., *Neurosteroid hydroxylase CYP7B: vivid reporter activity in dentate gyrus of gene-targeted mice and abolition of a widespread pathway of steroid and oxysterol hydroxylation.* J. Biol. Chem., 2001. **276**: p. 23937 - 23944.

64. Li-Hawkins, J., et al., *Disruption of the oxysterol 7α-hydroxylase gene in mice.* J. Biol. Chem., 2000. **275**: p. 16536-16542.

65. Russell, D.W., *Fifty years of advances in bile acid synthesis and metabolism.* J. Lipid Res., 2009. **50**: p. S120-125.

66. Danielsson, H., K. Einarsson, and G. Johansson, *Effect of biliary drainage on individual reactions in the conversion of cholesterol to taurocholic acid. Bile acids and steroids 180.* Eur. J. Biochem., 1967. **2**: p. 44-49.

67. Toll, A., et al., *7α-Hydroxylation of 25-hydroxycholesterol in liver microsomes. Evidence that the enzyme involved is different from cholesterol 7α-hydroxylase.* Eur.J.Biochem., 1994. **224**: p. 309-316.

68. Schwarz, M., et al., *Disruption of cholesterol 7α-hydroxylase gene in mice. II. Bile acid deficiency is overcome by induction of oxysterol 7α-hydroxylase.* J. Biol. Chem., 1996. **271**: p. 18024-18031.

69. Ishibashi, S., et al., *Disruption of cholesterol 7α-hydroxylase gene in mice. I. Postnatal lethality reversed by bile acid and vitamin supplementation.* J. Biol. Chem., 1996. **271**: p. 18017-18023.

70. Schwarz, M., et al., *Alternate pathways of bile acid synthesis in the cholesterol 7α-hydroxylase knockout mouse are not upregulated by either cholesterol or cholestyramine feeding.* J. Lipid Res., 2001. **42**: p. 1594-1603.

71. Li-Hawkins, J., et al., *Expression cloning of an oxysterol 7α-hydroxylase selective for 24-hydroxycholesterol.* J. Biol. Chem., 2000. **275**: p. 16543-16549.

72. Baulieu, E.E., P. Robel, and M. Schumacher, *Neurosteroids: beginning of the story.* Int. Rev. Neurobiol., 2001. **46**: p. 1-32.

73. Kuiper, G.G., et al., *Comparison of the ligand binding specificity and transcript tissue distribution of estrogen receptors alpha and beta.* Endocrinology, 1997. **138**: p. 863-870.

74. Sundin, M., et al., *Isolation and catalytic activity of cytochrome P-450 from ventral prostate of control rats.* J. Biol. Chem., 1987. **262**: p. 12293-12297.

75. Weihua, Z., et al., *An endocrine pathway in the prostate, ERbeta, AR, 5alpha-androstane-3beta,17beta-diol, and CYP7B1, regulates prostate growth.* Proc. Natl. Acad. Sci. U.S.A., 2002. **99**: p. 13589-13594.

76. Omoto, Y., et al., *Early onset of puberty and early ovarian failure in CYP7B1 knockout mice.* Proc. Natl. Acad. Sci. U.S.A., 2005. **102**: p. 2814-2819.

77. Umetani, M., et al., *27-Hydroxycholesterol is an endogenous SERM that inhibits the cardiovascular effects of estrogen.* Nat. Med., 2007. **13**: p. 1185-1192.

78. DuSell, C.D., et al., *27-hydroxycholesterol is an endogenous selective estrogen receptor modulator.* Mol. Endocrinol., 2008. **22**: p. 65-77.

79. Martin, C., et al., *CYP7B generates a selective estrogen receptor beta agonist in human prostate.* J. Clin. Endorinol. Metab., 2004. **89**: p. 2928-2935.

80. Pettersson, H., et al., *CYP7B1-mediated metabolism of dehydroepiandrosterone and 5alpha-androstane-3beta,17beta-diol--potential role(s) for estrogen signaling.* FEBS J., 2008. **275**: p. 1778-1789.

81. Diczfalusy, U., et al., *Marked up-regulation of cholesterol 25-hydroxylase expression by lipopolysaccharide.* J. Lipid Res., 2009. **50**: p. in press.

82. Dulos, J., et al., *CYP7B expression and activity in fibroblast-like synoviocytes from patients with rheumatoid arthritis: regulation by proinflammatory cytokines.* Athritis Rheum., 2005. **52**: p. 770-778.

83. Stoilov, I., et al., *The cytochromes P450 (CYP) response to allergic inflammation of the lung.* Arch. Biochem. Biophys., 2006. **456**: p. 30-38.

84. Setchell, K.D.R., et al., *Identification of a new inborn error in bile acid synthesis: mutation of the oxysterol 7α-hydroxylase gene causes severe neonatal liver disease.* J. Clin. Invest., 1998. **102**: p. 1690-1703.

85. Ueki, I., et al., *Neonatal cholestatic liver disease in an Asian patient with a homozygous mutation in the oxysterol 7alpha-hydroxylase gene.* J. Pediatr. Gastroenterol. Nutr., 2008. **46**: p. 465-469.

86. Tsaousidou, M.K., et al., *Sequence alterations within CYP7B1 implicate defective cholesterol homeostasis in motor-neuron degeneration.* Am. J. Hum. Genet., 2008. **82**: p. 510-515.

87. Biancheri, R., et al., *White matter lesions in spastic paraplegia with mutations in SPG5/CYP7B1.* Neuromuscul. Disord., 2009. **19**: p. 62-65.

88. Schüle, R., et al., *Analysis of CYP7B1 in non-consanguineous cases of hereditary spastic paraplegia.* Neurogenetics, 2009. **10**: p. 97-104.

89. Goizet, C., et al., *CYP7B1 mutations in pure and complex forms of hereditary spastic paraplegia type 5.* Brain, 2009. **132**: p. 1589-1600.

90. Criscuolo, C., et al., *Two novel CYP7B1 mutations in Italian families with SPG5: a clinical and genetic study.* J. Neurol., 2009. **256**: p. in press.

91. Salinas, S., et al., *Hereditary spastic paraplegia: clinical features and pathogenetic mechanisms.* Lancet Neurol., 2008. **7**: p. 1127-1138.

92. Clayton, P.T., et al., *Mutations in the sterol 27-hydroxylase gene (CYP27A) cause hepatitis of infancy as well as cerebrotendinous xanthomatosis.* J. Inherit. Metab. Dis., 2002. **25**: p. 501-513.

93. Pierre, G., et al., *Prospective treatment of cerebrotendinous xanthomatosis with cholic acid therapy.* J. Inherit. Metab. Dis., 2008. **32**: p. in press.

94. Bjorkhem, I., K.M. Boberg, and E. Leitersdorf, *Inborn errors in bile acid biosynthesis and storage of sterols other than cholesterol.*, in *The Metabolic and Molecular Bases of Inherited Disease.*, C.R. Scriver, et al., Editors. 2001, McGraw-Hill, Inc.: New York. p. 2961-2988.

95. Quehenberger, O., et al., *Lipidomics reveals a remarkable diversity of lipids in human plasma.* J. Lipid Res., 2010. **51**: p. 3299-3305.

96. McDonald, J.G., et al., *A comprehensive method for extraction and quantitative analysis of sterols and secosteroids from human plasma.* J. Lipid Res., 2012. **53**: p. in press.

97. Garcia, C.K., et al., *Autosomal recessive hypercholesterolemia caused by mutations in a putative LDL receptor adaptor protein.* Science, 2001. **292**: p. 1394-1398.

98. Berge, K.E., et al., *Accumulation of dietary cholesterol in sitosterolemia caused by mutations in adjacent ABC transporters.* Science, 2000. **290**: p. 1771-1775.

99. He, G., et al., *ARH is a modular adaptor protein that interacts with the LDL receptor, clathrin, and AP-2.* J. Biol. Chem., 2002. **277**: p. 44044-44049.

100. Yu, L., et al., *Overexpression of ABCG5 and ABCG8 promotes biliary cholesterol secretion and reduces fractional absorption of dietary cholesterol.* J. Clin. Invest., 2002. **110**: p. 671-680.

101. Victor, R.G., et al., *The Dallas Heart Study: a population-based probability sample for the multidisciplinary study of ethnic differences in cardiovascular health.* Am. J. Cardiol., 2004. **93**: p. 1473-1480.

102. Babiker, A. and U. Diczfalusy, *Transport of side-chain oxidized oxysterols in the human circulation.* Biochim. Biophys. Acta., 1998. **1392**: p. 333-339.

103. Cooke, G.M., *Identification and mechanism of action of phospholipids capable of modulating rat testicular microsomal 3 beta-hydroxysteroid dehydrogenase-isomerase activity in vitro.* Biol Reprod, 1989. **41**(3): p. 438-45.

104. Berge, K.E., et al., *Heritability of plasma noncholesterol sterols and relationship to DNA sequence polymorphism in ABCG5 and ABCG8.* J Lipid Res, 2002. **43**(3): p. 486-94.

105. Romeo, S., et al., *Genetic variation in PNPLA3 confers susceptibility to nonalcoholic fatty liver disease.* Nat. Genet., 2008. **40**: p. 1461-1465.

106. Lund, E.G., J.M. Guileyardo, and D.W. Russell, *cDNA cloning of cholesterol 24-hydroxylase, a regulator of cholesterol homeostasis in the brain.* Proc. Natl. Acad. Sci. USA, 1999. **96**: p. 7238-7243.

107. Solomon, A., et al., *Plasma levels of 24S-hydroxycholesterol reflect brain volumes in patients without objective cognitive impairment but not in those with Alzheimer's disease.* Neurosci. Lett., 2009. **462**: p. 89-93.

108. Bretillon, L., et al., *Plasma levels of 24S-hydroxycholesterol reflect the balance between cerebral production and hepatic metabolism and are inversely related to body surface.* J. Lipid Res., 2000. **41**: p. 840-845.

109. Gur, R.C., et al., *Gender differences in age effect on brain atrophy measured by magnetic resonance imaging.* Proc. Natl. Acad. Sci. U.S.A., 1991. **88**: p. 2845-2849.

110. Luria, A., et al., *Compensatory mechanism for homeostatic blood pressure regulation in Ephx2 gene-disrupted mice.* J Biol Chem, 2007. **282**(5): p. 2891-8.

111. Brown, A.J., *24(S),25-epoxycholesterol: a messenger for cholesterol homeostasis.* Int J Biochem Cell Biol, 2009. **41**(4): p. 744-7.

112. Matysik, S., H.H. Klunemann, and G. Schmitz, *Gas Chromatography-Tandem Mass Spectrometry Method for the Simultaneous Determination of Oxysterols, Plant Sterols, and Cholesterol Precursors.* Clin Chem, 2012.

113. McDonald, J.G., et al., *A comprehensive method for extraction and quantitative analysis of sterols and secosteroids from human plasma.* J Lipid Res, 2012. **53**(7): p. 1399-409.

114. Yu, L., et al., *Expression of ABCG5 and ABCG8 is required for regulation of biliary cholesterol secretion.* J Biol Chem, 2005. **280**(10): p. 8742-7.

115. Yu, L., et al., *Disruption of Abcg5 and Abcg8 in mice reveals their crucial role in biliary cholesterol secretion.* Proc Natl Acad Sci U S A, 2002. **99**(25): p. 16237-42.

116. Hubacek, J.A., et al., *Mutations in ATP-cassette binding proteins G5 (ABCG5) and G8 (ABCG8) causing sitosterolemia.* Hum Mutat, 2001. **18**(4): p. 359-60.

117. Arunabh, S., et al., *Body fat content and 25-hydroxyvitamin D levels in healthy women.* J Clin Endocrinol Metab, 2003. **88**(1): p. 157-61.

118. Lin, E., et al., *Contribution of adipose tissue to plasma 25-hydroxyvitamin D concentrations during weight loss following gastric bypass surgery.* Obesity (Silver Spring), 2011. **19**(3): p. 588-94.

119. Bretillon, L., et al., *Plasma levels of 24S-hydroxycholesterol reflect the balance between cerebral production and hepatic metabolism and are inversely related to body surface.* J Lipid Res, 2000. **41**(5): p. 840-5.

120. Lutjohann, D., et al., *Cholesterol homeostasis in human brain: evidence for an age-dependent flux of 24S-hydroxycholesterol from the brain into the circulation.* Proc Natl Acad Sci U S A, 1996. **93**(18): p. 9799-804.

121. Maeda, Y., et al., *Sex difference in serum 7 alpha-hydroxycholesterol levels in the rat reflect hepatic activity of 3 beta-hydroxy-delta 5-C27-steroid dehydrogenase and cholesterol 7 alpha-hydroxylase.* J Gastroenterol, 1997. **32**(4): p. 502-6.

122. Schwarz, M., et al., *Alternate pathways of bile acid synthesis in the cholesterol 7alpha-hydroxylase knockout mouse are not upregulated by either cholesterol or cholestyramine feeding.* J Lipid Res, 2001. **42**(10): p. 1594-603.

123. Sanchez, I., et al., *Ethnic differences in 25-hydroxyvitamin D levels and response to treatment in CKD.* Int Urol Nephrol, 2012.

124. McDonald, J.G., et al., *Identification and Quantitation of Sorbitol-Based Nuclear Clarifying Agents Extracted from Common Laboratory and Consumer Plasticware Made of Polypropylene.* Analytical Chemistry, 2008. **80**(14): p. 5532-5541.

125. Wynberg, H., *The Reimer-Tiemann Reaction.* Chemical Reviews, 1960. **60**(2): p. 169-184.

126. Paik, M.-J., et al., *Gas chromatographic-mass spectrometric analyses of cholesterol and its precursors in rat plasma as tert-butyldimethylsilyl derivatives.* Clinica Chimica Acta, 2008. **396**(1-2): p. 62-65.

127. Lund, E.G. and U. Diczfalusy, *Quantitation of Receptor Ligands by Mass Spectrometry*, in *Methods in Enzymology*, a.D.J.M. D.W. Russell, Editor. 2003, Academic Press. p. 24-37.

128. Quehenberger, O., et al., *Lipidomics reveals a remarkable diversity of lipids in human plasma.* Journal of Lipid Research, 2010. **51**(11): p. 3299-3305.